



The Journal of **MENA** Sciences

ISSN 2412- 9763 (Print)
ISSN 2412-8937 (Online)

Vol. 2, No. 2
February, 2016

THE JOURNAL OF **MIDDLE** **EAST** AND **NORTH AFRICA** SCIENCES

Editorial Board

A. Heidari	Faculty of Chemistry, California South University (CSU), Irvine, California, USA
Elham Shayegh	The American University of Iraq, Sulaimani, Iraq
Kwame Owusu	The American University of Iraq, Sulaimani, Iraq
Mervat Abou Oaf	The American University in Cairo, Egypt
Mohammed Abdulmumin	University of Ghana, Ghana
Mohammad Mahmoud	Al-Quds College, Jordan
Paul Boye	The University of Mines & Technology, Ghana
Reza Hashemian	Northern Illinois University, United States
Tara Faidhalla	The American University of Iraq, Sulaimani
Victor Temeng	The University of Mines & Technology, Ghana
Zaidul Islam Sarker	International Islamic University Malaysia, Malaysia

Table of Contents

No'	Articles	Page
1	Economic Freedom and Economic Performance: The Case MENA Countries <i>Noha Emara</i>	1
2	Electroless and Corrosion of Nickel-Phosphorus-Tungsten Alloy <i>M.S. Ali Eltoun</i>	16
3	STRESS & AUTOIMMUNE DISEASES <i>Hala L. Fayed</i>	25
4	Diagnostic Tools for Sensitive Estimation of Renal Function & Early Detection of Lupus Nephritis <i>Raji Amin • Sami A. Hakim • Hala L. Fayed • Alaa Khalifa • Fouad Khalil • Mahmoud Khedr • Mohamed Alshafee</i>	34
5	Influence of Genotype on the Expression of Host Plant Resistance in Soybean (Glycine Max (L.) Mirrill) to the Major Insect Pests of Soybean in Umudike <i>Chidi J. Harriman • Abraham A. Ngwuta • Chuka C. Onyishi • Nonso K. Ndulue • Amarachi C. Nwadinobi • Chinonmso M. Okoronkwo • Chinaza B. Onwuchekwa-Henry • N. Olori-Great</i>	48
6	Application of Thermal Imaging Sensor to Early Detect Powdery Mildew Disease in Wheat <i>Tarek Y. Bayoumi • A. A. Abdullah</i>	56



Economic Freedom and Economic Performance: The Case MENA Countries

Noha Emara

Economics Department, Rutgers University, United States
Noha.emara@rutgers.edu

Abstract: The recent political up-rise in the Middle East and North African (MENA) economies sparks the light on evaluating the so called structural reforms that aimed at achieving economic freedom. This paper examines the impact of liberal policies on output per worker in 139 countries with a case study on MENA economies. Using panel least square estimation with fixed effects for a sample of 139 countries over the period 1970-2008, the study estimates the impact of different aspects of economic freedom on output per worker and its components; physical capital, human capital, and productivity. The economic freedom measure encompasses different areas including the size of the government, the protection of property rights and enforcement of contracts, the access to sound money, the freedom to access international markets, and the laxness of regulation of credit, labor, and business. In line with the results of Alexandrakis and Livanis (2013), the study finds a non-uniform impact of different areas of economic freedom on output per worker, capital intensity, human capital per worker, or total factor productivity. For instance, while trade freedom, fiscal freedom, monetary freedom, investment freedom, financial freedom, and freedom from corruption enhances output per worker, through the increase in human capital per worker, it does worsen it through a negative impact on capital intensity and total factor productivity. Furthermore, the study finds a significant reverse causality that runs from enhancing either output per worker or its three components on the economic freedom measure. While increasing output per worker or human capital per worker is reflected in an improvement in economic freedom measures, the opposite is found for the increase in capital intensity or total factor productivity. An important policy implication in this respect suggests that liberal economic policies in MENA countries might not be a pre-requisite for their enhanced future productivity.

To cite this article

[Emara, N. (2016). Economic Freedom and Economic Performance: The Case MENA Countries. *J. Middle East North Afr. sci*, 2(2), 1-15]. (p-ISSN 2412- 9763) - (e-ISSN 2412-8937). <http://www.jomenas.org>. 1

JEL Classification Numbers: O16; O43; N20

Keywords: MENA; Economic Freedom; Political Freedoms; Productivity; Corruption.

1. Introduction

The lack of economic growth in many countries, particularly the MENA countries, has been one of the most important economic problems, both historically and today. Over the past decades, the growth performance of the MENA region has been disappointing relative to the rest of developing countries, and the MENA states are attempting to achieve development and economic growth. A number of studies have consistently shown a positive relationship between economic freedom and economic growth rates across countries (Barro 1996; Justensen 2008). Hence, by becoming economically freer, these countries could theoretically achieve economic integration and macroeconomic convergence. The purpose of the present paper is to investigate precisely how economic freedom impact economic performance in these countries, defined by

four main measures – output per worker, capital intensity, human capital per workers and capital and labor productivity, and focusing on output per worker. Specifically, using panel data for 140 countries over the period 1970-2008, a Non Linear Panel Least Square regression is used to estimate the impact of the different components of economic freedom on three main components of output per worker – capital intensity, human capital per worker and total factor productivity.

In the growth literature, there have been extensive discussions on the importance of economic freedom on economic growth. A leading paper by Easton and Walker (1997) presents cross-sectional estimates on the relationship between economic freedom and growth. They find that changes in economic freedom have a significant impact on the steady-state level of income.

Similarly, De Haan and Sturm (2000), examined how robust economic freedom is related to economic growth; using both level and changes in economic freedom, they regress the average GDP on explanatory variables and an indicator of economic freedom during the period 1975-1990 for 80 countries. Their results show that changes in economic freedom are robustly correlated with economic growth, but not the level of economic freedom. In contrast, Dawson (2003) explored the causal relationship between economic freedom and growth, through Granger causality tests, found that the overall level of economic freedom causes growth. Le Roux and Gorchach (2011) results confirm the direction of the causality. VegaGordillo and Alvarez-Arce (2003) also confirm these results. They find a positive relationship between economic, political freedom and growth, but no statistically significant causality from growth to economic freedom. They shed some additional lights on the link between economic and political freedom: economic freedom enhances political freedom more than democratic institutions enhance economic freedom. Their results suggest that both political and economic freedom foster economic growth. In addition, Justensen (2008) investigates the causal relationship between economic freedom and economic growth further, considering both direct and indirect effects through the investment channel. He runs Granger causality tests for both an aggregated measure of economic freedom (Fraser Institute, 2015) as well as its individual components using panel data for the period 1970-1999 and investment as the dependent variable, and finds that economic freedom causes economic growth through the investment channel. In all the studies which considered, the author did not find any statistically significant causality from growth to economic freedom. Cebula (2011) goes further by investigating what specific types of economic freedom measures are important for growth. He investigates the impact of 10 forms of economic freedom (as developed by the Heritage Foundation) on economic growth in OECD nations, and found that economic growth is positively correlated with several forms of economic freedom: monetary, business, investment, labor, fiscal, property rights freedoms and freedom from corruption. Regarding the size of the coefficients, a one-unit increase in the fiscal freedom index increase the growth rate by 1.01%, and an increase of one-unit in the business freedom index raises economic growth by 1.09%. Freedom from corruption has also quite a high coefficient of 0.8, the lowest being for the labor freedom index (0.42). Investment freedom and corruption freedom have the same effect on economic growth. According to Dawson's (2003),

both bivariate and multivariate tests for causality yield similar results, but in contrast, he found some bidirectional causal effects of the size of the government on economic growth that other authors did not find. He did not reach any conclusion on the direction of the causality between growth and came to the conclusion that money and price stability is endogenously determined with growth. Within the same lines, Carlsson and Lundström (2002) analyze the effects of each component of economic freedom in growth regressions using observation for 74 countries, over a period of 25 years. They find that some areas of freedom have a significant and sizeable effect on the growth of GDP, considering the sensitivity test suggested by Sala-i-Martin (1997), while some of the categories in the index are insignificant or significant but negatively correlated (such as financial freedom or freedom of trade). Consequently, this does not mean that increasing economic freedom, in general, is good for economic growth since, among the components of economic freedom, some having a counteracting impact on economic activity.

Heckelman and Stroup (2000), disaggregating the specific components and measuring their independent impact, came to the same conclusion. Running multivariate regressions with growth as the dependent variable against the different categories of the index of freedom (money and inflation, takings and discriminatory taxes, government operations and regulations, restraints on international trade), their analysis suggests that only 3 of the 14 components have an independent contributing effect on growth. Ultimately derived an empirically weighted summary index of growth-promoting economic freedoms.

In a similar way, this paper pursues the goal to uncover which part of economic freedom impacts (hinder or helps) Total Factor Productivity Growth (TFPG), using the Fraser Institute Index of Economic Freedom. This is a strand of the literature that has yet to be explored. Makdisi, Fattah, and Liman (2003) started to explore this area by studying the contribution of total factor productivity (TFP) to economic growth in the MENA countries. They found that only Egypt, Morocco, Tunisia and Turkey had positive TFPG; regressing TFPG on relevant variables such as institutions, inflation rate, initial income and initial enrollment in primary school, they found that institutions and the stock of human capital affect positively the TFPG, while the negative sign of the coefficient for initial income points to the existence of catching up effect at the TFPG level. The impact of economic freedom on TFPG remains yet to be studied, which is one of the aims of this paper. Policy-makers will benefit from focusing their

attention on those specific components of economic freedom that do contribute to economic performance, through their impact on output per worker and its different components. The structure of the paper is as follows. In the next section, the author lays out empirical specification. Section 3 describes the data set. Section 4 describes the empirical results, and the last section concludes.

2. Empirical Specification

This section estimates the impact of different areas of economic freedom on output per capita in MENA states. Following Jones and Hall, the author estimates the natural logarithm of output per worker as given by the following equation

$$(1) \ln y_{i,t} = \frac{\alpha}{1-\alpha} \ln k_{i,t} + \ln h_{i,t} + \ln A_{i,t}$$

Where $y_{i,t}$ stands for the output per worker, $k_{i,t}$ refers to the physical capital to output or capital intensity, $h_{i,t}$ refers to the human capital per worker, $A_{i,t}$ refers to the total factor productivity, and finally the subscript i and t refers to the country and the time period respectively.

Following Alexandrakis and Livanis (2013), output per worker is expected to be affected either directly or indirectly, by different areas of economic freedom such as the size of the government, the protection of property rights and enforcement of contracts, the access to sound money, the freedom to access international markets, and the laxness of regulation of credit, labor, and business. To examine this relationship, equation (2) estimates the direct effect of economic freedom on output per worker using Panel Least Square regression with regional dummies and period fixed effects (LSDV) for a sample of 139 countries over the period 1970-2008. The period of the study is divided into eight-five-years periods, where the last year contains only four years.

$$(2) \ln y_{i,t} = \beta_0 + \sum_{j=1}^5 \beta_j EF_{j,i,t-v} + d_i + d_t + e_{i,t}$$

Where $\ln y_{i,t}$ stands for the average over v period output per worker and $EF_{i,t-v}$ represents the economic freedom chain-linked overall index and its five components, each one in a turn at the beginning of the v years period, where v is equal to five years.

Next, the variables d_i and d_t stands for the regional dummy and the period dummy respectively, and

finally $e_{i,t}$ reflects all other factors affecting output per worker that are not included in the model or omitted variables.

To explore the channel through which economic freedom indirectly affects output per worker, the three independent variables of the equation (1) are estimated as follows;

$$(3) \frac{\alpha}{1-\alpha} \ln k_{i,t} = \beta_0 + \sum_{j=1}^5 \beta_j EF_{j,i,t-v} + d_i + d_t + u_{i,t}$$

$$(4) \ln h_{i,t} = \beta_0 + \sum_{j=1}^5 \beta_j EF_{j,i,t-v} + d_i + d_t + v_{i,t}$$

$$(5) \ln A_{i,t} = \beta_0 + \sum_{j=1}^5 \beta_j EF_{j,i,t-v} + d_i + d_t + w_{i,t}$$

Where $\ln k_{i,t}$, $\ln h_{i,t}$, and $\ln A_{i,t}$ are defined as the average of the v period physical capital to output, human capital per worker, and total factor productivity respectively. The variables $u_{i,t}$, $v_{i,t}$ and $w_{i,t}$ reflects the omitted variables of each model, and $EF_{i,t}$, d_i and d_t are defined in Equation (2) above.

3. Data

The data set consist of 139 countries spanning the period 1970-2008. The dataset was averaged into eight five years periods where the last period has only four years. The data on output per worker is constructed from the data on GDP per capita (constant 2000 \$US) and labor force collected from the World Development Indicators, World Bank database. The data on the Economic Freedom Index measures, are collected from the website of the Fraser Institute (2015). In addition to the chain-linked overall index, the author uses its five components covering five main policy areas: the size of the government, the protection of property rights and enforcement of contracts, the access to sound money, the freedom to access international markets, and the laxness of regulation of credit, labor, and business.

Next, data on stock of capital is constructed from the domestic investment, as known as gross capital formation (at constant prices) data compiled from the Penn World Tables. More specifically, using the perpetual inventory method and assuming that the capital equation is as follows;

$k_t = (1 - \delta)k_{t-1} + I_{t-1}$ where δ stands for depreciation and I_{t-1} denotes investment level of last period. Where the initial level of capital is equal to

$k_0 = \frac{I_0}{g + \delta}$. Following Hall and Jones (1999) and Alexandrakis and Livanis (2013), the depreciation rate is assumed equal to six percent and following Bernanke and Gurkayanak (2001) and Alexandrakis and Livanis (2013), g is equal to the rate of growth of GDP during the decade in which investment is taken at the initial year.

Next, the data on human capital are collected from Barro and Lee (2000) as the average years of schooling referring to educational attainment. Finally, following Alexandrakis and Livanis (2013), the data on productivity is constructed from the data of output per worker, human capital per worker, and

capital intensity as follows $A_{i,t} = \frac{y_{i,t}}{h_{i,t}k_{i,t}^{\alpha}}$ where α , or the share of physical capital, is assumed to be equal to 0.33 following Mankiw (1992).

4. Estimation Results

In this section, the coefficients of equation (2), (3), (4), and (5) are estimated and reported in Table (1). Each equation was estimated using LSDV and was repeated for each of the six measures of economic freedom each one in a turn. For seek of brevity, only the coefficients of the five measures of economic freedom are reported in the table.

As obvious from Column (1), any improvement in any of the five measures of economic freedom; the size of the government, the protection of property rights and enforcement of contracts, the access to sound money, the freedom to access international markets, and the laxness of regulation of credit, labor, and business. *** The coefficients are all positively and statistically significant at the one percent. This suggests that when the citizens of MENA countries can be allowed more control on their disposition of their own wealth, when they enjoy a stable currency and market determined prices, open wide opportunities in front of new and existing businesses, when they can enjoy wide access to financial intermediaries, and when they suffer less from bribery and dishonesty all will feed into higher output per worker or higher standard of living in general.

Next, to explore the channel through which economic freedom feeds into output per worker, equations (3), (4), and (5) are estimated and reported in the table above. It was surprising to find that the six measures of economic freedom, exerts negative

and significant impact on capital intensity, as shown in Column (2). Similarly, Column (4) shows that the enhancement in economic freedom measures seems to reduce productivity in MENA countries. All coefficients are negative and statistically significant except for the impact of trade freedom on productivity. The results seem to surprisingly suggest that the less freedom in trade, fiscal, monetary, investment, financial, and corruption the more is either the capital intensity or the total factor productivity. The results seem surprising, but in line with the results of Alexandrakis and Livanis (2013).

Finally, it was interesting to find that all six measures of economic freedom increase human capital per worker. As shown in Column (4), all coefficients are positive and statistically significant. This result might suggest that the positive impact of the enhancement in economic freedom measures on output per worker arises mainly from their positive impact on human capital per worker. This positive impact seems to out-weigh the negative impact of the enhancement of these measures on either capital intensity or total factor productivity.

The second part of the estimation procedure is related to the reverse causality. The main question here is whether liberal economic policies are pre-requisite or not for future economic productivity in the MENA region. To answer this question, the author estimates equations (2), (3), (4), and (5) but with switching the dependent and the independent variables. For example, when estimating the reverse causality of in equation (2), dependent variable is the economic freedom index and the dependent variable is output per worker. Each equation is estimated six times with each time one of the economic freedom measures is taken as the dependent variable each one in a turn. The results show a significant reverse causality that runs from enhancing either output per worker or its three components on the economic freedom measure. While increasing output per worker or human capital per worker is reflected in an improvement in economic freedom measures, the opposite is found for the increase in capital intensity or total factor productivity. An important policy implication in this respect suggests that liberal economic policies in MENA countries might not be a pre-requisite for their enhanced future productivity.

5. Conclusion

Improvement in any of the six measures of economic freedom; trade, fiscal, monetary, financial, investment, or corruption enhances output per worker. When the citizens of MENA countries can be allowed more control on their disposition of their own wealth, when they enjoy a stable currency and market determined prices, open wide opportunities in

front of new and existing businesses, when they can enjoy wide access to financial intermediaries, and when they suffer less from bribery and dishonesty all will feed into higher output per worker or higher standard of living in general.

In contrast to the results of Alexandrakis and Livanis (2013) and Bylde and Fernandez-Arias (2006), the results of this study suggest that enhancing economic freedom in MENA states feeds into higher output per worker only through its impact on human capital per worker. Both the capital intensity channel and the total factor productivity channel do not seem to boost output per worker. Furthermore, the results of the current study show a significant reverse causality running from either output per worker, capital intensity, human capital per worker, or total factor productivity to economic freedom measures. An important policy implication in this respect suggests that liberal economic policies in MENA countries might not be a pre-requisite for their enhanced future productivity. In a future extension of this study, the model will be estimated with instrumental variables to check on the robustness of these results.

Corresponding Author:

Noha Emara, Ph.D.
Economics Department,
Rutgers University, United States.
E-mail: Noha.emara@rutgers.edu

References

- Alexandrakis, C., & Livanis, G. (2013). Economic Freedom and Economic Performance in Latin America: A Panel Data Analysis. *Review of Development Economics*, 17(1), 34-48.
- Barro, R. J. (1996). Democracy and growth. *Journal of economic growth*, 1(1), 1-27.
- Carlsson, F., & Lundström, S. (2002). Economic freedom and growth: Decomposing the effects. *Public choice*, 112(3-4), 335-344.
- Cebula, R. J. (2011). Economic growth, ten forms of economic freedom, and political stability: An empirical study using panel data, 2003-2007. *Journal of Private Enterprise*, 26(2), 61-81.
- Dawson, J. W. (2003). Causality in the freedom-growth relationship. *European Journal of Political Economy*, 19(3), 479-495.
- De Haan, J., & Sturm, J. E. (2000). On the relationship between economic freedom and economic growth. *European Journal of Political Economy*, 16(2), 215-241.
- Easton, S. T., & Walker, M. A. (1997). Income, growth, and economic freedom. *The American Economic Review*, 328-332.
- Fraser Institute. (2015). *Economic Freedom Index measures*. Retrieved from <http://www.fraserinstitute.org/research?id=18849>
- Heckelman, J. C., & Stroup, M. D. (2000). Which Economic Freedoms Contribute to Growth?. *Kyklos*, 53(4), 527-544.
- Justesen, M. K. (2008). The effect of economic freedom on growth revisited: new evidence on causality from a panel of countries 1970-1999. *European Journal of Political Economy*, 24(3), 642-660.
- Le Roux, P., & Gorchach, V. (2011). An econometric analysis of the impact of economic freedom on economic growth in the SADC. *Studies in Economics and Econometrics*, 35(2), 1-14.
- Makdisi, S., Fattah, Z., & Liman, I. (2002). *Determination of Growth in the MENA Countries*. Arab Planning Institute Working Paper.
- Sala-i-Martin, X. X. (1997). I just ran two million regressions. *The American Economic Review*, 178-183.
- Vega-Gordillo, M., & Alvarez-Arce, J. L. (2003). Economic growth and freedom: a causality study. *Cato J.*, 23, 199.

Received January 7, 2016; revised January 13, 2016; accepted January 15, 2016; published online February 1, 2016.

Appendix

Figure 1. MENA Region Economic Freedom Index, 2008

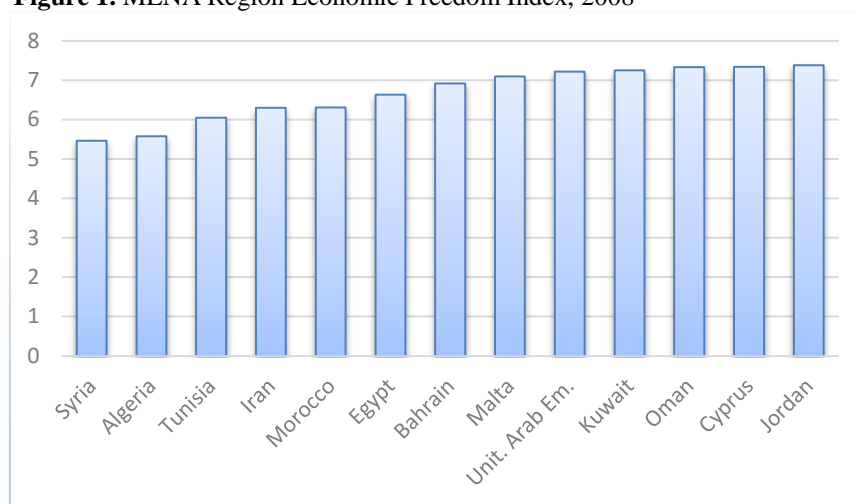


Table 2: The Effect of Economic Freedom on Output per Worker and its Components using Panel Fixed Effects Regression.

Regressors	All Countries				MENA & the Rest of the World			
	(1)	(2)	(3)	(4)	(1')	(2')	(3')	(4')
	Output per Worker regression	Capital Intensity regression	Human Capital per Worker regression	Productivity Regression	Output per Worker regression	Capital Intensity regression	Human Capital per Worker regression	Productivity Regression
<i>EF</i>	0.604***	-0.309***	-0.099	0.993***	0.647***	-0.309***	-0.054	1.025***
<i>EF*MENA</i>	-	-	-	-	-0.747**	-0.080	-0.628*	-1.094***
Overall R^2	0.310	0.130	0.0004	0.141	0.04	0.128	0.025	0.083
Within R^2	0.166	0.159	0.129	0.383	0.174	0.160	0.144	0.388
# Observations	658	598	637	474	658	598	637	474
# Countries	119	96	113	89	119	96	113	89
F(df, n)	17.67***	12.01***	6.40***	20.53***	9.84***	10.92***	5.88***	23.09***

* $p < 0.05$; ** $p < 0.01$; *** $p < 0.001$

Table 3: *The effect of Economic Freedom Indices on Output per Worker using Panel Fixed Effects Regression.*

	All Countries	MENA & the other Countries
Regressors: Output per Worker relative to USA	(1)	(2)
EF1	-	-
EF2	-	0.252**
EF3	0.183***	0.162**
EF4	-	-
EF5	-	-
EF1*MENA	-	-
EF2*MENA	-	-
EF3*MENA	-	-
EF4*MENA	-	-
EF5*MENA	-	-
Overall R^2	0.307	0.214
Within R^2	0.150	0.162
# Observations	592	592
# Countries	118	118
F(df, n)	5.87	4.73***

** $p < 0.01$; *** $p < 0.001$.

Table 4: *The effect of Economic Freedom Indices on Output per Worker through Capital using Panel Fixed Effects Regression.*

	All countries	MENA & the other Countries
Regressors		
Capital Intensity	(1)	(2)
EF1	-0.055*	-
EF2	-0.216***	-0.216***
EF3	-	-
EF4	-0.097**	-0.106**
EF5	-	-
EF1*MENA	-	-
EF2*MENA	-	-
EF3*MENA	-	-
EF4*MENA	-	-
EF5*MENA	-	-
Overall R^2	0.212	0.186
Within R^2	0.153	0.157
# Observations	516	516
# Countries	95	95
F(df, n)	5.81***	79349***

* $p < 0.05$; ** $p < 0.01$; *** $p < 0.001$

Table 5: *The effect of Economic Freedom Indices on Output per Worker through Human Capital using Panel Fixed Effects Regression.*

	All Countries	MENA & the other Countries
Regressors	(2)	(1)
EF1	-	-
EF2	-0.186*	-
EF3	-	-
EF4	-	-
EF5	-	-
EF1*MENA	-	-
EF2*MENA	-	-
EF3*MENA	-	-
EF4*MENA	-	-
EF5*MENA	-	-
Overall R^2	0.005	0.024
Within R^2	0.126	0.133
# Observations	569	569
# Countries	112	112
F(df, n)	2.53***	2.05**

* $p < 0.05$; ** $p < 0.01$; *** $p < 0.001$

Table 6: *The effect of Economic Freedom Indices on Output per Worker through Productivity using Panel Fixed Effects Regression.*

	All Countries	MENA & the other Countries
Regressors	(1)	(1)
EF1	-	-
EF2	0.812***	0.963***
EF3	0.317**	0.278**
EF4	-	-
EF5	-	-
EF1*MENA	-	-
EF2*MENA	-	-0.772**
EF3*MENA	-	-
EF4*MENA	-	-
EF5*MENA	-	-
Overall R^2	0.284	0.245
Within R^2	0.365	0.381
# Observations	437	437
# Countries	88	88
F(df, n)	10***	-

** $p < 0.01$; *** $p < 0.001$



Robustness Check using Prais-Winsten Regression procedure, Panel-Corrected Standard Errors, and Autoregressive errors

Table 7: *The Effect of Economic Freedom on Output per Worker and its Components using Prais-Winsten regression procedure, panel-corrected standard errors, and autoregressive errors.*

Regressors	All Countries				MENA & the Rest of the World			
	(1) Output per Worker regression	(2) Capital Intensity regression	(3) Human Capital per Worker regression	(4) Productivity Regression	(1') Output per Worker regression	(2') Capital Intensity regression	(3') Human Capital per Worker regression	(4') Productivity Regression
EF	0.577***	-0.134***	-	1.133***	0.622***	-0.132***	-	1.153***
EF*MENA	-	-	-	-	-0.585**	-	-	-0.619*
R^2	0.070	0.215	0.456	0.142	0.076	0.216	0.456	0.143
# Observations	539	598	637	385	539	598	637	385
# Countries	119	96	113	89	119	96	113	89
F(df, n)	62.85***	8.88***	0.00	42.60***	32.66***	4.48**	0.32	21.27***

* $p < 0.05$; ** $p < 0.01$; *** $p < 0.001$



Table 8: *The effect of Economic Freedom Indices on Output per Worker using Prais-Winsten regression procedure, panel-corrected standard errors, and autoregressive errors.*

	All Countries	MENA & the other Countries
Regressors:	(1)	(2)
EF1	0.087**	0.095**
EF2	0.151***	0.199***
EF3	0.102***	0.097**
EF4	-	-
EF5	0.246**	0.229*
EF1*MENA	-	-0.153*
EF2*MENA	-	-0.265***
EF3*MENA	-	-
EF4*MENA	-	-
EF5*MENA	-	-
R^2	0.092	0.106
# Observations	474	474
# Countries	118	118
F(df, n)	10.21	5.90

* $p < 0.05$; ** $p < 0.01$; *** $p < 0.001$



Table 9: *The effect of Economic Freedom Indices on Output per Worker through Capital using Prais-Winsten regression procedure, panel-corrected standard errors, and autoregressive errors.*

	All countries	MENA & the other Countries
Regressors	(1)	(2)
EF1	-0.065***	-0.062***
EF2	-0.080***	-0.090***
EF3	-	-
EF4	-	-
EF5	-	-
EF1*MENA	-	-0.186*
EF2*MENA	-	0.145**
EF3*MENA	-	-
EF4*MENA	-	-0.131*
EF5*MENA	-	-
R^2	0.264	0.266
# Observations	516	516
# Countries	95	95
F(df, n)	5.32***	471***

* $p < 0.05$; ** $p < 0.01$; *** $p < 0.001$



Table 10: *The effect of Economic Freedom Indices on Output per Worker through Human Capital using Prais-Winsten regression procedure, panel-corrected standard errors, and autoregressive errors.*

	All Countries	MENA & the other Countries
Regressors	(1)	(2)
EF1	-0.055**	0.057*
EF2	-	-0.091*
EF3	-	-
EF4	0.117***	0.145***
EF5	0.151**	0.130**
EF1*MENA	-	-
EF2*MENA	-	-
EF3*MENA	-	-
EF4*MENA	-	-0.415**
EF5*MENA	-	-
R^2	0.498	0.50
# Observations	569	569
# Countries	112	112
F(df, n)	3.77***	2.98***

* $p < 0.05$; ** $p < 0.01$; *** $p < 0.001$



Table 11: The effect of Economic Freedom Indices on Output per Worker through Productivity using Prais-Winsten regression procedure, panel-corrected standard errors, and autoregressive errors

	All Countries	MENA & the other Countries
Regressors	(1)	(2)
EF1	0.142*	0.141**
EF2	0.572***	0.641***
EF3	0.154*	0.143*
EF4	-	-
EF5	-	-
EF1*MENA	-	-
EF2*MENA	-	-0.853***
EF3*MENA	-	-0.292***
EF4*MENA	-	-
EF5*MENA	-	-
R^2	0.148	-
# Observations	349	349
# Countries	88	88
F(df, n)	9.84***	-

* $p < 0.05$; ** $p < 0.01$; *** $p < 0.001$



Electroless and Corrosion of Nickel-Phosphorus-Tungsten Alloy

M.S. Ali Eltoun

Department of Chemistry, Faculty of Science, Sudan University of Science and Technology, Khartoum, Sudan
abotrteell74@gmail.com

Abstract: At the present work Nickel-Phosphorous- tungsten alloy was electroless plating on copper substrate, different parameters which affect the electroless plating of this alloy were studied and the obtained coatings were characterized using different analytical techniques such as EDX (Energy Dispersive X-ray), XRD (X-ray Diffraction), SEM (Scanning Electron microscope), Potentiodynamic polarization curve (corrosion resistance), incorporation of tungsten on Ni-P matrix changed the crystallography and microstructure details of Ni-P ally and enhancement in corrosion and hardness were observed.

To cite this article

[Ali Eltoun, M. S. (2016). Electroless and Corrosion of Nickel-Phosphorus-Tungsten Alloy. *J. Middle East North Afr. sci.*, 2(2), 16-24]. (p-ISSN 2412- 9763) - (e-ISSN 2412-8937). <http://www.jomenas.org>. 2

Keywords: Electrolessplting; Polyalloy; Potentiodynamic polarization; Corrosion.

1. Introduction

Development of electroless nickel polyalloy deposits is considered as the most effective method to alter the chemical and physical properties of binary Ni-P alloy deposits. The transition metal is the preferred choice because of its high melting temperature, and, unusual mechanical properties.

It is a well-established fact that W cannot be electrodeposited from aqueous electrolytes, but can be codeposited with iron group metals such as nickel to form an alloy (Brenner, 1963), this is classified as induced codeposition.

Electroless ternary alloy with elements other than the iron family, namely, Ni-W-P, has been first reported by Pearlstein, Weightman, and Wick (1963). Codeposition of tungsten in binary Electroless Ni-P deposit improves the deposit characteristics such as wear resistance. The properties of the electroless Ni-W-P amorphous deposits were determined (Bangewi, Wangyu, Qinglong, & Xuanyuan, 1996). Ni-P based alloy films was prepared by autocatalytic plating and their structure, chemistry and corrosion behaviors in sulfuric acid solution were studied as a function of their composition (Lu & Zangari, 2002). The as-prepared Ni-based alloys are nanocrystalline, and their grain size decreases with increasing P content. The Addition of a third element (W or Mo) influences the observed grain size.

Electroless deposition of Ni-W-P alloy coatings onto metal substrates using H₂PO₂ as reducing agent from solutions containing nickel sulfate, sodium tungstate, sodium citrate, ammonium sulfate and other additives was studied (Du & Pritzker, 2003). Electroless Ni-P-W coatings were deposited on mild steel in alkaline solutions have been reported (Tien, Duh, & Chen, 2004). The tungsten addition into the nickel-phosphorus based coating, effectively, increases micro hardness and thermal stability (Balaraju & Rajam, 2005). They also possess good magnetic properties. The effect of copper and tungsten in alkaline electroless nickel baths has been studied in depositing Ni-Cu-P and Ni-W-P alloys and also the synergistic effect of ions in depositing Ni-W-Cu-P alloys (Balaraju & Rajam, 2005). Autocatalytic ternary Ni-Sn-P, Ni-W-P and quaternary Ni-W-Sn-P films were also studied (Balaraju & Rajam, 2006). Alkaline citrate-based baths were used and compared with binary Ni-P coatings, excellent properties such as high hardness, wear and corrosion resistance, a lot of interest has been created in the scientific community in developing electroless nickel alloys Hypophosphite reduced baths become more popular for many industrial applications due to their stability, ease of operation, and cost effectiveness.

Thermal stability of electroless Ni-W-P deposits, analyzed by DSC, is enhanced by the co-deposition of tungsten as compared to binary electroless Ni-P coating (Hu, Wang, Meng, & Rao, 2006). Quaternary Ni-W-Cu-P coatings deposited using alkaline-citrate-based nickel sulfate and nickel chloride baths were studied (Balaraju, Anandan, & Rajam, 2006). Incorporation of copper has a marginal influence on the nickel, phosphorus and tungsten contents of the coatings. XPS studies show that the addition of copper increases the elemental form of W in chloride-based deposits towards that of sulfate-based deposits. Copper has no detrimental effect on hardness, but improves the surface quality difference in hardness between ternary and quaternary deposits.

Composite four-component Ni-W-P-ZrO₂ coatings were electrolessly deposited from a bath with different concentrations of glycine, sodium tungstate (VI) and zirconium (IV) oxide at different pH values (Szczygieł & Turkiewicz, 2008).

The effect of experimental parameters, such as temperature, pH, nickel sulfate concentration, sodium hypophosphite concentration, sodium citrate concentration, and deposition time on the deposition rate of electroless deposition of Ni-P-W and Ni-P-Al₂O₃ were studied (Hamdy, Shoeib, Hady, & Salam, 2008). The result shown that, the coating brightness, coherence, corrosion and uniform surface distribution were improved due to addition of W and alumina. Ni-W-Cr-P alloy coatings prepared by electroless deposition on stainless steel have been reported by Jin et al. (2010). The effects of heat treatment on the structure and phase transformation behavior, microhardness of the Ni-W-Cr-P alloy coatings were investigated. The experimental results reveal that with an increase in the annealing temperature, micro hardness of Ni-W-Cr-P alloy coatings increased, reaching its maximum value at 700C, and then decreased slightly. Using a complexing agent such as citrate in electroless Ni-P such as citrate (Hamdy, Shoeib, Hady, & Salam, 2008), propylene glycol and urea (de Hazan, Werner, Z'graggen, Groteklaes, & Graule, 2008) are found to induce stability during plating. A survey of the literature shows that gluconate electrolytes have been used to electroplate metals such as nickel (Abd El Meguid, Abd El Rehim, & Moustafa, 1999), copper (El Rehim, Sayyah, & El Deeb, 2000), tin (Abd el Rehim, Sayyah, & El Deeb, 2000), and zinc (Rashwan, Mohammed, El Wahaab, & Kamel, 2000). No literature reference was found on the use of gluconate in electroless nickel plating. The objective of the present study is to obtain Ni-P-W from alkaline gluconate baths, studying the dependence of coating characteristics on several

electroless plating variables. Our work also characterizes the coatings by using different analytical techniques such as SEM, EDX and XRD and examines the coating hardness and corrosion resistance.

2. Experimental

2.1. Chemicals of electroless deposition:

All chemicals used were of analytical grade: Nickel sulfate hexa-hydrate (NiSO₄.6H₂O), Boric acid (H₃BO₃), Ammonium sulfate ((NH₄)₂SO₄), Sodium gluconate (C₆H₁₁O₇Na), Sodium tungstate (Na₂WO₄), Sodium hydroxide (NaOH), Sodium carbonate (Na₂CO₃), Hydrochloric acid (HCl), Sulfuric acid (H₂SO₄), Nitric acid (HNO₃), Acetone (C₂H₆O), Ethanol (C₂H₆O), Sodium hypophosphite (NaH₂PO₂), lead acetate (PbAc₂), Succinic acid (C₄H₆O₄), (Sodium dodecyl sulfate (SDS), (C₁₂H₂₃O₄SNa), Palladium chloride (PdCl₂).

2.2. Pretreatment of the substrates:

Before each run, the copper sheets cathodes (2X2cm²) were mechanically polished with different grades emery papers (360,800 and 1000) and then washed by distilled water, then degreased by ethanol (abs 95%) for 60 second, rinsed by distilled water, pickled by acidic solution (3HCl+1HNO₃), for 30 second, rinsed by distilled water, anodically polarized in concentrated Phosphoric acid for 2min at 4V for electro-polishing and rinsed by distilled water, the copper sheets were then dried with hot air to be ready for the electroplating process.

2.3. Activation of copper substrate:

After treating the copper substrate, it was immersed for 20 seconds in a dilute acidic solution of PdCl₂ (0.1 g/L PdCl₂ and 0.2 ml/L HCl 36%), followed by thorough rinsing, then the substrate was dried and weighed (9).

2.4. Experimental procedure of nickel electroless deposition:

The electrochemical cell was connected by holding only the copper substrate immersed into 250ml of the electroless solution for 60 min.

2.4.1. Bath composition of Nickel-phosphorus electrolessdeposition:

The plating bath composition and operating condition are shown in Table (1) below:

Table 1: *The plating bath composition and operating condition.*

Nickel sulfate	5-30 g/L
Sodium hypophosphite	5-40 g/L
Sodium gluconate	15-40 g/L
Succinic acid	3 g/L
SDS	0.5g/L
Lead acetate	2 mg/L
Time	20-100 min
Temperature	50-100 ⁰ C
pH	4-9
Stirring speed	150 rpm

The pH was measured using Microprocessor pH/mV/C Meter (Model CP 5943-45USA) and adjusted by adding NH₄OH or H₂SO₄ 20 % solutions; the temperature was adjusted using a thermostatically controlled bath.

2.4.2. Factors Affecting Electroless Ni-P alloy Coating:

The factors may be summarized as follows:

- (I). Base metal: Good quality base metal produces good quality electroless nickel coatings.
- (II). Pretreatment and cleaning: The substrate surface must be prepared to leave a clean, uniformly active, surface, and free from dirt and grease.
- (III). Electroless nickel process control; The process parameters are: Bath temperature, Bath pH, Nickel content, Reducing agent content, Complexing agent, and Deposition time

2.4.2.1. Effect of Temperature on Deposition Rate:

The effect of electroless nickel bath temperature was determined as a function of deposition rate (mg/cm².hr). The temperature was changed from 50-1000C.

2.4.2.2. Effect of pH:

The effect of pH on the deposition rate and phosphorus content was determined by changing the pH as a function of deposition rate and phosphorus content.

2.4.2.3. Effect of Nickel Salt (source of nickel ions):

Using the operating conditions in Table (1) nickel sulfate concentration was changed from 5-30 g/L as a function of deposition rate.

2.4.2.4. Effect of Sodium Hypophosphite (reducing agent):

The plating bath was prepared as in Table (1); the sodium hypophosphite concentration was changed from 5-40 g/L as a function of deposition rate and phosphorus content.

2.4.2.5. Effect of Sodium gluconate (complexing agent):

Copper cathode prepared and plated using the optimum bath solution, shown in Table (1) the gluconate concentration was changed from 15-40 g/L as a function of deposition rate.

2.4.2.6. Effect of plating time on the deposition rate:

The effect of time on the deposition rate was studied by changing the plating time from 20 to 100 min as a function of deposition rate.

2.5. Factors Affecting Electroless Ni-P-W alloy:

2.5.1. Bath composition of Ni-P-W electroless deposition:

The plating bath composition and operating conditions for Ni-P-W electroless deposition are shown in Table (2) below:

Table 2: *The plating bath composition and operating conditions for Ni-P-W electroless deposition*

Nickel sulfate	25 g/L
Sodium hypophosphite	15 g/L
Sodium gluconate	15 g/L
Ammonium sulfate	15 g/L
Sodium tungstate	5-25 g/L
Succinic acid	3 g/L
SDS	0.5g/L
Lead acetate	2 mg/L
Time	60 min
Temperature	900 C
pH	9
Stirring speed	150 rpm

2.6. Characterization of nickel alloys electroless deposits:

2.6.1. Coating investigation:

2.6.1.1. Coating chemical composition:

The composition was examined using the following procedures:

- 1) The coating layer is stripped using 10% H₂SO₄ solution. The object is then placed as an anode in an electroplating cell. The coating layer was dissolved in solution, diluted to 250 ml with bi-distilled water.
- 2) Analysis using Atomic absorption Spectrophotometer (Perkin Elymer3100, Germany).
- 3) The solution obtained is further diluted by dissolving 5ml in bi- distilled water to 250ml.
- 4) Nickel standard solutions for the elements to be detected were prepared (1g Ni metal in (1+1) HNO₃. Diluted to 1 L with 1 % (v/v) HNO₃), Ni- Hollow Cathode lamp, Air-Acetylene flame gases, wave length of 232 n

The results are confirmed in some samples with EDX analysis.

2.7. Coating Thickness:

Coating Thickness obtained was measured by taking a cross section of the coated layer using a coating thickness /Neophot2-Optical microscope (Germany).

2.8. Microstructure Characterization:

Metallographic examinations were carried out on the material under consideration, to correlate the parameters affecting mechanical properties, such as grain size and the distribution of the particles in the matrix, as well as the main phases and intermetallic phases present.

2.8.1. Scanning Electron Microscopy (SEM) and Energy Dispersive X-ray (EDX):

Microstructures of different deposits were characterized by scanning electron microscopy (SEM), and Energy Dispersive X-ray Spectroscopy (EDXS).

The specimens were coated with golden solution and were taken at room temperature by inserting the samples through the sample holder into the inside of the instrument; Photomicrographs at different zones and magnifications were taken for each specimen at 30 kV, and was used to define the distribution of the particles in the matrix and on the grain boundaries. Photomicrographs of Energy dispersive X-ray spectroscopy (EDXS) at 10 kV was also used to determine the distribution of elements in the particles that are present in the matrix and on grain boundaries.

2.8.2. X- Ray Diffraction (XRD):

XRD was performed in order to determine the constituent phases of surface and phase changes of different coated substrates. Using an X-Ray Diffractometer (Broker AXS-D8 X-ray diffractometer, ADVANCE, Germany), with a copper target ($\text{Cu}\lambda = 1.54060\text{\AA}$) and Nickel filter. Selected samples of each group were recorded; Data of XRD were based on Bragg's Equation:

$$(1) \quad n\lambda = 2d\sin\theta$$

Where n = Integral number, λ = Wave length, d = Interplanar space, and θ = Diffraction angle.

Crystallinity determination:

The average crystal size of the phases in the coating was calculated using *Debye-Scherer* formula:

$$(2) \quad D = k\lambda / B \cos\theta$$

Where D = crystal size nm, $K = 0.8$ -- 1.3 (usually close to unity e.g.0.9), λ is the wave length of the radiation $\lambda_{\text{Cu}} = 1.54056 \text{\AA}$, B is the full width at half maximum, and θ is the position of the maximum of diffraction.

The numerical procedures were facilitated with the use of computer software (PSI-Plot, poly software international, salt lake, UK).

2.9. Hardness measurements:

The Vickers microhardness of deposits was measured under 50 gm. The load microhardness of the specimen material using a Shimdzu Hardness tester. The diamond is pressed into the surface of the specimen material at 50 gm load. For 15 s (the diamond produces a square indentation and an average is taken of the diagonal lengths) which is measured using a microscope and an average of triplet readings was recorded.

2.10. Corrosion Resistance:

2.10.1. Polarization Tests:

Electrochemical experiments were performed using A VOLTA LAB 40 (Model PGZ301) with the aid of commercial software (Volta Master 4 version 7.08). A saturated calomel electrode (SCE) and a platinumized platinum black were used as reference and auxiliary electrodes respectively, with the plated substrate as a working electrode. The electrochemical cell was filled with 3.5% NaCl.

Linear polarization technique was carried out by subjecting the working electrode to a potential range of 205 mV below and above corrosion potential (E_{corr}) at a scan rate of 5 mV/Sec., corrosion rate was evaluated from the polarization curves by Tafel extrapolation with the aid of the commercial software (Volta Master 4 version 7.08).

Volta Master 4 calculates and displays the corrosion rate as Corr. in the $\mu\text{m}/\text{year}$: this rate is calculated from the corrosion current density found i_{corr} , the density, D , and the atomic mass, M , and valence, V , entered in the Tafel dialogue box. The calculation is performed as follows:

$$(3) \quad \text{Corr.rate } (\mu\text{m}/\text{year}) = \frac{i_{\text{corr.}} (\text{A}/\text{cm}^2) \times M (\text{g})}{D (\text{g}/\text{cm}^3) \times V} \times 3270$$

With: $3270 = 0.01 \times [1 \text{ year (in seconds) } / 96497.8]$ and $96497.8 = 1 \text{ Faraday in Coulombs.}$

3. Results and Discussion

3.1. Ni-P alloy electrolessdeposition:

From data in table (1) systematic studies were carried out to investigate the appropriate conditions for Ni-P electroless plating, and this step was done only in the way that these conditions can be used in Ni-P-W alloy electroless plating and not discussed further here.

The obtained optimum conditions of Ni-P electroless plating were shown on the table (3).

Table 3: optimum conditions of Ni-P electroless plating

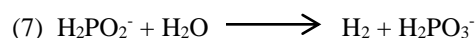
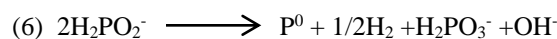
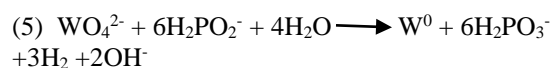
Nickel sulfate	25 g/L
Sodium hypophosphite	15 g/L
Sodium gluconate	15 g/L
Ammonium sulfate	15 g/L
Succinic acid	3 g/L
SDS	0.5g/L
Lead acetate	2 mg/L
Time	60 min
Temperature	90 ⁰ C
pH	9
Stirring speed	150 rpm

3.2. Ni-P-W alloy electrolessdeposition:

3.2.1. Effect of Sodium Tungstate concentration on Ni-P-W alloy:

Figs (1, 2) show the effect of sodium tungstate concentration on the deposition rate and W% in Ni-P-W alloy. The deposition rate is slightly decreased with increasing sodium tungstate concentration in the plating bath, consequently the alloy tungstate content increased and nickel content decreased. The phosphorus content slightly decreased with increase sodium tungstate concentration. This is due to increase of the metals ion ratio to hypophosphite ions in the bath. Du and Pritzker (2003), reported that Ni²⁺ ions participate in W and P deposition, H₂ evolution and H₂PO₂⁻ oxidation and that H₂PO₂⁻ ions participate in cathodic reduction. This indicates that the partial reactions for the Ni-W-P system do not occur independently of one another. Finally, they proposed a mechanism for the deposition of Ni-P-W alloy that incorporates the following features: (i) produced H₂ originates primarily from the hypophosphite reducing agent rather than H₂O and (ii) oxidation and reduction reactions mediated by radicals play very important roles in addition to anodic and cathodic processes involving direct electron transfer. These characteristics ensure that metal deposition is always accompanied by H₂ evolution. With this in mind, one might expect the predominant overall reactions during Ni-W-P

electroless plating in an alkaline solution to be the following:



These reactions reflect the overall stoichiometry of the processes, but not the possible mechanistic steps or interactions between the various reactants.

From Fig (3), it is clear that the deposition rate of Ni-P-W alloy increased with increasing the pH of the solution. This could be attributed to the increase of the driving force of the reducing agent as a result of the increase of which needs the addition of ammonia solution, which is a type of ligand able to enhance electron transmission, thus increasing reducing the rate of metal ions when it is incorporated with complexing agent.

The result of energy dispersive X-ray for Ni-P and Ni91%-P3%-W6% alloys were shown in Figs (4, 5) respectively.

The X-ray diffraction pattern of the as-plated Ni-W-P deposit is illustrated in Fig (7). The reflections corresponding to the (111), (200) and (220) planes of a Face Centered Cubic (FCC) phase of nickel could be observed and it was consisted of a mixture of amorphous, Ni and Ni₃P. The original amorphous structure of Ni-P which has a single peak at about 42 Fig (6) was converted. This result agreed with the results obtained by Jin et.al (2010) and Aal, El-Sheikh, and Ahmed (2009). The grain size was 55.75nm.

3.3. Characterization of Ni-P-W alloy:

3.3.1. Morphology of Ni-P-W alloy:

The original amorphous structure of Ni-P alloy Fig (8) was converted to a compact structure with spherical nodules in the case of the morphological structure of Ni91%-P3%-W6% alloy Fig (9). Bright and coherent coatings, uniform in appearance.

3.3.2. Microhardness:

The microhardness of Ni91%-P3%-W6% (W 5g/L), was observed to be 650HV50.

3.3.3. Corrosion behavior Ni-P-W alloy:

The Potentiodynamic polarization curve of Ni-P and Ni-P-W coatings were shown in Figs (10,

11) respectively, and Ni-P-W has higher corrosion resistance in comparison with Ni-P. The potentiodynamic curves shown that, the corrosion current density of the coated Ni-P-W% alloy was lower than that of the Ni-p alloy. For the two curves, once the scanned potential exceeded E_{corr} , the corrosion current density of the samples continually increased. However, the increase of the corrosion current density of the coated Ni-P-W alloy was less than that of the Ni-P alloy. This implied that the anodic dissolution reaction of the Ni-W-Al₂O₃ coating was restrained, which effectively decreased the corrosion sensitivity of the coated sample in NaCl solution.

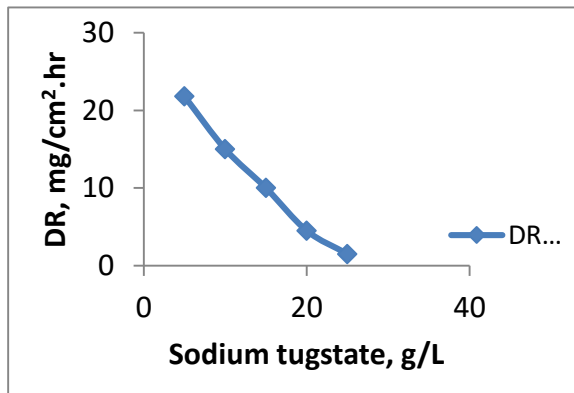


Figure 1. Effect of sodium tungstate g/L on DR from a bath containing NiSO₄.6H₂O 25g/L, Sodium hypophosphite 15g/L, Am. Sulfate 15 g/L, sodium dodecyl sulfate 0.1g/L, Succinic acid 0.3g/L, Sodium gluconate 15g/L, time 60 min, pH 9, temperature 900C.

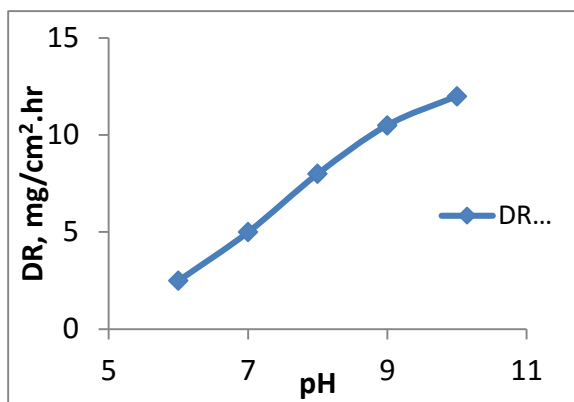


Figure 2. Effect of pH in the DR of Ni-P-W alloy from a bath containing NiSO₄.6H₂O 25g/L, Sodium hypophosphite 15g/L, sodium tungstate 15g/L, Am. Sulfate 15 g/l, sodium dodecyl sulfate 0.1g/L, Succinic acid 0.3g/L, Sodium gluconate 15g/L, time 60 min, temperature 900C.

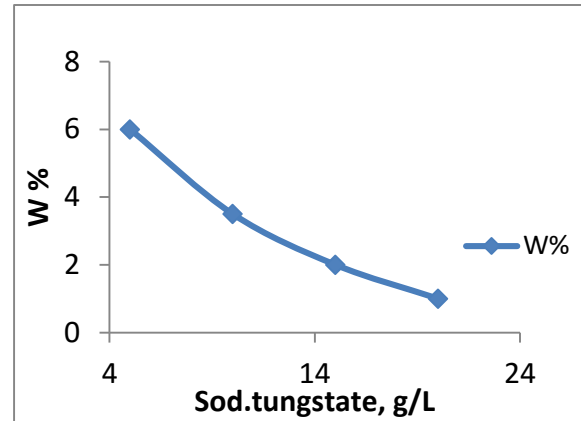


Figure 3. Effect of sodium tungstate g/L in W% in Ni-P-W alloy from a bath containing NiSO₄.6H₂O 25g/L, Sodium hypophosphite 15g/L, Am. Sulfate 15 g/L, sodium dodecyl sulfate 0.1g/L, Succinic acid 0.3g/L, Sodium gluconate 15g/L, time 60 min, pH 9, temperature 900C.

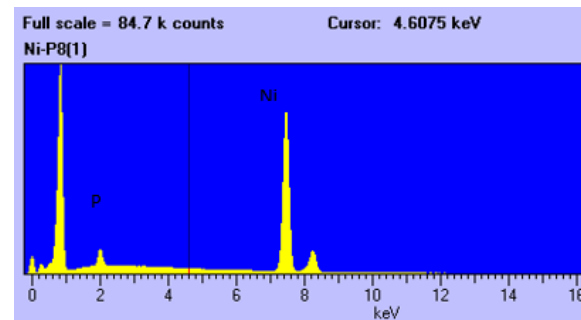


Figure 4. EDX chart of Ni88%-P12% alloy obtained from a bath containing NiSO₄.6H₂O 25g/L, Sodium hypophosphite 15g/L, Am. Sulfate 15 g/L, sodium dodecyl sulfate 0.1g/L, Succinic acid 0.3g/L, Sodium gluconate 15g/L, time 60 min, pH 9, temperature 900C.

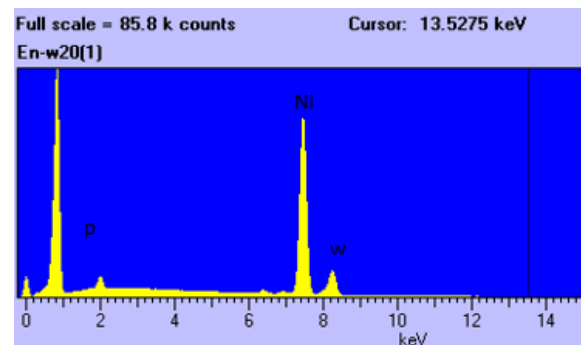


Figure 5. EDX chart of Ni91%-P3%-W6% alloy obtained from a bath containing NiSO₄.6H₂O 25g/L, Sodium hypophosphite 15g/L, sodium tungsten 5g/L, Am. Sulfate 15 g/L, sodium dodecyl

sulfate 0.1g/L, Succinic acid 0.3g/L, Sodium gluconate 15g/L, time 60 min, pH 9, temperature 900C.

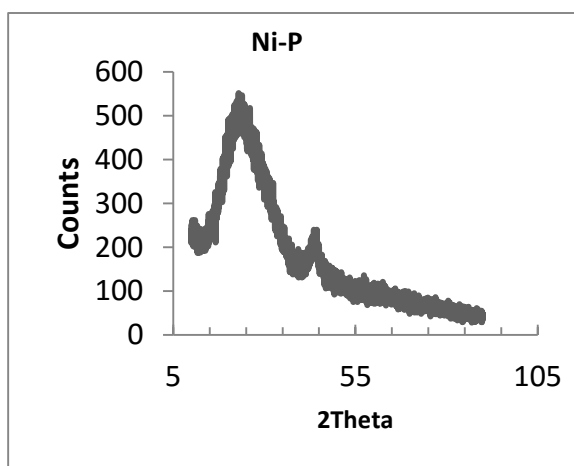


Figure 6. XRD chart of Ni-P alloy obtained from a bath containing NiSO₄.6H₂O 25g/L, Sodium hypophosphite 15g/L, Am. Sulfate 15 g/L, sodium dodecyl sulfate 0.1g/L, Succinic acid 0.3g/L, Sodium gluconate 15g/L, time 60 min, pH 9, temperature 900C.

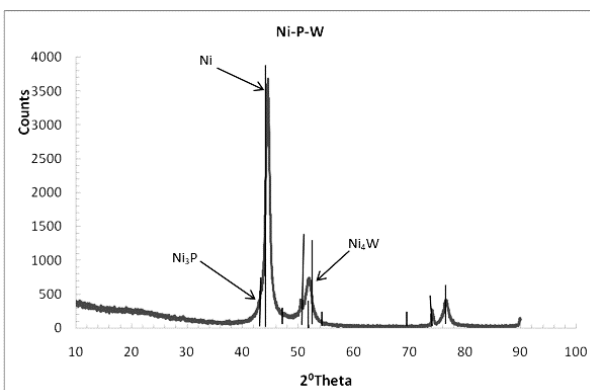


Figure 7. XRD chart of Ni91%-P3%-W6% alloy obtained from a bath containing NiSO₄.6H₂O 25g/L, Sodium hypophosphite 15g/L, sodium tungsten 5g/L, Am. Sulfate 15 g/L, sodium dodecyl sulfate 0.1g/L, Succinic acid 0.3g/L, Sodium gluconate 15g/L, time 60 min, pH 9, temperature 900C.

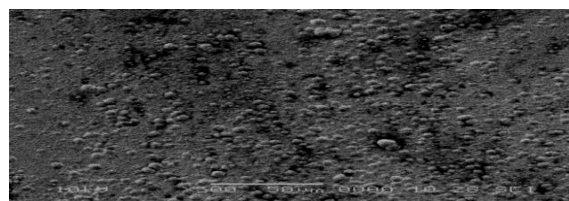


Figure 8. SEM of Ni-P alloy obtained from a bath containing NiSO₄.6H₂O 25g/L, Sodium hypophosphite 15g/L, Am. Sulfate 15 g/L, sodium dodecyl sulfate 0.1g/L, Succinic acid 0.3g/L, Sodium gluconate 15g/L, time 60 min, pH 9, temperature 900C.

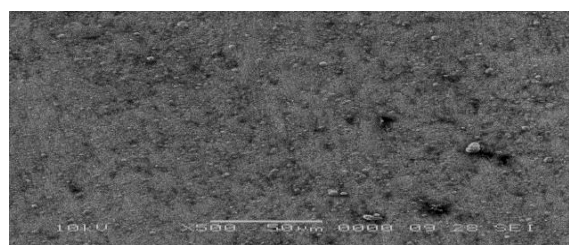


Figure 9. SEM of Ni91%-P3%-W6% alloy obtained from a bath containing NiSO₄.6H₂O 25g/L, Sodium hypophosphite 15g/L, sodium tungsten 5g/L, Am. Sulfate 15 g/L, sodium dodecyl sulfate 0.1g/L, Succinic acid 0.3g/L, Sodium gluconate 15g/L, time 60 min, pH 9, temperature 900C.

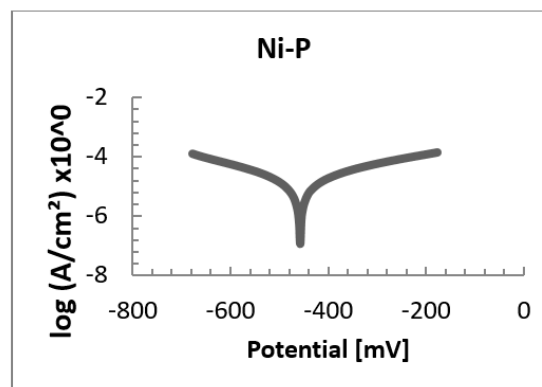


Figure 11. Corrosion behavior of Ni-P alloy obtained from a bath containing NiSO₄.6H₂O 25g/L, Sodium hypophosphite 15g/L, Am. Sulfate 15 g/L, sodium dodecyl sulfate 0.1g/L, Succinic acid 0.3g/L, Sodium gluconate 15g/L, time 60 min, pH 9, temperature 900C.

Table 4. Data of Potentiodynamic curve of Ni96-P4 alloy

E (i=0) mV	i corrosion $\mu\text{A}/\text{cm}^2$	Rp kohm.cm ²	Beta a mV/ decade	Beta c mV/ decade	Corrosion Rate $\mu\text{m}/\text{Y}$
-225	0.2848	57.64	72.74	-89.7	3.296

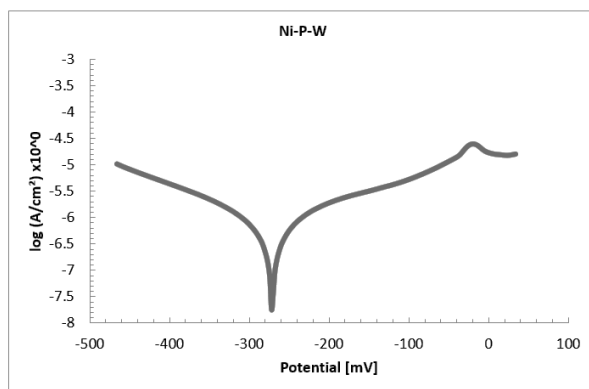


Figure 12. corrosion behavior of Ni94%-P2.5%-W3.5% alloy obtained from a bath containing NiSO₄.6H₂O 25g/L, Sodium hypophosphite 15g/L, sodium tungsten 5g/L, Am. Sulfate 15 g/L, sodium dodecyl sulfate 0.1g/L, Succinic acid 0.3g/L, Sodium gluconate 15g/L, time 60 min, pH 9, temperature 900C.

Table 5. Corrosion data of Ni94%-P2.5%-W3.5% alloy

E (i=0) mV	i corrosion $\mu\text{A}/\text{cm}^2$	Rp Kohm.cm ²	Beta a mV/ decade	Beta c mV/ decade	Corrosion rate, $\mu\text{m}/\text{Y}$
-270.0	0.224	28.015	48.984	-55.530	2.620

4. Conclusion:

At the present work Ni-P and Ni-P-W alloys were electroless plated from alkaline hypophosphite gluconate baths, the factors affected the plating conditions were studied. X-ray diffraction and SEM analysis shown that the morphological details, of as plated Ni-P coatings were greatly affected by the incorporation of W on the Ni-P matrix. Enhancement in hardness and corrosion resistance was also observed upon introducing of W on Ni-P coatings.

Corresponding Author:

M.S. Ali Eltoun, Ph.D.

Department of Chemistry, Faculty of Science, Sudan University of Science and Technology, Khartoum, Sudan.

E-mail: abotteell74@gmail.com

References

- 1- Aal, A. A., El-Sheikh, S. M., & Ahmed, Y. M. Z. (2009). Electrodeposited composite coating of Ni-W-P with nano-sized rod-and spherical-shaped SiC particles. *Materials Research Bulletin*, 44(1), 151-159.
- 2- Abd el Rehim, S. S., Sayyah, S. M., & El Deeb, M. M. (2000). Electroplating of tin from acidic gluconate baths. *Plating and surface finishing*, 87(9), 93-98.
- 3- Abd El Meguid, E. A., Abd El Rehim, S. S., & Moustafa, E. M. (1999). The electroplating of nickel from aqueous gluconate baths. *Transactions of the Institute of Metal Finishing*, 77, 188-191.
- 4- Balaraju, J. N., Anandan, C., & Rajam, K. S. (2006). Influence of codeposition of copper on the structure and morphology of electroless Ni-W-P alloys from sulphate-and chloride-based baths. *Surface and Coatings Technology*, 200(12), 3675-3681.
- 5- Balaraju, J. N., & Rajam, K. S. (2005). Electroless deposition of Ni-Cu-P, Ni-W-P and Ni-W-Cu-P alloys. *Surface and coatings technology*, 195(2), 154-161.
- 6- Balaraju, J. N., & Rajam, K. S. (2006). Influence of particle size on the microstructure, hardness and corrosion resistance of electroless Ni-P-Al 2 O 3 composite coatings. *Surface and Coatings Technology*, 200(12), 3933-3941.
- 7- Bangwei, Z., Wangyu, H., Xuanyuan, Q., Qinglong, Z., Heng, Z., & Zhaosheng, T. (1996). Preparation, formation and corrosion for Ni-WP amorphous alloys by electroless plating. *Transactions of the Institute of Metal Finishing*, 74, 69-71.
- 8- Brenner, A. (1963), Electrodeposition of Alloys. Principle and practice, *Academic Press*, New York, pp 345.
- 9- de Hazan, Y., Werner, D., Z'graggen, M., Groteklaes, M., & Graule, T. (2008). Homogeneous Ni-P/Al 2 O 3 nanocomposite coatings from stable dispersions in electroless nickel baths. *Journal of colloid and interface science*, 328(1), 103-109.
- 10- Du, N., & Pritzker, M. (2003). Investigation of electroless plating of Ni-W-P alloy films. *Journal of applied electrochemistry*, 33(11), 1001-1009.
- 11- El Rehim, S. A., Sayyah, S. M., & El Deeb, M. M. (2000). Electroplating of copper films on steel substrates from acidic gluconate baths. *Applied Surface Science*, 165(4), 249-254.

- 12- Hamdy, A. S., Shoeib, M. A., Hady, H., & Salam, O. A. (2008). Electroless deposition of ternary Ni–P alloy coatings containing tungsten or nano-scattered alumina composite on steel. *Journal of applied electrochemistry*, 38(3), 385-394.
- 13- Hu, Y. J., Wang, T. X., Meng, J. L., & Rao, Q. Y. (2006). Structure and phase transformation behaviour of electroless Ni–W–P on aluminium alloy. *Surface and Coatings Technology*, 201(3), 988-992.
- 14- Jin, Y., Fan, J., Mou, K., Wang, X., Ding, Q., Li, Y., & Liu, C. (2010). Structural and phase transformation behaviour of electroless Ni–W–Cr–P alloy coatings on stainless steel. *Inorganic Materials*, 46(6), 631-638.
- 15- Lu, G., & Zangari, G. (2002). Corrosion resistance of ternary Ni–P based alloys in sulfuric acid solutions. *Electrochimica Acta*, 47(18), 2969-2979.
- 16- Pearlstein, F., Weightman, R., & Wick, R. (1963). Nickel-Tungsten electroless deposition. *Metal Finishing*, 61, 77.
- 17- Rashwan, S. M., Mohammed, A. E., El Wahaab, S. A., & Kamel, M. M. (2000). Mansoura Science Bulletin A. *Chemistry*, 27, 121.
- 18- Szczygieł, B., & Turkiewicz, A. (2008). The effect of suspension bath composition on the composition, topography and structure of electrolessly deposited composite four-component Ni–W–P–ZrO₂ coatings. *Applied Surface Science*, 254(22), 7410-7416.
- 19- Tien, S. K., Duh, J. G., & Chen, Y. I. (2004). Structure, thermal stability and mechanical properties of electroless Ni–P–W alloy coatings during cycle test. *Surface and Coatings Technology*, 177, 532-536.

Received January 13, 2016; revised January 15, 2016; accepted January 15, 2016; published online February 1, 2016.



STRESS & AUTOIMMUNE DISEASES

Hala L. Fayed

Rheumatology & Rehabilitation Department, Kasr Al Ainy School of Medicine, Cairo University, Egypt
halafayed@yahoo.com

Abstract: Incidences of autoimmune diseases are rising; the numbers of cases are tripled over the last few decades. There are more than eighty illnesses caused by autoimmunity. It has been estimated that autoimmune diseases are among the ten leading causes of death among women in all age groups up to 65 years. The etiology of autoimmune diseases is multifactorial: Genetic, hormonal, environmental, immunological factors, together with host susceptibility are all considered important in their development. The cause of this worldwide epidemic lies primarily in our environment and the toxic world in which we live, as various stressors have been implicated in the induction and perpetuation of many autoimmune diseases. Various stressors including physical, chemical, biological, and psychological have been shown to be responsible for this growing epidemic. Understanding the pathogenic modes of actions of various stressors e.g. molecular mimicry, role of cytokines, Toll-like receptors signaling pathways, role of stress proteins (heat shock proteins), role of reactive species, in addition to neuroendocrine immune systems interactions foster the advent in targeted therapeutic era. New strategies have been introduced and are being studied to overcome effects of oxidative stress at the cellular level for subsequent use as new therapies for autoimmune diseases e.g. targeting intracellular signaling pathways for various proinflammatory cytokines, DNA vaccines, anti-inflammatory neuropeptides, and more. The better understanding of these etiopathogenetic mechanisms can move us from the era of controlling or treating autoimmune diseases to a new era of preventing these diseases.

To cite this article

[Fayed, H. L. (2016). Stress & Autoimmune Diseases. *J. Middle East North Afr. sci*, 2(2), 25-33]. (p-ISSN 2412-9763) - (e-ISSN 2412-8937). <http://www.jomenas.org>. 3

Keywords: Autoimmune disease; Stress; Immune System; Autoimmune disorders.

1. Introduction

Autoimmune Disease (AIDx) is a condition in which the body immune system recognizes and attacks host tissues causing tissue destruction. It results from failure to sustain tolerance to self-molecules, i.e. a state of loss of immune tolerance (Bolon, 2012). It occurs when a self-antigen induces a specific adaptive immune response which the body cannot eliminate entirely, leading to chronic inflammation and tissue damage. Dozens of AIDx involving one or multiple organ systems afflict 3% or more of people worldwide (>75% women). It has been estimated that autoimmune diseases are among the ten leading causes of death among women in all age groups up to 65 years.

The etiology of autoimmune diseases is multifactorial; genetic, hormonal, environmental, immunological factors, together with host susceptibility are all considered important in their development (Ecrolini & Miller, 2009).

Genetic Factors: Many genes--over 20 different ones, each of which showed a small effect in contribution to susceptibility to autoimmune inflammatory diseases. However, genetic predisposition is only a minor risk factor; Low concordance rates were observed in monozygotic twins. In addition, geographic distribution was an additional risk factor for disease risk.

Hormonal Factors: Neuroendocrine hormones triggered during stress may lead to immune dysregulation, altered or amplified cytokine production, resulting in impaired host defense and autoimmune diseases. Blunting of the brain hormonal stress response is an important contributor to the development of autoimmune diseases. The reason for this is that chronic stress leads to impaired limbic-hypothalamic-pituitary-adrenal axis (LHPA) with reduced secretion of cortisol (this potent anti-inflammatory hormone that is released from the adrenal glands in response to stress); The LHPA axis becomes less responsive to stress potentially resulting



in an impaired capacity to cope with stressors. Several autoimmune diseases are mediated by neuroendocrine-immune (NEI) network dysregulation, including autoimmune rheumatic diseases: rheumatoid arthritis, systemic lupus erythematosus, Sjögren's syndrome, as well as other autoimmune inflammatory diseases: Atherosclerosis, Graves' disease, type-I diabetes mellitus, among others (Butts & Sternberg, 2008).

Immunologic Factors: Autoreactive T cells i.e. reduced deletion or enhanced activation of autoreactive CD4+ T-helper (Th) lymphocytes; Defective immunomodulation by CD4+ regulatory (Treg) and CD8+ suppressor (Ts) T-lymphocytes; Autoreactive B cells & autoantibody production; Cytokine dysregulation i.e. dysregulated signaling (leading to a relative increase in pro-inflammatory cytokines); Role of complement.

Therefore, there were questions:

- 1) What is the cause of this growing epidemic?
- 2) Why is this number of cases tripled over the last few decades?
- 3) How does the toxic world in which we live cause the rates of autoimmune diseases to overshoot?

Top scientists in this field agree that the cause of this epidemic (which is worldwide) lies primarily in our environment, and in all the toxins, industrial fumes, heavy metals, chemicals, pesticides, infectious agents, as well as increasing psychological stress with long working hours, sleep deprivation, and unhealthy dieting and lifestyle

Stress is a stimulus or a succession of stimuli tending to disrupt the homeostasis of an organism. It is the response of the brain to unpleasant events. It is a ubiquitous and unavoidable experience of daily life, whether it arises from the external environment or from within the body (Butts & Sternberg, 2008).

Stimuli acting as potential stressors are numerous, and include: physical stressors, chemical stressors, biological stressors, and psychological stressors. Over 1,400 physical and chemical reactions in conjunction with greater than 30 hormones and neurotransmitters are involved in body's stress response.

In recent years, much has been learned about the effect of various stressors on the immune function, and the role of the stress response in various autoimmune diseases. A large number of potential stressors have been implicated in the development of autoimmune disease (Cataldi, 2010).

4) How stress can cause or worsen disease?

5) How understanding the cross-talks between the brain and the immune system can help us structure our lives to help us heal?

Many retrospective studies found that a high proportion (up to 80%) of patients reported uncommon stress (physical, mental, emotional ...etc.) before disease onset. Not only does stress cause disease, but the disease itself also causes significant stress in the patients, creating a vicious cycle. Thus, different stress reactions should be discussed with autoimmune patients, and obligatory questionnaires about trigger factors should include inquiries about common triggers; infection, trauma, psychological stress...etc. (Stojanovich & Marisavljevich, 2008).

Physical Stress: Various physical agents that may act as potential stressor include: Ionizing radiation, Non-physiological oxygen levels (hypoxia, hyperoxia), Ultraviolet rays (UVR), Heat exposure, strenuous physical activity and over exhaustion

Chemical Stress: Several environmental and occupational chemical exposures are considered as triggers for autoimmunity, including: Silica dust and lupus, use of permanent hair dyes in women was associated with a borderline increase in the risk of developing Systemic Lupus Erythematosus (SLE) in the CLU study (Cooper et al, 2001), Vinyl chloride and organic solvents in scleroderma, Mercury, gold or perchloroethylene in autoimmune kidney disease, and Polybrominated biphenyls in autoimmune thyroid disease.

Environmental chemicals may also contribute to autoimmune liver disease: non-alcoholic steatohepatitis/ NASH). Not only foreign chemicals and agents have been associated with induction of autoimmunity, but also an intrinsic hormonal exposure, such as estrogens, which might explain the sexual dimorphism in autoimmunity. Better understanding of these environmental risk factors will likely lead to an explanation of the mechanisms of onset and progression of autoimmune diseases and may lead to effective preventive involvement in specific high-risk groups.

Psychological Stress: continued psychological stress (mental or emotional) can compromise brain function with impaired concentration, memory, and learning. It can damage the hippocampus responsible for pain predisposing to chronic pain & fatigue syndromes. It can result in immune dysfunction that results in autoimmune disease after frequent activation of the autonomic nervous system in the case of chronic stresses. Associations between psychological stress (mental or emotional stress) and depressive disorders as well as autoimmune disease have been established.



Many reviews discuss the possible role of psychological stress, and the major stress-related hormones, in the pathogenesis of various autoimmune diseases, and presume that the stress-triggered neuroendocrine hormones lead to immune dysregulation, which ultimately results in autoimmune disease by altering or amplifying cytokine production (Slavich & Irwin 2014; Stojanovich & Marisavljevic, 2008).

A retrospective cohort study of 15,357 adults has examined the effect of cumulative childhood stress and increased risk of developing autoimmune diseases in adults. Adverse Childhood Experiences (ACEs) included childhood physical, emotional, or sexual abuse, witnessing domestic violence, mental illness, or parental divorce.

The outcome was hospitalizations for any of 21 selected autoimmune diseases. Sixty-four percent (64%) reported at least one ACE.

First hospitalization for any autoimmune disease increased with increasing number of ACEs ($p < 0.05$). Persons with >2 ACEs compared to those with no ACEs showed a 70% increased risk for hospitalizations with Th1, 80% increased risk for Th2, and 100% increased risk for rheumatic diseases ($p < 0.05$).

This study concluded that childhood traumatic stresses increased the likelihood of hospitalization with a diagnosed autoimmune disease decades into adulthood. These findings are consistent with recent biological studies on the impact of early life stresses on subsequent inflammatory responses (Dube, 2009).

Biological Stress: Infectious agents and/or their products have been implicated in the pathogenesis of autoimmune diseases. Chronic bacterial and viral infections are associated with a variety of autoimmune diseases involving chronic inflammation, including rheumatic conditions as well as chronic fatigue syndromes. Possible mechanisms of bacterial & viral involvement as etiological agents or in the exacerbation of these diseases have been investigated intensively. An auto-regulatory loop might exist in the interaction of bacteria with the host and in pathogenic signal processing. These studies reveal potential therapeutic targets (Sherbet, 2009).

Evidence of various *Mycoplasma* species infections has been strongly associated with Rheumatoid Arthritis (RA); there is often systemic infection of more than one species. *Mycoplasma* antigens induce both cell-mediated and humoral immune responses. Besides, *H. influenzae*, *Bordetella*, *Yersinia*, *Chlamydia pneumoniae*, *Borrelia burgdorferi*, *Proteus mirabilis*, & staphylococcal enterotoxins A & B represent possible infecting organisms as well.

Bacterial infections associated with other autoimmune conditions: Demyelinating diseases as Multiple sclerosis (MS), Landry-Guillain-Barre (LGB) syndrome ...are possibly a consequence of autoimmune condition or infection by viral or bacterial agents with the resultant development of demyelinating plaques. LGB syndrome has been associated with *Mycoplasma pneumoniae*, *Campylobacter jejuni* & *Haemophilus influenzae* infection. Moreover, serology and PCR have provided ample evidence of *Chlamydia pneumoniae*, *Borrelia burgdorferi*, and *Mycoplasma* species, among others in MS, ALS, Alzheimer's and Parkinson's disease.

A tentative relationship between MS and streptococcal infection has been suggested (Sherbet, 2009; Casserly et al., 2007). Possible modes of pathogenic action of bacteria: the role of cytokines, Toll-like receptor signaling, interaction of heat shock proteins with the immune system, and role of reactive oxygen & nitrogen species (ROS/RNS)

Viral Infection: Various viral infections are sometimes associated with the initiation or exacerbation of autoimmune diseases. Viruses like Epstein-Barr virus (EBV), parvovirus, cytomegalovirus, rotavirus, coxsackie B-1, hepatitis B & C virus, rubella, human herpesvirus-1, -6 and -7 and other viral infections showed association with several autoimmune diseases. EBV is known as an infamous viral agent that can encourage the initiation and perpetuation of different autoimmune diseases; systemic lupus erythematosus, Sjögren's syndrome, multiple sclerosis, autoimmune thyroiditis, autoimmune hepatitis, and Kawasaki disease. Virus-like inclusions were found in the renal biopsy tissue of SLE patients. Various viral infections have been implicated in Type-I diabetes as well (Barzilai et al., 2007).

Possible modes of pathogenic action of viruses: Molecular mimicry between Epstein-Barr virus and human antigens: The involvement of HLA antigens in the pathogenesis of various autoimmune diseases has been suggested to be due to the molecular similarities between certain bacterial or viral antigens and HLA or other human antigens.

Viral persistence: Evidence that the human microbiota accumulates during a lifetime, and a variety of persistence mechanisms are coming to light. In one model, obstruction of VDR nuclear-receptor-transcription prevents the innate immune system from making key antimicrobials, allowing the microbes to persist. Genes from these microbes must necessarily impact disease progression. Recent efforts to decrease this VDR-perverting microbiota in patients with autoimmune disease have resulted in reversal of autoimmune processes. As the NIH Human Microbiome Project continues to better

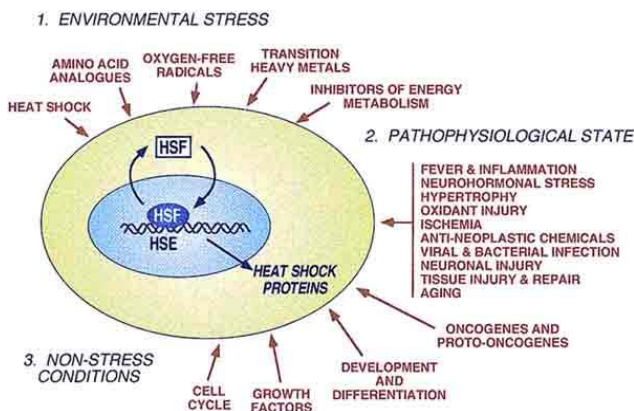
characterize the human metagenome, new insights into autoimmune pathogenesis are beginning to emerge (Proal et al., 2009).

Autoreactive T & B cells creating immortal cells by loss of apoptosis, production of autoantibodies, and role of cytokines: There is strong evidence that bacterial and viral antigens induce the synthesis of many pro-inflammatory cytokines with consequent implication in a wide range of autoimmune diseases.

Induction of Toll-like receptor (TLR) signaling: TLRs are transmembrane receptors that represent the first line of defense against microbial antigens, and can activate immune cell responses. They can recognize pathogen-associated molecular patterns (PAMPs) of infectious agents, including LPS, viral RNA, and unmethylated CpG-oligonucleotides. Exposure of cells to LPS or other toxins induces TLR signaling mechanisms with expression of different pro-inflammatory interleukins and interferons.

Phosphatidyl inositol-3-kinase (PI3K) is thought to participate in the TLR signaling pathway. PI3K activation is commonly observed after stimulation with various TLR ligands. The resultant activation of serine-threonine protein kinase Akt leads to increased expression of various proinflammatory cytokines including IL-12 & TNF. This provides a novel therapeutic approach (Hazeki et al., 2007).

Role of Heat-shock proteins (stress proteins):



6) What are Heat-Shock Proteins (HSPs)?

HSPs are a group of proteins that are present in all cells in all life forms, but are mostly known as stress proteins because their expression is increased when the cells undergo various types of environmental stresses.

They have a variety of functions for monitoring cell's proteins: Help new or distorted proteins fold into their correct shape, which essential for their

function, act as 'chaperones,' is ensuring that the cell's proteins are in the right conformations and in the right place at the right time, transport old proteins to removal areas inside the cell, shuttle proteins from one compartment to another inside the cell (cell trafficking), play a role in the presentation of specific proteins sites or peptides to the cell surface to help the immune system recognize diseased cells.

Although HSPs represent an important initial line of defense against various stressors, they may represent immune-dominant antigens/ autoantigens that are presented to T cells bearing gamma delta receptors.

They have the ability to influence both innate and adaptive immune responses inducing the expression of various interleukins contributing to autoimmune disease. A growing body of evidence suggests that auto-reactivity in chronic inflammatory arthritis involves gamma delta cells, which recognize epitopes of the stress proteins. This supports the notion that HSPs actually play a role in autoimmune processes.

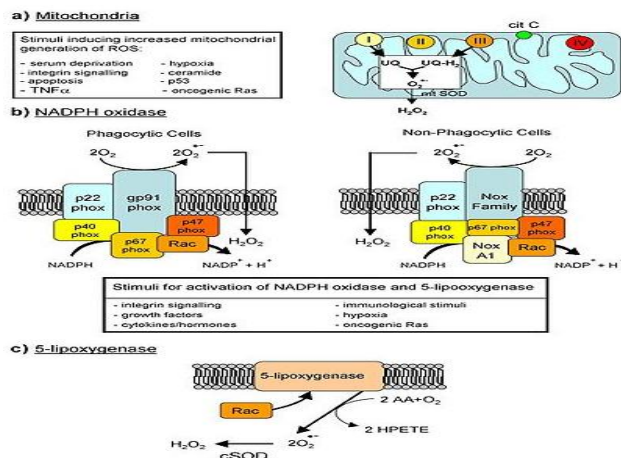
Alternate mechanisms for T cell stimulation by stress proteins is molecular mimicry of the DR susceptibility locus for RA by a stress protein epitope in gram-negative bacteria. The capacity of certain stress proteins to bind to multiple proteins in the nucleus and cytoplasm both physiologically and during stress or injury to cells, suggests that stress proteins may be important elements in the "immunogenic particle" concept of the origin of autoantibodies. Autoantibodies to a number of stress proteins have been identified in RA, AS, & SLE (Sherbet, 2009).

Role of Reactive Species (RS): Reactive Oxygen Species (ROS) and Reactive Nitrogen Species (RNS), e.g. nitric oxide, [NO] are "two-faced" products. They are well recognized for playing a dual role as both beneficial and deleterious species. ROS and RNS are normally generated by tightly regulated enzymes; NADPH oxidase and NOS, respectively. Many of ROS-mediated responses protect cells against oxidative stress and maintain "redox homeostasis".

Beneficial effects of ROS/RNS e.g. superoxide radical & nitric oxide occur at low/moderate concentrations where they act as molecular signals that regulate a series of physiological processes: Defense against infectious agents, Maintenance of vascular tone, Control of ventilation, Erythropoietin production, Cellular signaling pathways in various physiological processes, Induction of a mitogenic response (Coaccioli et al., 2010).

Normally in the organism, damage by ROS is counteracted with natural antioxidants: Enzymatic antioxidants: glutathione peroxidases, superoxide

dismutase (Cu-Zn SOD, Mn SOD), and catalase. Non-enzymatic antioxidants: thiol antioxidants (glutathione, thioredoxin), ubiquinol, uric acid, essential minerals (selenium, molybdenum,..) carotenoids, vitamin C, vitamin E (tocopherol), and flavonoids (Valko et al., 2007).



Reactive Oxygen Species (ROS):

Overproduction of ROS can be induced by various endogenous and exogenous factors and results in oxidative stress; a deleterious process that can be an important mediator of damage to cell structures, including lipids & membranes, proteins and DNA.

ROS act as second messenger by activating p38 mitogen-activated protein kinase (MAPK), activator protein-1 (AP-1), Nuclear Factor Kappa B (NFkB) with subsequent activation of transcription factors involved in the inflammatory cascade (Valko et al., 2006).

This redox imbalance can initiate a wide range of toxic oxidative reactions in the cell including: Initiation of lipid peroxidation, Oxidations of amino acids in proteins, direct inhibition of mitochondrial respiratory chain enzymes, Inactivation of specific enzymes by oxidation of co-factors, Inhibition of membrane sodium/potassium ATPase activity, Inactivation of membrane sodium channels, Damage of DNA, Oxidative cellular stress induced by environmental factors, such as cigarette smoke, UV or ionizing radiation, bacterial or viral infection, or any number of oxidizing xenobiotic compounds, triggers a wide range of pro inflammatory cellular responses. ROS are capable of initiating DNA single strand breakage, with subsequent activation of the nuclear enzyme Poly ADP Ribose Synthase (PARS), leading to eventual severe energy depletion of the cells, and necrotic-type cell death.

Excessive increase in Reactive Species (RS) production has been implicated in the pathogenesis of various autoimmune, demyelinating, and chronic

inflammatory disorders: atherosclerosis, cardiovascular diseases, hypertension, diabetes mellitus, RA, ischemia/reperfusion injury, and ageing by activating specific signaling pathways which lead to transcription of genes involved in production of proinflammatory cytokines and other inflammatory mediators hence perpetuating the inflammatory cascade (Moroni et al., 2010).

Various studies have evaluated the oxidative stress in various autoimmune rheumatic diseases; RA, SLE, APS, PsA as well as other autoimmune diseases, and found significantly higher levels of Serum Hydroperoxide Concentration (SHC) with significant reduction in Total Antioxidant Capacity (TAC) and Thiolic Capacity (TC), concluding etiopathogenic role for RS in these diseases (Coaccioli et al., 2010; Moroni et al., 2010)

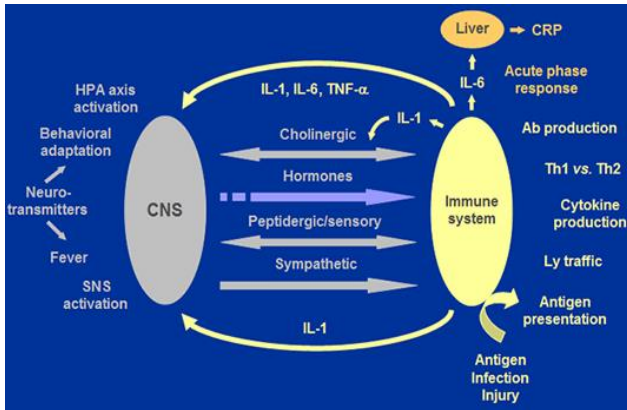
Reactive Nitrogen Species (RNS): Nitric oxide (NO) is synthesized from L-arginine by the enzyme nitric oxide synthase (NOS). Two constitutive NOS isoforms [endothelial NOS (eNOS) and neuronal NOS (nNOS)] are formed and play important roles in the regulation of vascular tone and homeostasis. Cytokine-inducible NOS (iNOS) generates excessive amounts of NO. This is required for bacterial clearance during infection. The general and overall effects would be bactericidal /cytotoxic in nature. iNOS exerts deleterious effects and has been implicated in the pathogenesis of a number of autoimmune, inflammatory, neurodegenerative diseases: RA, SLE, MS among others; all show associated synthesis of NO and their toxic products. Up-regulation of the iNOS has an important role in the expression of pro-inflammatory mediators in inflammation, and can be responsible for sustained inflammation, and as a cytotoxic molecule with a pivotal role in apoptosis at the joints of RA patients (Predonzani et al., 2015).

Neuro - Endocrine - Immune System Interactions: Inflammatory responses are modulated by a bidirectional communication between the Neuro-Endocrine System (NES) & Immune System (IS). Many lines of research have established the numerous routes by which the Immune System (IS) and the Central Nervous System (CNS) communicate.

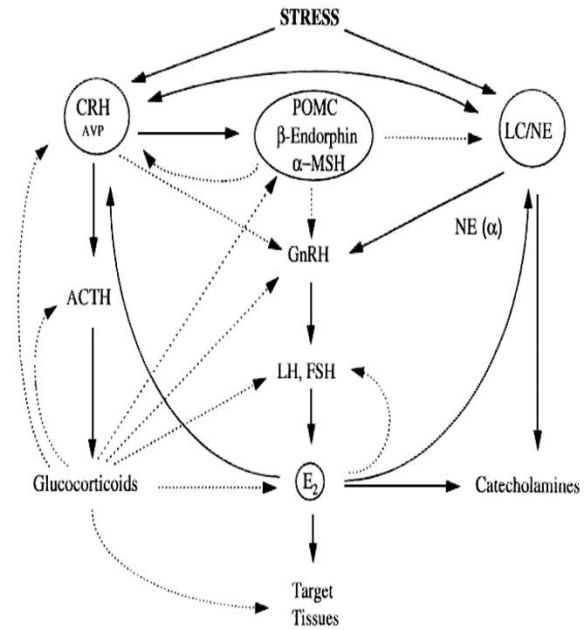
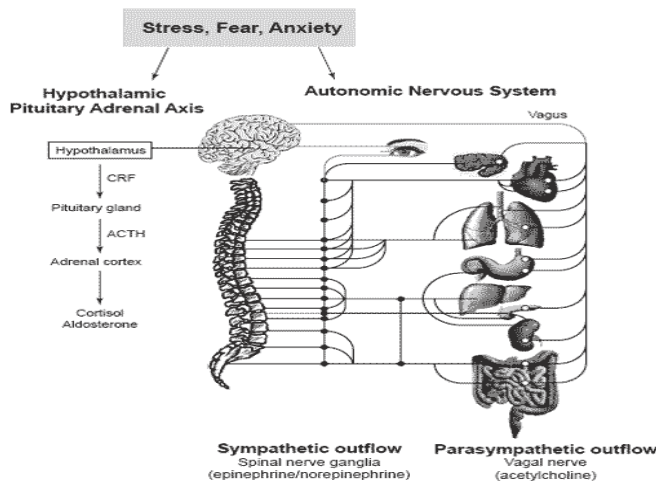
The immune system signals the Central Nervous System (CNS) through immune mediators and cytokines that can cross the blood-brain barrier, or signal indirectly through the vagus nerve or second messengers. The CNS signals the immune system through hormonal pathways, including the Limbic - Hypothalamic - Pituitary - Adrenal axis (LHPA) and the hormones of the neuroendocrine stress response, and through neuronal pathways, including the Autonomic Nervous System (ANS). Interactions between the CNS and IS play an important role in

modulating host susceptibility or resistance to inflammatory diseases.

NES produces neuropeptides and hormones which can modulate the activity of the immune system. It also secretes proinflammatory cytokines (IL-1 β , IL-6, & TNF α). On the other hand, the IS produces cytokines, which can modulate the neuroendocrine system. It produces neuropeptides (CRH, ACTH, AVP, POMC, PRL, & GH). Therefore, both systems can modulate the activity of one another (Marques-Deak et al., 2005).

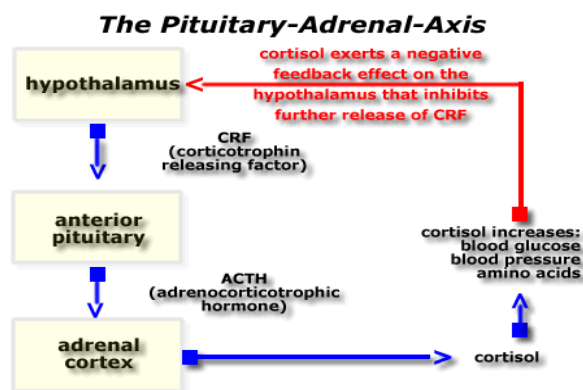


Adaptive response to various stress stimuli involves activation of: Limbic-Hypothalamus-Pituitary-Adrenal (LHPA) axis and Sympathetic autonomic nervous system (SANS).



The Limbic-Hypothalamus-Pituitary-Adrenal (LHPA) axis: Whenever a person is subjected to acute stress, whether an internal or external stressor, the limbic system of the brain triggers the hypothalamus to secrete Corticotropin-Releasing Hormone (CRH). In the hypothalamus, cytokines (IL-1 β , IL-6, & TNF α) activate the production of CRH & AVP which are stimulatory factors for adrenocorticotrophic hormone (ACTH) release in the pituitary gland, and consequent cortisol production in the adrenal cortex. Cortisol will in turn inhibit the production of CRH & AVP in the hypothalamus as well as ACTH in the pituitary gland. The released glucocorticoids have anti-inflammatory and immunomodulatory effect, causing a shift in patterns of cytokine production from a TH1- to a TH2-type pattern.

When cortisol blood levels become excessive, this turns off CRH release in a negative feedback loop. CRH also stimulates the production of a pituitary-derived cytokine: Macrophage Migration Inhibitory Factor (MIF) which counteracts the immunosuppressive effects of cortisol on T cells and macrophages with consequent production of IL-1 β , TNF α , IL-6 promoting inflammatory response. Moreover, local production of CRH, AVP, & PRL has shown to contribute to chronic inflammation (Eskandari et al., 2003).



Sympathetic Autonomic Nervous System (SANS): Sympathetic noradrenergic and peptidergic fibers innervate lymphoid organs. This provides an additional physical link to neural modulation of the immune response. Neutrophils, macrophages, Natural killer cells, T & B lymphocytes were found to express adrenergic receptors on their surfaces.

Acute stress: If the stresses in our life are only occasional, and we take adequate time for rest, relaxation and sleep to restore LHPA equilibrium, then occasional stress cortisol release will not be a problem, i.e. some cortisol is essential for life.

Excessive stress: When the body is subject to excessive stress that exceeds the body capability of healing, circumstances of stress, overcome the negative feedback regulation of the LHPA axis, together with SNS overstimulation with excessive production of stress hormones (cortisol, epinephrine & norepinephrine), i.e. excessive cortisol is equally damaging.

Chronic stress: Prolonged unresolved stress can result in defective LHPA axis response which can be one of the factors responsible for a shift from acute to chronic phase of inflammation, and can be an important contributor to the development of various autoimmune diseases. As a consequence of this LHPA axis dysfunction, there is a lower diurnal cortisol level in RA patients, and lower cortisol response to surgical stress.

Many autoimmune diseases and disease states of chronic inflammation are accompanied by alterations in the complex interactions between the endocrine, nervous and immune systems (Silverman & Sternberg, 2008).

Thus, treatment of autoimmune diseases needs multidisciplinary care interventions that target patients' disease symptoms and help them cope with their illness; it should include stress management and behavioral intervention to prevent stress-related immune imbalance (Stojanovich & Marisavijevich, 2008).

In an ideal world, we would make lifelong stress management an integral part of our daily life. We would: Sleep eight to nine hours nightly, Take relaxing breaks during the day, Take frequent mini-vacations from work to restore LHPA & SANS equilibrium, Utilize stress reduction techniques such as meditation, quiet prayer, massage, relaxation techniques...etc., Have regular aerobic exercise: take brisk 30-to-60-minute walks daily in the open air, Live in quiet homes without chronic noise stress from loud TVs, stereos, traffic...etc., Follow healthy eating habits: Eat only nutritious foods: fresh fruits & vegetables, fish, poultry, whole grain, and low fat, take a multivitamin supplement daily to boost the immune system, our air and water should be clean, Avoid tobacco, alcohol, Avoid stimulants such as pseudoephedrine, Avoid chemical stressors such as heavy metals: lead, mercury, pesticides..... Etc., and pharmacologic management of anxiety.

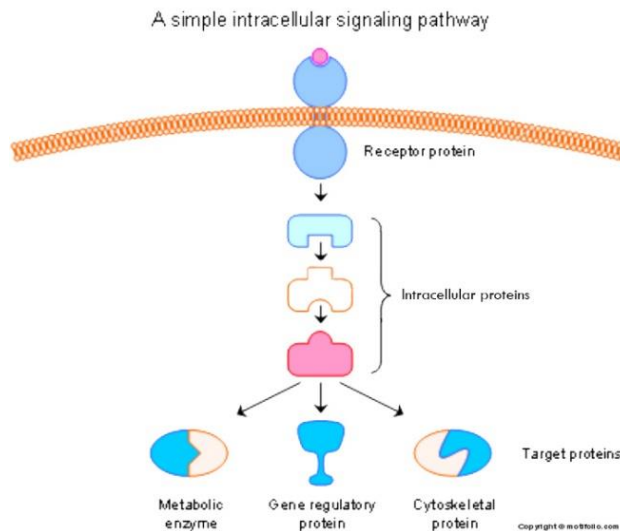
Antioxidants: Antioxidants can help reduce the oxidative damage to our cells by capturing damaging free radicals: Vitamin A, C, and E (tocopherol) supplements. Trace elements: Cu, Zn, Mn, Se, molybdenum. Pharmacological preparations that provide the proper nutrients needed to promote the body's own ability to manufacture and absorb glutathione (GSH). The depletion of glutathione and the cofactors to recycle glutathione between its oxidized and reduced states may play a key role in the loss of self and chemical tolerance. There is some evidence that glutathione depletion activates iNOS which in turn promotes T lymphocyte activation i.e. increased iNOS activity promotes lymphocyte activation. Inducible NO synthase (iNOS) can be expressed in macrophages and is able to induce NO production. Ultimately, Treg failure and barrier breakdown. Others supports the production and function of superoxide dismutase (SOD) and catalase (CAT); two vital antioxidants produced by the body to fight the potent free radical superoxide.

Flavonoids: Evidence suggests that flavonoids have potential neuroprotective effects controlling neuro-inflammatory processes contributing to the cascade of events culminating in the neuronal damage in neurodegenerative disorders; Parkinson's and Alzheimer's disease. They have been shown to be highly effective in preventing age-related cognitive decline and neurodegeneration, and that they may express such ability through a multitude of physiological functions, including an ability to modulate the brain's immune system. They also show potential to inhibit neuro-inflammation through an attenuation of microglial activation and associated cytokine release, iNOS expression, nitric oxide production and NADPH oxidase activity.

Current evidence indicates that the regulation of these immune events appear to be mediated by their actions on intracellular signaling pathways, including the nuclear factor- κ B (NF- κ B) cascade and mitogen-activated protein kinase (MAPK) pathway.

Novel Therapeutic Targets: Advances in our understanding of the cellular and molecular mechanisms in rheumatic disease fostered the advent of targeted therapeutics era: Targeting stress proteins /Heat Shock Proteins (HSPs), anti-inflammatory neuropeptides/ neuro-hormones, Inhibitors of iNOS, and inhibitors of intracellular cell signaling pathways e.g. p38 MAPK (mitogen-activated protein kinase), ERK (extra-cellular regulating kinase), JNK (c-Jun-N-terminal kinase), Phosphatidylinositol 3-kinases (PI3K) Jak-Stat (Janus kinase & signal transducer & activator of transcription).

Controlling Cell Signaling: Every cell in an organism is exposed to hundreds of different signals from its environment. The cell can respond to these signals in a variety of ways, and does so independently. However, all of these independent actions come together in a very complex and interconnected pathway of communication that governs basic cellular activities and coordinates cell actions. The ability of cells to perceive and correctly respond to their microenvironment is the basis of development, tissue repair, and immunity as well as normal tissue homeostasis. Errors in cellular information processing can be responsible for diseases such as cancer, autoimmunity, and diabetes. By understanding the fundamentals of cell signaling, researchers hope to be able to develop new drugs and treat them selectively and effectively. As intracellular signaling pathways transmit environmental information to the cytoplasm and subsequently to the nucleus, where they regulate cellular responses and gene transcription and as various intracellular signaling pathways are involved in the initiation & persistence of inflammation, Small molecules can be designed to block intracellular enzymes that control these cell signaling pathways, hence abolishing related effects of inflammation & tissue damage.



Targeting Stress Protein /Heat Shock Proteins:

Targeting stress proteins through the engineering of DNA vaccines containing the heat-shock protein gene from mycobacteria in order to intervene in autoimmune processes. Instrumental HSPs include HSP 90, 70, 65, 60, 40 and 27 (Santos et al., 2009).

Anti-Inflammatory Neuropeptides: Resolution of inflammation and re-establishment of immune homeostasis and maintenance of tolerance: Vasoactive intestinal peptide (VIP), Urocortin (UC), Adrenomedullin (AM), Alpha melanocyte stimulating hormone (α MSH), Cortistatin, and Ghrelin (Delgado & Ganea, 2008).

iNOS inhibitors: Recently it has been demonstrated that treatment with NG-monomethyl L-arginine (L-NMMA); an inducible Nitric Oxide Synthase (iNOS) inhibitor prevents the activation of Poly ADP Ribose Synthase (PARS), and prevents the organ injury associated with inflammation. It has been shown to reduce urinary markers of systemic oxidant stress in proliferative lupus nephritis.

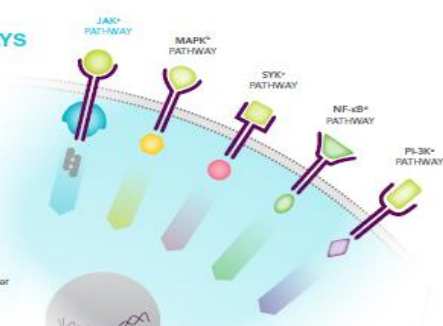
2. Conclusion:

To sum up, with more understanding of the etiology and trigger factors of autoimmune and chronic inflammatory diseases, as well as different pathogenetic mechanisms more therapeutic targets can be identified that can offer novel treatments or even preventive measures for the rising epidemic of autoimmune and chronic inflammatory diseases. With continuous serious efforts in the field the best is yet to come.

INTRACELLULAR SIGNALING PATHWAYS

Intracellular pathways offer many options for inhibition of cytokine signaling²

- JAK pathways are one of several intracellular hubs in the inflammatory cytokine network²



¹ Janus kinase.
² Mitogen-activated protein kinase.
³ Signal tyrosine kinase.
⁴ Nuclear factor kappa-light-chain-enhancer of activated B cells.
⁵ Phosphoinositide 3-kinase.

Corresponding Author:

Hala L. Fayed, MSc, MD.

Rheumatology & Rehabilitation Department, Kasr Al Ainy School of Medicine, Cairo University, Egypt.

E-mail: halafayed@yahoo.com**References**

- 1- Barzilai, O., Sherer, Y., Ram, M., Izhaky, D., Anaya, J. M., & Shoenfeld, Y. (2007). Epstein-Barr virus and cytomegalovirus in autoimmune diseases. *Annals of the New York Academy of Sciences*, 1108(1), 567-577.
- 2- Bolon, B. (2012). Cellular and molecular mechanisms of autoimmune disease. *Toxicologic pathology*, 40(2), 216-229.
- 3- Butts, C. L., & Sternberg, E. M. (2008). Neuroendocrine factors alter host defense by modulating immune function. *Cellular immunology*, 252(1), 7-15.
- 4- Casserly, G., Barry, T., Tourtellotte, W. W., & Hogan, E. L. (2007). Absence of Mycoplasma-specific DNA sequence in brain, blood and CSF of patients with multiple sclerosis (MS): A study by PCR and real-time PCR. *Journal of the neurological sciences*, 253(1), 48-52.
- 5- Cataldi, A. (2010). Cell responses to oxidative stressors. *Current pharmaceutical design*, 16(12), 1387-1395.
- 6- Coaccioli, S., Standoli, M. L., Biondi, R., Panaccione, A., Landucci, P., Del Giorno, R. ... & Puxeddu, A. (2009). Assessment of the oxidative stress markers in patients with chronic renal insufficiency undergoing dialysis treatment. *La Clinica terapeutica*, 161(5), 441-444.
- 7- Cooper, G. S., Dooley, M. A., Treadwell, E. L., St Clair, E. W., & Gilkeson, G. S. (2001). Smoking and use of hair treatments in relation to risk of developing systemic lupus erythematosus. *The Journal of rheumatology*, 28(12), 2653-2656.
- 8- Dube, S. R., Fairweather, D., Pearson, W. S., Felitti, V. J., Anda, R. F., & Croft, J. B. (2009). Cumulative childhood stress and autoimmune diseases in adults. *Psychosomatic medicine*, 71(2), 243-250.
- 9- Ercolini, A. M., & Miller, S. D. (2009). The role of infections in autoimmune disease. *Clinical & Experimental Immunology*, 155(1), 1-15.
- 10- Eskandari, F., Webster, J. I., & Sternberg, E. M. (2003). Neural immune pathways and their connection to inflammatory diseases. *Arthritis Research and Therapy*, 5(6), 251-265.
- 11- Hazeki, K., Nigorikawa, K., & Hazeki, O. (2007). Role of phosphoinositide 3-kinase in innate immunity. *Biological and Pharmaceutical Bulletin*, 30(9), 1617-1623.
- 12- Moroni, G., Novembrino, C., Quaglini, S., De Giuseppe, R., Gallelli, B., Uva, V. ... & Bamonti, F. (2010). Oxidative stress and homocysteine metabolism in patients with lupus nephritis. *Lupus*, 19:65-72.
- 13- Predonzani, A., Calì, B., Agnellini, A. H., & Molon, B. (2015). Spotlights on immunological effects of reactive nitrogen species: When inflammation says nitric oxide. *World journal of experimental medicine*, 5(2), 64-76.
- 14- Proal, A. D., Albert, P. J., & Marshall, T. (2009). Autoimmune disease in the era of the metagenome. *Autoimmunity reviews*, 8(8), 677-681.
- 15- Sherbet, G. S. G. (2009). Bacterial Infections and the Pathogenesis of Autoimmune Conditions. *British Journal of Medical Practitioners*, 2(1), 6-13.
- 16- Slavich, G. M., & Irwin, M. R. (2014). From stress to inflammation and major depressive disorder: A social signal transduction theory of depression. *Psychological bulletin*, 140(3), 774-815.
- 17- Stojanovich, L., & Marisavljevic, D. (2008). Stress as a trigger of autoimmune disease. *Autoimmunity reviews*, 7(3), 209-213.
- 18- Valko, M., Leibfritz, D., Moncol, J., Cronin, M. T., Mazur, M., & Telser, J. (2007). Free radicals and antioxidants in normal physiological functions and human disease. *The international journal of biochemistry & cell biology*, 39(1), 44-84.
- 19- Valko, M., Rhodes, C. J., Moncol, J., Izakovic, M. M., & Mazur, M. (2006). Free radicals, metals and antioxidants in oxidative stress-induced cancer. *Chemico-biological interactions*, 160(1), 1-40.

Received January 17, 2016; revised January 20, 2016; accepted January 20, 2016; published online February 1, 2016.



Diagnostic Tools for Sensitive Estimation of Renal Function & Early Detection of Lupus Nephritis

Raji Amin^{1,2*} • Sami A. Hakim^{1,2} • Hala L. Fayed^{2,3} • Alaa Khalifa⁴,
Fouad Khalil^{5,6} • Mahmoud Khedr⁷ • Mohamed Alshafee⁸

¹Assistant Professor of Rheumatology & Rehabilitation, Faculty of Medicine, Al-Azhar University, Cairo, Egypt

²Consultant Rheumatology, King Fahd Specialized Hospital, Buraidah, Kingdom of Saudi Arabia

³Lecturer of Rheumatology & Rehabilitation, Faculty of Medicine, Cairo University, Cairo, Egypt

⁴Consultant Radiology, King Fahd Specialized Hospital, Buraidah, Kingdom of Saudi Arabia

⁵Lecturer of Nuclear Medicine, Radiology Department, Faculty of Medicine, Minia University, Minia, Egypt

⁶Consultant Nuclear Medicine, Radiology Department, Buraidah, Kingdom of Saudi Arabia

⁷Associate Professor, Internal Medicine, Qassim University, Buraidah, Kingdom of Saudi Arabia

⁸Consultant Nephrology King Fahd Specialized Hospital, Buraidah, Kingdom of Saudi Arabia

halafayed@yahoo.com

ABSTRACT

Introduction: Systemic Lupus Erythematosus (SLE) is a systemic autoimmune disease where the immune system mistakenly attacks the body cells and tissues, resulting in a state of chronic inflammation and tissue damage. SLE is characterized by unpredictable course, with periods of flares alternating with remissions. It can affect any part or body tissues, including heart, joints, skin, lungs, liver, nervous system, blood vessels, but still the kidney affection is one of the most commonly involved visceral organs in SLE. Although only approximately 50% of patients with SLE develop clinically evident renal disease, biopsy studies demonstrate some degree of renal involvement in most patients. Acute or chronic renal impairment may develop with lupus nephritis leading to acute or end stage renal disease. Early recognition and management of these cases can reduce the percentage of development of end stage renal disease among these patients to less than 5% of cases. Nephron is the functioning unit of the kidney, whose function is always effected as an early response to inflammation; this function can be evaluated through the estimation of the glomerular filtration rate (secretory function) as well as its excretory function. So searching for a more sensitive and specific indicator for early detection of disease flare or activity depends on the estimation of the nephron function.

Aims of the study: The aims of the study are: to evaluate the most sensitive and accurate diagnostic tool to assess glomerular function and glomerular filtration rate (GFR) in lupus nephritis patients, in relation to clinical manifestations and laboratory indices, as a trial for early detection of lupus nephritis, to investigate whether dynamic renal ^{99m}Tc-DTPA Glomerular Filtration Rate (GFR) is a more sensitive indicator of the degree of renal involvement in lupus nephritis patients than laboratory measurement of serum creatinine level and creatinine clearance (CrCl) through estimated Glomerular Filtration Rate (eGFR) formulae, and to assess renal morphology by static renal ^{99m}Tc-DMSA, as well as split function of both kidneys in view of renal ultrasonography (U/S).

Patients & Methods: Twenty-eight patients with biopsy-proven lupus nephritis selected according to WHO classification for renal staging. The disease activity was recorded using Systemic Lupus Erythematosus Disease Activity Index (SLEDAI) to detect active disease requiring increased treatment for activity. Immunological profiles, including ANA, anti-dsDNA, complement levels (C3, C4) were assessed. Kidney function tests, including serum creatinine, blood urea nitrogen (BUN), creatinine clearance (CrCl), glomerular filtration rate (GFR) using Cockcroft–Gault (CG), the 4-variable abbreviated Modification of Diet in Renal Disease (MDRD) and Chronic Kidney Disease Epidemiology Collaboration Formula (CKD-EPI) method, urinalysis with microscopy, 24 hours urinary proteins, as well as total serum proteins and serum albumin were measured. Dynamic ^{99m}Tc-DTPA radioisotope renal scan was done for all patients as a part of assessment of renal GFR in all patients in the study group. Another static study was done using ^{99m}Tc-DMSA to assess the morphological status as well as the split function of both kidneys in view of renal ultrasonography.



Results: This study was carried out on 28 patients: 9 males (32.1%) and 19 females (67.9%). Their age ranged from (16 - 44 years) with a mean age (23.57 ± 9.57 years). Their height ranged from (147 - 169cm) with a mean height (155.14 ± 7.97) and weight ranged from (37- 84.5 kg) with a mean weight (59.66 ± 16.69). As regards the renal histopathology results, 4 patients (14.28%) had mesangial glomerulonephritis, 15 patients (53.57%) had focal proliferative glomerulonephritis, 6 patients (21.42%) had diffuse proliferative glomerulonephritis, and 3 patients (10.71%) had membranous glomerulonephritis. In patients with impaired renal function the ^{99m}Tc -DTPA GFR values and C-G estimated GFR values was decreased significantly with P value < 0.05 , however, that GFR values obtained by the C-G estimated formula showed a total bias ($-15 \text{ ml/min/1.73m}^2$) and relative bias (-21%). Whereas, the estimated GFR obtained by MDRD, and CKD-EPI equations are still markedly underestimating the GFR values, among the same group of patients with total bias (-28 & $-26 \text{ ml/min/1.73m}^2$) and relative bias (-40% & -37%) respectively. MDRD as well as CKD-EPI equations for estimation of GFR tend to underestimate the GFR value among patients with impaired renal functions. In the patients group with preserved (normal or near normal renal function) the measured GFR by ^{99m}Tc -DTPA dynamic renal scintigraphy showed a comparable results to that obtained from the C-G equations total bias ($-5 \text{ ml/min/1.73m}^2$) and relative bias (-5%), whereas, the GFR values are much higher in equations of MDRD, and CKD-EPI with a total bias ($+5$ & $+10 \text{ ml/min/1.73m}^2$) and a relative bias ($+5\%$ & $+10\%$) respectively. MDRD as well as CKD-EPI equations for estimation of GFR tend to overestimate the GFR value among patients with normal or near normal renal functions. There was a significant decrease in the ^{99m}Tc -DTPA measured GFR value among patients with stage III and stage IV glomerulonephritis, with a P value < 0.05 . Whereas, the GFR values obtained by the C-G formula showed significant decrease only among patients with stage IV glomerulonephritis (P value = 0.016). On the other hand, (MDRD & CKD-EPI formulae) showed insignificant decreased GFR values among patients with stage III & stage IV glomerulonephritis, but they showed significantly increased GFR values among patients with stage II & stage V glomerulonephritis.

Conclusion: ^{99m}Tc -DTPA as a glomerular agent provides a sensitive, physiological, reliable, accurate and reproducible method for assessment of renal function throughout different disease stages in patients with confirmed diagnosis of lupus nephritis (LN), when compared to other methods evaluating renal function in these patients. It provided a proper evaluation of the nephron function, including renal blood flow condition, the secretory function of the nephrons, as well as nephron's excretory function before and after intravenous diuretics injection. Besides, ^{99m}Tc -DMSA as a tubular agent provides a sensitive morphological image of the kidney that can help in estimation of the split function of both kidneys as well as evaluation of the disease course, compared to the traditional morphological imaging modalities (renal ultrasonography).

To cite this article

[Amin, R., Hakim, S. A., Fayed, H. L., Khalifa, A., Khalil, F., Khedr, M., & Alshafee, M. (2016). Diagnostic Tools for Sensitive Estimation of Renal Function & Early Detection of Lupus Nephritis. *J. Middle East North Afr. sci*, 2(2), 34-47]. (p-ISSN 2412- 9763) - (e-ISSN 2412-8937). <http://www.jomenas.org>. 4

Keywords: Renal isotopes scan in SLE/lupus nephritis, GFR-DTPA, DMSA, early lupus nephritis.

1. Introduction:

Systemic lupus erythematosus (SLE) is a prototypic autoimmune disease characterized by the production of antibodies to components of the cell nucleus in association with a diverse array of clinical manifestations. The typical age of onset of SLE falls during the reproductive years, and postpartum and during periods of rapid hormonal changes (Mok & Lau, 2003).

Lupus comprises a range of multisystem disorders involving the deposition of aberrant immune complexes into tissues. Inflammation occurs as a result of autoantibodies attacking organ systems (Childs, 2006).

The primary pathological findings in patients with SLE are those of inflammation, vasculitis, immune complex deposition, and vasculopathy. The exact etiology of SLE is unknown. SLE may coexist with other organ specific autoimmune diseases such as hemolytic anemia, immune thrombocytopenic purpura, and thyroiditis (Mok & Lau, 2003).

It causes inflammation in the tissues of the brain, endothelial cells, gastrointestinal, genitourinary, joints, kidneys, muscles, and skin (Childs, 2006). Renal disease is one of the most common and most serious manifestations of SLE. Systemic lupus erythematosus may present with renal manifestations that frequently are difficult to categorize and lupus nephritis is an important

predictor of poor outcome. The type and spectrum of renal injury may remain undiagnosed until full-blown nephritic and/or nephritic syndrome appears with increased risk of end-stage renal disease. These abnormalities occur within the first few years after the diagnosis of lupus is made on clinical grounds and with the support of laboratory tests in high-risk patients (Ortega et al., 2010).

Renal involvement in SLE adversely affects its ultimate prognosis in terms of patient survival and renal survival (survival without the need for renal replacement therapy) rates, as well as quality of life, including work disability (Mok et al., 1999). The glomerulus is the most common site of kidney involvement by lupus. However, the renal interstitium and tubules, as well as the vasculature, may also be affected (Cross & Jayne, 2005). Early recognition of renal disease and close monitoring for progress after treatment is an essential part of management.

The clinical course of SLE is characterized by periods of remissions and acute or chronic relapses. Despite the overall improvement in the care of SLE in the past two decades, the prognosis of lupus nephritis remains unsatisfactory. Up to 25% of patients still develop end-stage renal failure 10 years after onset of renal disease. Relapses occur frequently in patients with Lupus nephritis, so early disease relapse detection allows proper early treatment. Treatment is based on preventive measures, reversal of inflammation, and prevention of organ impairment and alleviation of symptoms (Ortega et al., 2010).

In order to improve the prognosis of lupus nephritis in SLE, more sensitive and specific diagnostic tools for the onset or relapse of renal disease activity in patients with SLE may allow earlier institution of treatment and even preventive strategies so that the efficacy of existing therapies can be enhanced while treatment-related complications can be minimized (Mok, 2010).

Renal biopsy is the gold standard for assessing renal activity and hence guiding the treatment. Early recognition of renal disease and close monitoring for progress after treatment is an essential part of management (Ortega et al., 2010). Here, we are trying to find a sensitive and accurate diagnostic tool for early detection of lupus nephritis or relapse. Many trials were used to assess nephron function through estimating the glomerular filtration rate (GFR). Calculation of GFR using an empirical mathematical formula has been encouraged as a simple, rapid and reliable means of assessing kidney function. But there are now fewer than 46 different prediction equations currently available, although the two most commonly used are the Cockcroft-Gault (C-G), and Modification of Diet in Renal Disease (MDRD) formulas (Levey et al., 1999), and more recently, Chronic Kidney Disease

Epidemiology Collaboration (CKD-EPI) equation (Levey et al., 2009).

Estimation of GFR proven to be less prone to errors than using 24-hour urine collections for creatinine clearance and is recommended by guideline-issuing organizations like the National Kidney Foundation (NKF) that recommended to estimate GFR with prediction equations based on serum creatinine determinations (Botev et al., 2009).

The Cockcroft-Gault (C-G) formula is based on serum creatinine, age, sex and body weight (Cockcroft & Gault, 1976). Many MDRD equations were used; the most commonly used one is the abbreviated (simplified) 4-variable MDRD equation which relies entirely on determination of serum creatinine, eliminating the need for urea and albumin and so allows estimation of the GFR even if albumin is not checked. It provides computer-generated estimates of GFR with minimal impact on accuracy. (Levey et al., 2000).

CKD guidelines have provided definitions of CKD, and recommend an estimated glomerular filtration rate (GFR) as the best overall measure of kidney function. Unlike measures of creatinine or urea clearance, the MDRD equation does not require 24-hour urine collection, which is prone to errors and is inconvenient for patients (Levey et al., 2000).

The new Chronic Kidney Disease Epidemiology Collaboration Formula (CKD-EPI) equation was developed by Levey and his colleagues in 2009 in an effort to create a formula more accurate than the MDRD formula, especially when actual GFR is greater than 60 ml/min per 1.73 m² (Levey et al., 2009).

Radionuclide renal studies can assess both renal function through the dynamic study with a glomerular agent like (99mTc-DTPA) and morphology through the static imaging using tubular agent like (99mTc-DMSA). Scintigraphy with 99mTc-dimercapto succinic acid (DMSA) is considered a reference method for assessment of parenchymal lesions and estimation of differential kidney function (Smokvina et al., 2005).

2. Patients & Methods:

This study was carried out on 28 SLE patients who were attending the outpatient clinic, or were admitted to the inpatient unit of the Rheumatology Department at King Fahd Specialist Hospital (KFSH) - Buraidah - Kingdom of Saudi Arabia (KSA).

All Patients fulfilled the updated revised criteria of the American College of Rheumatology for classification of Systemic Lupus Erythematosus (Hochberg, 1997). Clinical and laboratory evidence of renal disease was defined as varying combinations of the following: 3+ proteinuria, urine protein > 0.5

gm/24h, creatinine clearance < 60 ml/min, diastolic blood pressure > 90 mmHg or serum creatinine >150 μ mol/l, (1.5 mg/dl).

The clinical disease activity was recorded using the Systemic Lupus Erythematosus Disease Activity Index (SLEDAI). It is a weighted cumulative index of lupus disease activity. The SLEDAI is an index that measures disease activity by weighting the importance of each organ system involved. Activity categories have been defined on the basis of SLEDAI scores: no activity (SLEDAI = 0), mild activity (SLEDAI = 1-5), moderate activity (SLEDAI = 6-10), high activity (SLEDAI = 11-19), and very high activity (SLEDAI 20).

A flare of SLE has been defined as an increase in SLEDAI > 3, and a SLEDAI score > 5 is associated with a probability of initiating or changing therapy in more than 50% of instances (Bombardier et al., 1992). Disease activity was recorded first at the time of renal biopsy and at the time of DTPA assessment.

All patients were diagnosed histopathologically by renal biopsy. These biopsies were performed during the course of assessment and management of the disease. Renal biopsy was done by ultrasound- guided percutaneous puncture and all renal biopsies were assessed by a pathologist and classified according to the abbreviated International Society of Nephrology/ Renal

Pathology Society (ISN/RPS) classification of lupus nephritis (2003):

Class I Minimal mesangial lupus nephritis.

Class II Mesangial proliferative lupus nephritis.

Class III Focal lupus nephritis (a).

Class IV Diffuse segmental (IV-S) or global (IV-G) lupus nephritis (b) Class V Membranous lupus nephritis (c).

Class VI Advanced sclerosing lupus nephritis.

(a) Indicate the proportion of glomeruli with active and with sclerotic lesions.

(b) Indicate the proportion of glomeruli with fibrinoid necrosis and cellular crescents.

(c) Class V may occur in combination with class III or IV in which case both will be diagnosed. Indicate and grade (mild, moderate, severe) tubular atrophy, interstitial inflammation and fibrosis, severity of arteriosclerosis or other vascular lesions (Weening et al., 2004).

All patients were subjected to thorough history taking, full clinical examination, and relevant laboratory investigations.

Laboratory investigations included: CBC, including hemoglobin levels, total leucocyte count, lymphocyte count, and platelet count, Erythrocyte

Sedimentation Rate (ESR) by Westergren method, complement levels (C3 and C4), antinuclear antibodies (ANA), anti-double stranded DNA

antibodies (anti-dsDNA) using the indirect immunofluorescent antibody test, blood chemistry, including serum urea, serum creatinine, serum total proteins, serum albumin, serum calcium, serum phosphorus, routine urine analysis with microscopy for presence of pus cells, presence of RBCs, and abnormal sediments (casts). In addition, 24 hour urine proteins as well as creatinine clearance were done.

Ultrasonography (U/S) assessment for both kidneys was done by the aid of state of the art (General Electric Ultrasound Machine, Logic 9 model), and by using a deep probe (3-5 MHz). Images were taken while the patients were at supine as well as at lateral positions.

Estimation of glomerular filtration rate (GFR) using three formulae namely Cockcroft-Gault (C-G) Modification of Diet in Renal Disease (MDRD) and Chronic Kidney Disease Epidemiology Collaboration (CKD- EPI) Formulae was performed.

Glomerular filtration rate (GFR) is accepted as the best overall measure of kidney function. Normal values, which are related to age, sex, and body size, are approximately 130 ml per minute per 1.73 m² in young men and 120 ml per minute per 1.73 m² in young women, taking into consideration that mean values decline with a person's age.

The Cockcroft-Gault (C-G) formula is based on serum creatinine, age, sex and body weight (Cockcroft & Gault, 1976).

The CKD-EPI (Chronic Kidney Disease Epidemiology Collaboration) formula was developed by Levey and his colleagues in 2009 in an effort to create a formula more accurate than the MDRD formula, especially when actual GFR is greater than 60 ml/min per 1.73 m² (Levey et al., 2009).

Measurement of GFR uses dynamic ^{99m}Tc-DTPA renal isotope scan: Individuals then underwent renal dynamic ^{99m}Tc-DTPA and static ^{99m}Tc-DMSA studies with proper hydration confirmed before starting the study. Explanation of the technique of the study and all the recommended precautions was done before insertion of the IV line. Dynamic ^{99m}Tc-DTPA renal isotope scan was performed as follows: ^{99m}Tc-DTPA was dosed at 100 μ Ci/Kg (with total adult dose about 300MBq) was injected intravenously according to the following imaging protocol:

A pre-syringe image was taken for 60 seconds for the prepared radioactive dose before being injected inside the patient with detector posterior to the syringe).

Injection of the patient was done in the gamma camera room while the dynamic phases of the study were being taken by the aid of state of the art large field of view gamma camera fitted with low energy general purpose (LEGP) collimator, with energy peak at ^{99m}Tc (140 Kev and 20% window) and adjusted at

the region of interest (kidneys at posterior view). Serial dynamic images were taken every 1 second for 60 seconds. Then, second group dynamic images were taken every 15 seconds for 29 minutes. At the 10th minute, 40mg IV furosemide injection was done.

A post-syringe image was taken for 60 seconds for the residual ^{99m}Tc - DTPA radioactive dose after being injected inside the patient with the detector being posterior to the syringe.

Patient's weight and height were taken for further processing of the imaging data for further evaluation of the GFR of the patient as well as split function of both kidneys by using (Gates' equation and technique).

Static ^{99m}Tc -DMSA scan was performed as follows:

- 1) Adjustment of the dose of the ^{99m}Tc -DMSA at $50\mu\text{Ci/Kg}$, with total adult dose about $100\text{MBq} = 2.7\text{ mCi}$. Injection of the patient was done in the preparation (injection) room.
- 2) Wait for 120 minutes before taking anterior & posterior images for the patient in the gamma camera room by the aid of state of the art large field of view gamma camera fitted with LEGP collimator, with energy peak at ^{99m}Tc (140 Kev and 20% window).
- 3) Imaging field was adjusted in the kidney area (site of interest) taking into consideration the upper parts of the urinary bladder to appear at the bottom of the field of view. The duration of imaging was for 500-1000 K. count.

Exclusion Criteria:

Patients excluded from our study include: a patient with malnutrition, a patient under age of 16 years or more than 45 years, pregnant females or a patient with hyperthyroidism. In addition, a patient in remission or has a disease activity less than 6 according to SLEDAI score.

Statistical Methods:

The performance of C-G, MDRD, and CKD-EPI formulae was assessed by the following criteria, in which mGFR is deemed as the true value for comparison purposes:

Total bias = mean difference between eGFR and mGFR values.

Relative bias = mean percentage difference; that is, $[(\text{eGFR} - \text{mGFR})/\text{mGFR}] \times 100$.

3. Results:

This study was carried out on 28 patients: 9 males (32.1%) and 19 females (67.9%). Their age ranged from 16 years to 44 years with mean age (23.57 ± 9.57 years), their height ranged from 147 - 169 cm with mean height (155.14 ± 7.97), and their weight ranged from 37 - 84.5 Kg with mean weight

(59.66 ± 16.69). All patients had biopsy-proven lupus nephritis with disease duration ranging between 4 weeks and 24 weeks with mean disease duration (16.9 ± 4.54 weeks). According to SLEDAI score, eighteen patients (64.3%) had mild to moderate disease flare with SLEDAI score ranging between 6-10, and ten patients (35.7%) had severe disease flare with SLEDAI score ≤ 11 .

As regards the renal histopathology results; 15 patients (53.57%) had focal proliferative glomerulonephritis, 6 patients (21.42%) had diffuse proliferative glomerulonephritis, 4 patients (14.28%) had mesangial glomerulonephritis, and 3 patients (10.71%) had membranous glomerulonephritis.

Six out of the 28 patients (21.4%) had associated bronchial asthma. During the disease course, 6 out of the 28 patients (21.4%) developed diabetes. All patients in study group were normotensive.

Demographic results of our study revealed that the 24-hour urine protein level ranged between 0.71–7.22 gm/day with mean (2.24 ± 2.10 gm/d), whereas, the total serum protein level ranged between 40.9 – 67.9 gm/dl with mean (52.78 ± 11.59), whereas serum albumin level ranged between 15-33 gm/dl with mean (25.13 ± 7.58 $\mu\text{mol/l}$).

Serum creatinine level ranged between 85-209 $\mu\text{mol/l}$ with a mean (125.4 ± 29.15), 24-hour urinary creatinine level ranged between 3680-8592 mg/day with mean value (6135.2 ± 1206.84); whereas, the creatinine clearance ranged between 25-106 ml/min, with mean (76.86 ± 17.43).

Immunological profile for patients of the study group revealed that the Anti- dsDNA serum level ranged from 64-787 U/mL, with mean (238.89 ± 195.76), whereas, serum Complement-3 (C3) ranged from 0.3-1.0 g/L with mean (0.71 ± 0.28), and Complement-4 (C4) ranged from 0.8-1.0 g/L with mean (0.58 ± 0.34), Table (1) showed this demographic data.

Table (2) showed the demographic data for the patients as regard the results of the total renal GFR estimated and/or measured by different methods, and revealed that the Total renal GFR calculated by Cockcroft-Gault (C-G) ranged from 34.62 – 106.64 ml/min/1.73m² with mean value (76.31 ± 26.36), whereas this value ranged from 42-120 ml/min/1.73m² with mean value (84 ± 24.02) when calculated by MDRD. By the CKD-EPI method, estimated total renal GFR value ranged from 48 – 132 ml/min/1.73m² with mean value (100.92 ± 26.55). On Dynamic renal study to assess the renal GFR using ^{99m}Tc -DTPA, total renal GFR value ranged from 27-106 ml/min/1.73m² with mean value (84.63 ± 24.9).

Table 1: Demographic Data of Patients in the Study Group:

Parameters	Minimum and Maximum	Average	Mean ± SD
Age in years	16-44	23.57	23.57± 9.57
Weight	37-84	47.50	
Height	147-169	153	155.15±7.89
Duration of Renal disease (weeks)	4-24	14	16.9 ± 4.54
24-h urinary protein (gm/day).	0.71 – 7.22	2.23	2.24 ± 2.10
Total serum protein (gm/dl)	40.9 - 67.9	52.78	52.78±11.59
Serum albumin (gm/dl)	15-33	25.13	25.13±7.58
Serum creatinine (umol/l)	85-209	125.4	125.4±29.15
creatinine24h urine (mg/day)	3680-8592	6135.5	6135.6±1206.84
Creatinine clearance	25-106	76.86	76.86±17.43
Anti-dsDNA	64.00-787.00	239	238.89±195.76
C3	0.30-1.0	0.7	0.71±0.28
C4	0.8-1.0	0.5	0.58±0.34

Table 2: Demographic data of the total Glomerular Filtration Rate (GFR) estimated and/or measured by different modalities for study group:

Parameters	Range	Mean ± SD
C-G - GFR	34.62-106.64	76.31±26.36
MDRD	42.00-120.00	84.00±24.02
CKDEPI	48.00-132.00	100.92±26.55
^{99m} Tc-DTPA TOTAL GFR	27-106	84.63±24.90
Split Lt kidney Function %	47-54	50.5±5.08
Split Rt kidney Function %	46-53	49.5±5.08
Rt kidney DTPA - GFR	27-54	38.24±12.93
Lt kidney DTP - GFR	26-53	41.37±12.30

In comparison between the total estimated and/or measured renal GFR by different methods and the renal function among patients included in the study revealed that: there was a significant decrease in the GFR values obtained by ^{99m}Tc-DTPA as well

as C-G formula in patients with impaired renal function (serum creatinine > 135 μmol/min) P value < 0.05, whereas, the total renal GFR estimated by MDRD and CKD-EPI formulae, decrease insignificantly in patients with impaired renal function (serum creatinine > 135 μmol/min) p value > 0.05. All methods gives a significant normal GFR values in patients with preserved renal function P value = 0.0001 table (3).

Table 3: Comparison between different methods of GFR estimation in view of renal function:

Parameter	Patients with impaired renal function (18)	P value	Patients with preserved renal function (10)	P Value
Total ^{99m} Tc-DTPA - mGFR	70.31±7.86	0.002*	95.25±6.75	0.0001*
C-G - eGFR	54.94±3.14	0.049*	90.72±5.21	0.0001*
MDRD - eGFR	42.62±5.36	0.66	100.78±9.32	0.0001*
CKD-EPI- eGFR	44.28±7.64	0.55	110.97±8.61	0.0001*

*P value < 0.05 is considered to be significant.

Comparison between the GFR values obtained by different GFR estimation methods in patients with impaired renal function revealed that in patients with impaired renal function the ^{99m}Tc-DTPA GFR values and C-G estimated GFR values was decreased significantly with P value <0.05, however, that GFR values obtained by C-G estimated formula showed a total bias (– 15 ml/min/1.73m²) and relative bias (- 21%). Whereas, the estimated GFR obtained by MDRD, and CKD-EPI equations are still markedly underestimating the GFR values, among the same group of patients with total bias (-28 & -26 ml/min/1.73m²) and relative bias (-40% & - 37%) respectively.

MDRD as well as CKD-EPI equations for estimation of GFR tend to underestimate the GFR value among patients with impaired renal functions table (4).

Table 4: Comparison between different methods of GFR estimation in view of impaired renal function:

Parameter	Total ^{99m} Tc-DTPA - mGFR	P value	Total bias	Relative bias
	70.31±7.86			
C-G eGFR	54.94±3.14	0.0409*	-15	-21%
MDRD eGFR	42.62±5.36	0.0001*	-28	-40%
CKD-EPI eGFR	44.28±7.64	0.00004*	-26	-37%

*P value < 0.05 is considered to be significant.

In patients group with preserved (normal or near normal renal function) the measured GFR by 99mTc-DTPA dynamic renal scintigraphy showed a comparable results to that obtained by the C-G equations total bias (-5 ml/min/1.73m²) and relative bias (-5%), whereas, the GFR values are much higher in equations of MDRD, and CKD-EPI with a total bias (+5 & + 10 ml/min/1.73m²) and a relative bias (+5% & +10%) respectively.

MDRD as well as CKD-EPI equations for estimation of GFR tend to overestimate the GFR value among patients with normal or near normal renal functions table (5).

Table 5: Comparison between different methods of GFR estimation in view of normal renal function:

Parameter	Total 99mTc-DTPA -mGFR	P value	Total bias	Relative bias
	95.25±6.75			
C-G - eGFR	90.72±5.21	0.28	-5	-5%
MDRD - eGFR	100.78±9.32	0.07	+5	+5%
CKD-EPI- eGFR	110.97±8.61	0.076	+10	+10%

*P value < 0.05 is considered to be significant.

Comparison between the GFR values (obtained by different methods of estimated and/or measured GFR) and the renal histopathological data revealed that: there was a significant decrease in the 99mTc-DTPA measured GFR value among patients with stage III and stage IV glomerulonephritis, with P value < 0.05, Whereas, the GFR values obtained by C-G formula showed significant decrease only among patients with stage IV glomerulonephritis (P value = 0.016). Both methods gave significant normal values among patients with stage II and stage V glomerulonephritis, P value = 0.0001. On the other hand, (MDRD & CKD-EPI formulae) showed insignificant decreased GFR values among patients with stage III & stage IV glomerulonephritis, but they showed significantly increased GFR values among patients with stage II & stage V glomerulonephritis table (6).

Case Presentation

A 31 years old female patient diagnosed as systemic lupus erythematosus with diffuse proliferative glomerulonephritis and secondary antiphospholipid syndrome, as well as hypothyroidism secondary to autoimmune thyroiditis, under L-thyroxine 50ug daily. She developed high blood sugar level.

Table 6: Comparison between different methods of GFR estimation in view of the histopathology results:

Parameter	Stage II mesangial lupus nephritis (4)14.28%	Stage III focal lupus nephritis (15) 53.57%	Stage IV diffuse lupus nephritis (6) 21.42%	Stage V membranous lupus nephritis (3) 10.71%
Total	93±2.4	75±5.3	64±3.6	103±2.9
99mTc-DTPA - mGFR	P value =0.001*	P value =0.05*	P value= 0.0002*	P value = 0.0001*
C-G - eGFR	90±2.6 P value =0.0001*	55±1.7 P value =0.9	49±4.3 P value=0.016*	98±8.6 P value = 0.0001*
MDRD - eGFR	110±4.5 P value =0.001*	41±2.2 P value=0.33	37±1.6 P value=0.18	115±4.9 P value = 0.0001*
CKD-EPI- eGFR	120±6.5 P value= 0.001*	45±2.7 P value = 0.55	40±2.4 P value = 0.11	130±4.8 P value = 0.0001*

*P value < 0.05 is considered to be significant.

Patient is on: Cellcept 1gm PO BID, Prednisolone 40 mg PO OD, Hydroxychloroquine 200 mg PO BID, Folic Acid 2mg PO OD, Calcium Carbonate 1200 mg PO BID, Alpha Hydroxy Cholecalciferol 1 µg PO OD, L-Thyroxine 50 µg PO OD, ASA 81 mg PO OD, Omeprazole 40 mg PO OD.

At the time of the renal isotope scanning patient was admitted at the hospital with rapidly progressive glomerulonephritis and renal impairment. Laboratory studies were done for the patient and their results were as follow: WBC 8.1× 1000/uL, Hb 10.5 g/dL, PLT 360× 1000/uL, s. urea 13.8, s. creatinine 148, s. uric acid 414, creatinine clearance 28, total proteins 38.66, s. albumin 13.54, s. K 3.8, s. Ca 2.04, s. P 1.26, RBS 8.5, ESR 28 mm/Hr, C3 0.5, C4 0.28, anti-dsDNA 84.5, urinalysis 3+ albumin, Pus cells 10 cells / HPF, and 24- hour urinary proteins were 6 g/d.

Patient received IV pulse methylprednisolone at a dose 1 g/d for 5 consecutive days followed by high dose oral Prednisolone at a dose of 1mg/kg/day, together with IV pulse cyclophosphamide 0.75 g/ m² BSA with gradual withdrawal of oral prednisolone later on after stabilization of renal function.

Estimated total renal GFR by (C-G) method = 61 ml/min. Estimated total renal GFR by (MDRD) method = 46ml/min. Estimated total renal GFR by (CKD-EPI) method = 49 ml/min.

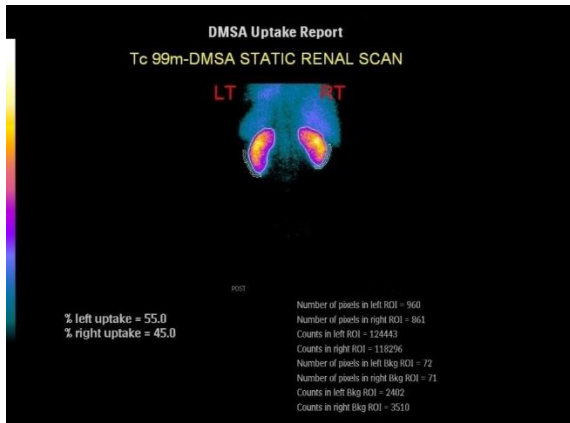


Figure 1(A): 99mTc-DMSA static image showed enhanced background radioactivity with fine heterogeneous cortical radiotracer distribution pattern at both kidneys (reflects parenchymal edema). Left kidney split function 55% & right kidney split function 45%.

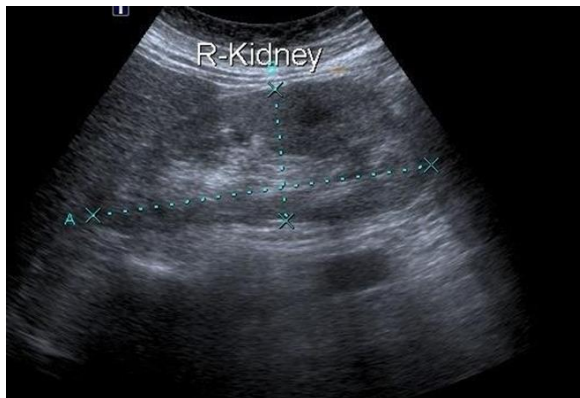


Figure 1(B): U/S both kidneys were of average size, normal site, and normal parenchymal thickness, echogenic Grade-1 nephropathy, with no calculi or backpressure changes.

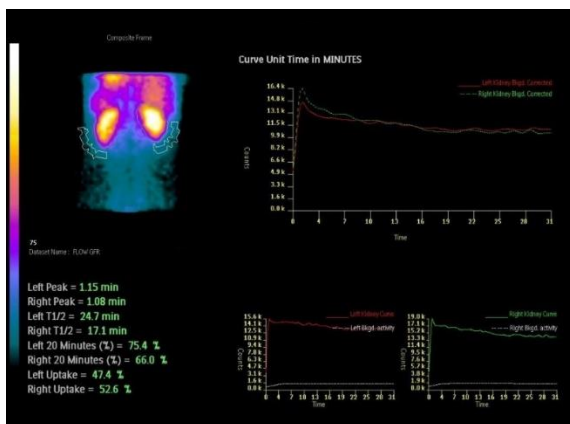


Figure 1(C): 99mTc-DTPA renogram curves showed proper perfusion of both kidneys (vascular phase), with suboptimal radiotracer handling (secretory phase) and prolonged parenchymal transit time of

radioactivity as well as delayed clearance of radioactivity from both kidneys.

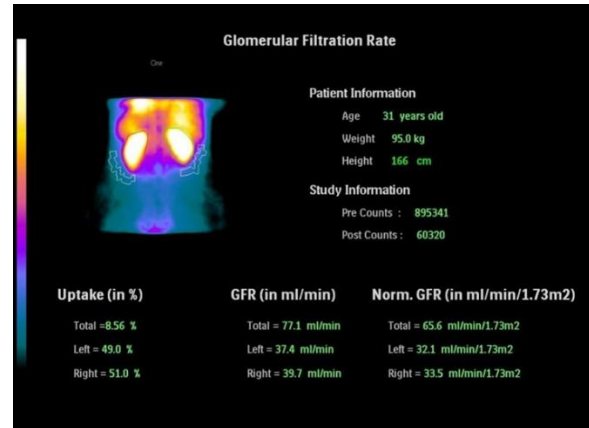


Figure 1(D): 99mTc-DTPA GFR data showed, reduced total renal GFR= 77.1 ml/min, (normal range for her age and sex = 90-110 ml/min), left kidney's GFR = 37.4 ml/min and right kidney's GFR = 39.7 ml/min.

4. Discussion:

Lupus nephritis remains a common complication and major determinant of outcome in SLE (Ortega et al., 2010). Survival of patients with lupus nephritis has significantly improved over the last decades due to increasing treatment options than in the past. However, the optimal treatment of lupus nephritis is still a challenge to the clinician (Bertsias et al., 2008). Early management of lupus nephritis is dependent on early detection of nephritis in SLE patient (Lightstone, 2010).

The best overall index of renal function is considered to be the glomerular filtration rate (GFR) (Botev et al., 2009). Attributes of the GFR as an overall index include the following: (1) it is a direct measure of renal function. (2) It is reduced prior to the onset of symptoms of renal failure. (3) In chronic renal diseases, the reduction in GFR correlates with the severity of some of the structural features of the end-stage kidney, such as the extent of tubule-interstitial sclerosis (Levey, 1990).

The regular measurement of serum creatinine levels is easy to perform and is currently the most common method. However because creatinine is invariably reabsorbed by the renal tubules, serum creatinine and creatinine clearance measurements tend to underestimate the GFR in the context of hyper filtration and overestimate the GFR in the context of hypo filtration (Shemesh et al., 1985).

There are several methods for estimating GFR: A traditional method is to measure 24-hour creatinine clearance which tends to underestimate hyper filtration and overestimate low GFR levels. This

technique is subject to errors in urine collection unless great care is taken (NEBG for CKD, 2009).

Calculation of GFR using an empirical mathematical formula has been encouraged as a simple, rapid and reliable means of assessing kidney function. But there are now fewer than 46 different prediction equations currently available, although the two most commonly used are the Cockcroft-Gault (C-G), and Modification of Diet in Renal Disease (MDRD) formulas (Kemperman et al., 2002; Levey et al., 1999) and more recently, Chronic Kidney Disease Epidemiology Collaboration (CKD-EPI) equation (Levey et al., 2009).

Many organizations recommend the use of equations that estimate the glomerular filtration rate (GFR) to facilitate the detection, evaluation, and management of chronic kidney disease (CKD). Indeed, many clinical laboratories already report estimated GFR (eGFR) values whenever the serum creatinine level is measured (Stevens et al., 2006). In addition, for optimal approximation of GFR from serum creatinine measurements allowances need to be made for age, gender, height and weight of the individual. If the variables are taken into account, as in the Cockcroft-Gault (C-G) and Modification of Diet in Renal Disease (MDRD) equations, a satisfactory index of GFR can be achieved. This is particularly important in thin elderly female people whose baseline serum creatinine levels may be as low as 40-50 μM . In these people delay in referral until the serum creatinine rises above 110 μM would imply that more than 50% of kidney function had been lost (NEBG of CKD, 2009; Levey et al, 1999).

The C-G formula estimates creatinine clearance (CrCl) instead of GFR. Because creatinine is not only filtered by the glomeruli but also secreted by the tubules, CrCl overestimates the GFR (Shemesh et al., 1985). Besides, Cockcroft Gault (C-G) equations consistently overestimate measured GFR in people with normal renal function. It tends to underestimate GFR at levels less than 60 ml/min but is more accurate at higher levels (Botev et al., 2009).

The MDRD equation is based on serum creatinine, age and sex. The MDRD formula tends to underestimate GFR at levels greater than 60 ml/min but is more accurate at lower levels. The Chronic Kidney Disease Epidemiology Collaboration (CKD-EPI) formula was developed to address the systematic underestimation of the glomerular filtration rate (GFR) by the Modification of Diet in Renal Disease (MDRD) Study equation in patients with a relatively well-preserved kidney function (White et al., 2010).

Estimated GFR by Modification of Diet in Renal Disease (MDRD) Study equation and Chronic Kidney Disease Epidemiology Collaboration (CKD-

EPI) can be used in patients who are in the hospital. However, it is important to pay attention to potential inaccuracies due to the non-steady state of serum creatinine, co-morbidities that cause, and the use of medications that interfere with the measurement of serum creatinine (Botev et al., 2009).

The GFR estimates appear to provide a substantial improvement over the measurement of serum creatinine alone in the clinical assessment of kidney function. GFR estimates may be inaccurate in the non-steady state and in people in whom non-GFR determinants differ greatly from those in whom the estimating equation was developed. If GFR estimates are likely inaccurate or if decisions based on inaccurate estimates may have adverse consequences, a measured GFR (mGFR) is an important confirmatory test (Stevens & Levey, 2009).

The National Kidney Foundation recommends GFR estimates for the definition, classification, screening, and monitoring of kidney diseases. Prediction equations based on serum creatinine values were chosen both for adults Cockcroft-Gault (C-G) and Modification of Diet in Renal Disease (MDRD). Because these prediction equations based on serum creatinine may still have a high level of bias, depending on creatinine assay calibration, especially in the normal or near-normal GFR range (Soares et al., 2009).

The MDRD equation generally outperforms the C-G equation but, and low precision with, at best, approximately 80% of estimated GFR in the "Accuracy range" of 70-130% of the measured GFR value, even in patients with known CKD (Soares et al., 2009).

Recently, the National Kidney Disease Education Program (NKDEP) recommends reporting estimated GFR values greater than or equal to 60 mL/min/1.73 m² simply as ≤ 60 mL/min/1.73 m², and not as an exact number when using the MDRD Study equation. For values below 60 mL/min/1.73 m², the report should give the numerical estimate rounded to a whole number (e.g., "32 mL/min/1.73 m²").

There are three reasons for this recommendation:

Inter-laboratory differences in calibration of creatinine assays and the imprecision of the measurements have their greatest impact in the near-normal range and, therefore, lead to greater inaccuracies for values ≤ 60 mL/min/1.73 m² (Myers et al., 2006).

The MDRD Study equation has been most extensively evaluated in people with CKD and reduced GFR, and is less accurate for persons with normal or mildly impaired kidney function (Poggio et al., 2005; Rule et al, 2004; Lin et al, 2003; Bostom et al, 2002; Stoves et al, 2002).

Quantification of estimated GFR values below 60 mL/min/1.73m² has more clinical implications for classification of kidney function than values above this level (Myers et al., 2006). The new Chronic Kidney Disease Epidemiology Collaboration Formula (CKD-EPI) equation was developed to address the systematic underestimation of the glomerular filtration rate (GFR) by the Modification of Diet in Renal Disease (MDRD) Study equation in patients with a relatively well-preserved kidney function (White et al., 2010). It performed better than the Modification of Diet in Renal Disease Study (MDRD) equation, especially at higher GFR, with less bias and greater accuracy (Levey et al., 2009).

An accurate measure of GFR can be undertaken using low molecular weight markers of kidney function such as inulin, iohexolol technetium (Labeled DTPA) (Mathew & Australasian Creatinine Consensus Working Group 2005). Other methods for assessment of GFR include the renal inulin clearance (Cin) (K/DOQI, 2002). However, it cannot be used routinely in daily practice because of its complexity as a test. Previously, some studies reported that Cio overestimates Cin in normal subjects and lupus nephropathy (Petri et al., 1988), and 125I-iothalamate is excreted not only by glomerular filtration but also by tubular secretion (Botev et al., 2009).

As a consequence, alternative filtration markers and clearance methods have been developed and validated. The most widely used alternative filtration marker in the United States is 99mTechnetium labeled di-ethylene triamine Penta acetic acid (DTPA). 99mTc-DTPA is excreted almost entirely by glomerular filtration, 99mTc-DTPA is widely used for dynamic kidney imaging, and its clearance from circulation reflects the condition of the renal arterial blood flow (perfusion), as well as the glomerular filtration rate (GFR) (Vladisav & Bogicevic, 1997).

The 99mTc-DTPA renography which was introduced by Gates (Gates, 1982), is considered to be more accurate than 24 hours creatinine clearance and is recommended for clinical use in patients with reduced renal function (Petersen et al., 1999). In 99mTc-DTPA renography, the GFR is calculated without the need for blood or urine sampling (Prigent et al., 1999).

Besides, 99mTc-DTPA dynamic renal scintigraphy is generally the most important imaging methods routinely used for the evaluation of kidney function. Additionally, the diagnostic information about pre-renal as well as post-renal underlying pathology can be obtained simultaneously with renal scintigraphy and this information has a potential benefit for patient management. Also the capability

of studying both kidneys separately offers a great benefit to assess the split function of each kidney (Tansel et al., 2006), and to draw the treating physician's attention of for the most affected kidney to be the site of further investigation including biopsy aiming at reaching early and proper diagnosis.

Radionuclide renal studies can assess both renal function through the dynamic study with glomerular agent like (99mTc-DTPA) and morphology through the static imaging using tubular agent like (99mTc-DMSA). Considering mechanisms of renal handling of radiopharmaceuticals, the glomerular filtration rate is estimated by 99mTc-DTPA, measurement of absolute as well as split clearances of this radiopharmaceutical provides quantitative information concerning overall and split renal functions. The functional information given by radionuclide methods, are sensitive, reproducible, noninvasive, with low radiation burden to the patient make them favorable for both diagnostic and monitoring tools of various renal diseases (Bogicevic & Stefanovic, 1997).

In Parenchymal diseases: Urographic finding is often normal in patients with a relatively mild impairment of the renal function, while radionuclide methods are very sensitive, even in the initial stage of disease. Renal hypofunction is manifested by low radiopharmaceutical uptake, prolonged transit time and decreased clearance value. By using radiopharmaceuticals with different mechanisms of renal handling, it is possible to estimate the extent of renal dysfunction, as well as to monitor the changes characteristic for disease in the advanced stage. Dynamic kidney scintigraphy and determination of 99mTc-DTPA clearance indicates impairment of both the glomerular and tubular function (Bogicevic et al., 1993; Bogicevic et al., 1989).

Determination of 99mTc-DMSA renal fixation showed decreased uptake in glomerulonephritis patients (Bogicevic & Stefanovic, 1997). Our study results showed that there was a significant decrease in the 99mTc-DTPA measured GFR value among patients with stage III and stage IV glomerulonephritis, with P value < 0.05, Whereas, the GFR values obtained by C-G formula showed significant decrease only among patients with stage IV glomerulonephritis (P value = 0.016). On the other hand, (MDRD & CKD-EPI formulae) showed insignificant decreased GFR values among patients with stage III & stage IV glomerulonephritis.

In patients with impaired renal function 99mTc-DTPA measured GFR values and C-G estimated GFR values was decreased significantly with P value < 0.05, however, that GFR values obtained by C-G estimated formula showed a total bias (- 15 ml/min/1.73m²) and relative bias (-21%).

Whereas, the estimated GFR obtained by MDRD, and CKD-EPI equations are still markedly underestimating the GFR values, among the same group of patients with total bias (-28 & -26 ml/min/1.73m²) and relative bias (-40% & - 37%) respectively.

MDRD as well as CKD-EPI equations for estimation of GFR tend to underestimate the GFR value among patients with impaired renal functions. In patients group with preserved (normal or near normal renal function) the measured GFR by ^{99m}Tc-DTPA dynamic renal scintigraphy showed a comparable results to that obtained by the C-G equations total bias (-5 ml/min/1.73m²) and relative bias (-5%), whereas, the GFR values are much higher in equations of MDRD, and CKD-EPI with a total bias (+5 & + 10 ml/min/1.73m²) and a relative bias (+5% & +10%) respectively.

MDRD as well as CKD-EPI equations for estimation of GFR tend to overestimate the GFR value among patients with normal or near normal renal functions. Cirillo, in 2010 stated that estimates of GFR by equations of the Modification of Diet in Renal Disease (MDRD) study can be unreliable for high-normal GFR because that study did not enroll individuals without kidney disease. Moreover, GFR estimates can be biased by inter assay creatinine differences or unusual levels of creatinine generation (muscle mass) or of renal tubular creatinine secretion.

In the study of Botev and his colleagues in 2009, the C-G and MDRD formulae showed some limitations in their ability to properly estimate the mGFR by Cin. Both formulae had accuracy of approximately 70% of the GFR estimates within \pm 30% of mGFR and approximately 60% of the population was classified correctly in the five GFR groups defined by the K/DOQI-CKD classification (Botev et al., 2009).

Dopuda and coworkers in 2008, in agreement with our results stated that, the most frequent method for the assessment of glomerular filtration rate (GFR) in clinical practice is clearance of creatinine and clearance of ^{99m}Tc-DTPA. Calculation of GFR is corrected for the background and depth of the kidney and finally expressed as a percentage of the net injected counts.

Soares and his colleagues in 2009, in agreement with our results stated that an extensive evaluation of the MDRD equation showed good accuracy in populations with low GFRs (<60mL/min/1.73m²), but worse performance for patients with near-normal GFRs, where underestimation is a problem. Therefore, the MDRD equation appears to be unsuitable for identifying early stages of kidney disease. In addition, other controversial issue with both C-G and MDRD

equations is the influence of patient ethnicity. As regards the CKD-EPI, they stated that it performed better than MDRD study equation especially at higher GFR with less bias and greater accuracy.

Assadi and coworkers in 2008 showed the same results of our study that determination of GFR by the C-G method tended to overestimate or underestimate GFR but the DTPA-GFR method resulted in less error in estimation of GFR. Because of the low cost and negligible radiation burden, this method might be preferred for routine practice.

In the study by Prigent in 2008 he showed that prediction equations based on serum creatinine have limitations especially in the normal or near- normal GFR range. The MDRD equation generally outperforms the C-G equation but may still have a high level of bias, depending on creatinine assay calibration, and low precision with, at best, approximately 80% of estimated GFR in the "accuracy range" of 70-130% of the measured GFR value, even in patients with known CKD. According to Kidney Disease Improving Global Outcomes (KDIGO) recommendations, many indications remain for GFR measurements using a clearance method. In that context, it should be recalled that radiolabeled-tracer plasma or urinary clearance methods, are safe, simple, accurate and reproducible.

Kozlova and coworkers in 2002 summarized our results and stated that the dynamic scintigraphy provides qualitative and quantitative assessment of renal circulation in patients with confirmed diagnosis of SLE. ^{99m}Tc-DTPA dynamic renal scintigraphy can evaluate the effective renal blood flow, which is commonly affected in SLE patients with symptoms of renal disorders.

In agreement with our results too, Prigent and his colleagues in 1999 showed that the ^{99m}Tc-DTPA renography is considered to be more accurate than 24 hours creatinine clearance and is recommended for clinical use in patients with reduced renal function. In ^{99m}Tc-DTPA renography, the GFR is calculated without the need for blood or urine sampling.

Conclusion

The results of this study concluded that ^{99m}Tc-DTPA dynamic renal scintigraphy, is a physiological, sensitive, reliable, safe, simple, accurate and reproducible technique to evaluate renal GFR and hence renal function in patient with early lupus nephritis especially those with normal or near normal renal function. Also, it provides proper evaluation of each kidney separately, so it is easily to detect the most affected kidney which gives a good chance for the treating physician to properly investigate it especially if biopsy procedure is planned to be done and consequently allow proper

histopathological diagnosis, staging, as well as early treatment. For already diagnosed cases it has high accurate diagnostic value that is needed by clinicians as a guide for lupus nephritis therapy. Also ^{99m}Tc -DTPA dynamic renal scan is a universal and simple technique that could assess the GFR without the need for any special equations for race or gender evaluation.

^{99m}Tc -DMSA static renal imaging can provide a good imaging marker for active underlying inflammatory process through its effect on the renal parenchyma (parenchymal edema), as well as its role in assessment of split renal functional indices.

Corresponding Author:

Hala L. Fayed,

Consultant Rheumatology, King Fahd Specialized Hospital, Buraidah, Kingdom of Saudi Arabia,
Lecturer of Rheumatology & Rehabilitation, Faculty of Medicine, Cairo University, Cairo, Egypt.

E-mail: halafayed@yahoo.com

References

- 1- Assadi, M., Eftekhari, M., Hozhabrosadati, M., Saghari, M., Ebrahimi, A., Nabipour, I. ... & Assadi, S. (2008). Comparison of methods for determination of glomerular filtration rate: low and high-dose Tc-^{99m} -DTPA renography, predicted creatinine clearance method, and plasma sample method. *International urology and nephrology*, 40(4), 1059-1065.
- 2- Balci, T. A., Ciftci, I., & Karaoglu, A. (2006). Incidental DTPA and DMSA uptake during renal scanning in unknown bone metastases. *Annals of Nuclear Medicine*, 20(5), 365-369.
- 3- Bertias, G. K., Ioannidis, J. P. A., Boletis, J., Bombardieri, S., Cervera, R., Dostal, C., ... & Isenberg, D. (2008). EULAR recommendations for the management of Systemic Lupus Erythematosus (SLE) Report of a Task Force of the European Standing Committee for International Clinical Studies Including Therapeutics (ESCISIT)*. *Annals of the Rheumatic Diseases*, 67: 195-205.
- 4- Bogicevic M, Antic S, Rajic M, Ilic S, & Stefanovic V. (1989). Radionuclide study of kidney function in some parenchymal kidney diseases. *Mak Med Pregled*, 5:51-53.
- 5- Bogicevi M, Rajic M, & Stefanovic V. (1993). Tubular fixation of ^{99m}Tc - dimercaptosuccinate in parenchymal renal diseases. *Srparhcellek*, 121:113-116.
- 6- Bogicevic M & Vladisav S. (1997) Evaluation of Renal Function by Radionuclide Methods. *The Scientific Journal FACTA UNIVERSITATIS. Medicine and Biology*; 4(1): 3 – 11.
- 7- Bombardier, C., Gladman, D. D., Urowitz, M. B., Caron, D., Chang, C. H., Austin, A. ... & Esdaile, J. (1992). Derivation of the SLEDAI. A disease activity index for lupus patients. *Arthritis & Rheumatism*, 35(6), 630-640.
- 8- Bostom, A. G., Kronenberg, F., & Ritz, E. (2002). Predictive performance of renal function equations for patients with chronic kidney disease and normal serum creatinine levels. *Journal of the American Society of Nephrology*, 13 (8), 2140-2144.
- 9- Botev, R., Mallié, J. P., Couchoud, C., Schück, O., Fauvel, J. P., Wetzels, J. F., ... & Cirillo, M. (2009). Estimating glomerular filtration rate: Cockcroft–Gault and Modification of Diet in Renal Disease formulas compared to renal inulin clearance. *Clinical Journal of the American Society of Nephrology*, 4(5), 899-906.
- 10- Childs S. G. (2006). The pathogenesis of SLE. *Orthop Nurs*; 25 (2):140-5; quiz 146-7.
- 11- Cirillo, M. (2010). Evaluation of glomerular filtration rate and of albuminuria/proteinuria. *J Nephrol*, 23(2), 125-32.
- 12- Cockcroft, D. W., & Gault, M. H. (1976). Prediction of creatinine clearance from serum creatinine. *Nephron*, 16(1), 31-41.
- 13- Cross, J., & Jayne, D. (2005). Diagnosis and treatment of kidney disease. *Best Practice & Research Clinical Rheumatology*, 19(5), 785-798.
- 14- Dopuđa, M., Ajdinović, B., Jauković, L., Petrović, M., & Janković, Z. (2008). Influence of the background activity region selection on the measurement of glomerular filtration rate using the Gates method. *Vojnosanitetski pregljed*, 65 (10), 729-732.
- 15- Gates, G. F. (1982). Glomerular filtration rate: estimation from fractional renal accumulation of ^{99m}Tc -DTPA (stannous). *American Journal of Roentgenology*, 138(3), 565-570.
- 16- Hochberg, M. C. (1997). Updating the American College of Rheumatology revised criteria for the classification of systemic lupus erythematosus. *Arthritis & Rheumatism*, 40 (9), 1725-1725.
- 17- Eknoyan, G., & Levin, N. W. (2002). K/DOQI clinical practice guidelines for chronic kidney disease: Evaluation, classification, and stratification-Foreword. *American Journal of Kidney Diseases*, 39(2), S14-S266.
- 18- Kemperman, F. A., Krediet, R. T., & Arisz, L. (2002). Formula-derived prediction of the glomerular filtration rate from plasma creatinine concentration. *Nephron*, 91(4), 547-558.
- 19- Kozlova, L. K., Baltaeva, T. A., & Gañutdinova, E. (2002). [Renal hemodynamics in patients with systemic lupus erythematosus as shown by renal

- scintigraphy]. *Klinicheskaia meditsina*, 80(12), 48-53.
- 20- Levey, A. S., Bosch, J. P., Lewis, J. B., Greene, T., Rogers, N., & Roth, D. (1999). A more accurate method to estimate glomerular filtration rate from serum creatinine: a new prediction equation. *Annals of Internal Medicine*, 130(6), 461-470.
 - 21- Levey, A. S., Bosch, J. P., Lewis, J. B., SHAHRIARI, A. R., Rogers, N., & Roth, D. (2000). A simplified equation to predict glomerular filtration rate from serum creatinine. *J Am Soc Nephrol*; 11: A0828.
 - 22- Levey, A. S. (1990). Measurement of renal function in chronic renal disease. *Kidney international*, 38(1), 167.
 - 23- Levey, A. S., Stevens, L. A., Schmid, C. H., Zhang, Y. L., Castro, A. F., Feldman, H. I., ... & Coresh, J. (2009). A new equation to estimate glomerular filtration rate. *Annals of internal medicine*, 150(9), 604-612.
 - 24- Lightstone, L. (2010). Lupus nephritis: where are we now? *Current Opinion in Rheumatology*, 22(3), 252-256.
 - 25- Lin, J., Knight, E. L., Hogan, M. L., & Singh, A. K. (2003). A comparison of prediction equations for estimating glomerular filtration rate in adults without kidney disease. *Journal of the American Society of Nephrology*, 14(10), 2573-2580.
 - 26- Matthews, D. R., Charbonnel, B. H., Hanefeld, M., Brunetti, P., & Scherthaner, G. (2005). Long - term therapy with addition of pioglitazone to metformin compared with the addition of gliclazide to metformin in patients with type 2 diabetes: a randomized, comparative study. *Diabetes/metabolism research and reviews*, 21(2), 167-174.
 - 27- Mok, C. C. (2010). Biomarkers for lupus nephritis: a critical appraisal. *Bio Med Research International*, 2010.
 - 28- Mok, C. C., & Lau, C. S. (2003). Pathogenesis of systemic lupus erythematosus. *Journal of Clinical Pathology*, 56(7), 481-490.
 - 29- Mok, C. C., Wong, R. W. S., & Lau, C. S. (1999). Lupus nephritis in Southern Chinese patients: clinic-pathologic findings and long-term outcome. *American Journal of Kidney Diseases*, 34(2), 315-323.
 - 30- Myers, G. L., Miller, W. G., Coresh, J., Fleming, J., Greenberg, N., Greene, T., ... & Eckfeldt, J. H. (2006). Recommendations for improving serum creatinine measurement: a report from the Laboratory Working Group of the National Kidney Disease Education Program. *Clinical Chemistry*, 52(1), 5-18.
 - 31- National Evidence Based Guideline for Diagnosis, Prevention and Management of Chronic Kidney Disease in Type II Diabetes. (2009). prepared by: CARI Guidelines Centre for Kidney Research & NHMRC Centre of Clinical Research Excellence - The Children's Hospital at West mead. In collaboration with: The Diabetes Unit Menzies Centre for Health Policy - The University of Sydney. For the: Diabetes Australia Guideline Development Consortium. Approved by NHMRC on 12 June 2009.
 - 32- Ortega, L. M., Schultz, D. R., Lenz, O., Pardo, V., & Contreras, G. N. (2010). Review: Lupus nephritis: pathologic features, epidemiology and a guide to therapeutic decisions. *Lupus*, 19(5), 557-574.
 - 33- Petersen, L. J., Petersen, J. R., Talleruphuus, U., Møller, M. L., Ladefoged, S. D., Mehlsen, J., & Jensen, H. A. (1999). Glomerular filtration rate estimated from the uptake phase of 99mTc-DTPA renography in chronic renal failure. *Nephrology Dialysis Transplantation*, 14(7), 1673-1678.
 - 34- Petri, M., Bockenstedt, L., Colman, J., Whiting-O'Keefe, Q., Fitz, G., Sebastian, A., & Hellmann, D. (1988). Serial assessment of glomerular filtration rate in lupus nephropathy. *Kidney Int*, 34(6), 832-839.
 - 35- Poggio, E. D., Wang, X., Greene, T., Van Lente, F., & Hall, P. M. (2005). Performance of the modification of diet in renal disease and Cockcroft-Gault equations in the estimation of GFR in health and in chronic kidney disease. *Journal of the American Society of Nephrology*, 16(2), 459-466.
 - 36- Prigent, A., Cosgriff, P., Gates, G. F., Graneurs, G., Fine, E. J., Itoh, K. ... & Taylor, A. (1999, April). Consensus report on quality control of quantitative measurements of renal function obtained from the renogram: International Consensus Committee from the Scientific Committee of Radionuclides in Nephrourology. *In Seminars in Nuclear Medicine*. 29(2), 146-159.
 - 37- Prigent, A. (2008, January). Monitoring renal function and limitations of renal function tests. *In Seminars in nuclear medicine*. 38(1), 32-46.
 - 38- Rule, A. D., Gussak, H. M., Pond, G. R., Bergstralh, E. J., Stegall, M. D., Cosio, F. G., & Larson, T. S. (2004). Measured and estimated GFR in healthy potential kidney donors. *American Journal of Kidney Diseases*, 43(1), 112-119.
 - 39- Shemesh, O., Golbetz, H., KRIss, J. P., & Myers, B. D. (1985). Limitations of creatinine as a

- filtration marker in glomerulopathic patients. *Kidney Int*, 28(5), 830-838.
- 40- Smokvina, A., Grbac-Ivanković, S., Giroto, N., Subat Dežulović, M., Saina, G., & Miletić Barković, M. (2005). The renal parenchyma evaluation: MAG3 vs. DMSA. *Collegium antropologicum*, 29 (2), 649-654.
- 41- Soares, A. A., Eyff, T. F., Campani, R. B., Ritter, L., Camargo, J. L., & Silveiro, S. P. (2009). Glomerular filtration rate measurement and prediction equations. *Clinical Chemistry and Laboratory Medicine*, 47(9), 1023-1032.
- 42- Stevens, L. A., & Levey, A. S. (2009). Measured GFR as a confirmatory test for estimated GFR. *Journal of the American Society of Nephrology*, 20(11), 2305-2313.
- 43- Stevens, L. A., Schmid, C. H., Greene, T., Li, L., Beck, G. J., Joffe, M. M. ... & Levey, A. S. (2009). Factors other than glomerular filtration rate affect serum cystatin C levels. *Kidney International*, 75 (6), 652-660.
- 44- Stevens, L. A., Coresh, J., Greene, T., & Levey, A. S. (2006). Assessing kidney function—measured and estimated glomerular filtration rate. *New England Journal of Medicine*, 354(23), 2473-2483.
- 45- Stoves, J., Lindley, E. J., Barnfield, M. C., Burniston, M. T., & Newstead, C. G. (2002). MDRD equation estimates of glomerular filtration rate in potential living kidney donors and renal transplant recipients with impaired graft function. *Nephrology Dialysis Transplantation*, 17(11), 2036-2037.
- 46- Vladisav S & Bogicevic M. (1997). Evaluation of Renal Function by Radionuclide Methods. *Medicine and Biology*. 4(1), 3 – 11.
- 47- Weening, J. J., D'AGATI, V. I. V. E. T. T. E., Schwartz, M. M., Seshan, S. V., Alpers, C. E., Appel, G. B., ... & Fogo, A. B. (2004). The classification of glomerulonephritis in systemic lupus erythematosus revisited. *Kidney International*, 65(2), 521-530.
- 48- White, C. A., Akbari, A., Doucette, S., Fergusson, D., & Knoll, G. A. (2010). Estimating glomerular filtration rate in kidney transplantation: is the new chronic kidney disease epidemiology collaboration equation any better? *Clinical Chemistry*, 56 (3), 474-477.

Received January 20, 2016; revised January 27, 2016; accepted January 27, 2016; published online February 1, 2016.



Influence of Genotype on the Expression of Host Plant Resistance in Soybean (*Glycine Max (L.) Mirrill*) to the Major Insect Pests of Soybean in Umudike

Chidi J. Harriman^{1*} • Abraham A. Ngwuta² • Chuka C. Onyishi² • Nonso K. Ndulue³
Amarachi C. Nwadinobi¹ • Chinonmso M. Okoronkwo¹ • Chinaza B. Onwuchekwa-Henry¹ • N. Olori-Great¹

¹Department of Agronomy, Michael Okpara University of Agriculture, Umudike, Abia State.

²Department of Crop Science and Technology, Federal University of Technology, Owerri, Imo State.

³Department of Agricultural Technology, Anambra State College of Agriculture, Mgbakwu, Awka.

harrimanchidi@gmail.com

Abstract: Due to low annual production output of soybean grains in Nigeria which was attributed to insect pests infestation, six soybean genotypes were screened for major insect pests resistance in the National Root Crops Research Institute (NRCRI), Umudike. The trials were arranged in the Randomized Complete Block Design with four replicates during 2014 and 2015 growing seasons under the tropical climatic conditions. Analyses were done by pooling over two years due to insignificant genotype X year interactions. Rank summation index (RSI) results showed that TG X 1448 (V6) with RSI value of 17 had overall best performance in terms of resistance, yield and other yield related attributes. Result obtained from correlation indicated that grain yield was significantly and positively correlated with pod number per plant ($r = 0.907^*$) and seed number per pod ($r = 0.691^*$). Conversely, significant and negative correlation was recorded between grain yield and number of damage pod per plant ($r = -0.616^*$). Compared to the simple correlation analysis, path analysis of grain yield and its traits demonstrated that pod number per plant and pod length evolved the highest positive direct influence, 1.80 and 0.65 respectively. Hence, selection for these traits could bring improvement in yield and yield components.

To cite this article

[Harriman, C. J., Ngwuta, A. A., Onyishi, C. C., Ndulue, N. K., Nwadinobi, A. C., Okoronkwo, C. M., Onwuchekwa-Henry, C. B., & Olori-Great, N. (2016). Influence of Genotype on the Expression of Host Plant Resistance in Soybean (*Glycine Max (L.) Mirrill*) to the Major Insect Pests of Soybean in Umudike. *J. Middle East North Afr. sci*, 2(2), 48-55]. (p-ISSN 2412- 9763) - (e-ISSN 2412-8937). <http://www.jomenas.org>. 5

Keywords: soybean, insect pests resistance, correlation, rank summation index, path coefficient analysis

1. Introduction

Soybean (*Glycine max (L.) Merrill*), a *legume* has been grown for three millennia in Asia and recently, has been successfully cultivated around the world. Today, the world's top producers of soybean are the United States, Brazil, Argentina, China and India (ASA, 2012). Soybean is one of the few plants that provide a complete protein as it contains all eight amino acids essential for human health. It is the world's most important source of vegetable oil that is a rich source of vitamin E in human nutrition (Giller and Dashiell, 2007).

Soybean has an average protein content of 40% and is more protein-rich than any of the common vegetable sources. Soybean seeds also contain about 20% oil on a dry matter basis, and this is 85% unsaturated and cholesterol-free (Dugje *et al.*, 2009).

Soybean therefore, serves as a cheap source of protein in meeting human dietary requirement in poor

countries of the World, such as Nigeria. Soybean is widely cultivated in the tropical, subtropical and temperate regions of the world (Giller and Dashiell, 2007). The crop can be successfully grown in many states in Nigeria using low agricultural input. Soybean cultivation in Nigeria has expanded as a result of its nutritive and economic importance and diverse domestic usage.

Despite global effort to increase soybean production, Nigeria has a very low annual production of 439,000t/ha, accounting for only 0.25% of the world annual output of 173 million tons between 1999 and 2003 (FAO, 2005). This low annual production output of soybean grains in Nigeria could be attributed to pests infestation (Tefera, 2011), as crop production is generally difficult in the tropics because of the favourable conditions which promote pest development (Orawu *et al.*, 2001).

The Aphids, *Aphis glycines* (Matsumura) (Hemiptera: Aphididae), Soybean Looper,

Chrysodeixincludens (Walker) (Lepidoptera: Noctuidae), Bean leaf beetle, *Cerotoma trifurcate* (Förster) (Coleoptera: Chrysomelidae), and Green stink bug (*Acrosternumhilare*) and Brown stink bug (*Euchistuservus*) are pests of major economic importance during its three growth stages (seedling, flowering and fruiting).

According to Ragsdale *et al.* (2007), these insects have the ability to reduce plant height, pod set, seed size and the amount of protein in seeds and have been known to reduce yields by as much as 40%. Aphids are the first insect pest in the United States capable of wide-spread damage in soybeans (Ragsdale *et al.*, 2004). For averting losses due to these pests, whole reliance has been on pesticides as a tool of pest control and foreign exchange worth millions of dollars is being spent every year (Anonymous, 2001). The continuous and indiscriminate use of large quantities of synthetic insecticides, besides creating health hazards to human and animal life, as well as environmental pollution, has also resulted in the crop failure in different parts of the world, outbreak of secondary pests and development of resistance to insecticides in large number of insects (Rahman *et al.*, 2006; Raju *et al.*, 2007; Naik *et al.*, 2008; Ghosh and Senapati, 2009).

In view of existing situation and importance of soybean for Nigeria, it is necessary to explore control measures such as host plant resistance (HPR) that is safe, cheap, easy to adopt and effective. HPR results from genetically-based changes in the morphology (leaf shape, stature and hairiness), chemistry (levels of toxins, growth retardants) or phenology (influence of climate on annual phenomena such as flowering) of the plant. HPR is often targeted at specific pests and provides a crop variety with a level of in-built protection against the pest. According to Snelling (1941), resistance includes those characteristics which enable a plant to avoid, tolerate, or recover from the attacks of insects under conditions that would cause greater injury to other plants of the same species.

There are three categories of HPR: antibiosis, anti xenosis, and tolerance. Antibiosis occurs when feeding on a host plant has a negative impact on the survival and egg production, development, feeding, oviposition, egg hatching, orientation, or fecundity of the herbivore, or any combination of the three. Antixenosis, or 'non preference', occurs when the herbivore determines the host-plant is an unsuitable food source and feeds very little, if at all. Tolerance is distinct from antibiosis and anti xenosis; as opposed to being defined by its effect on a herbivore, tolerance is defined as an increased threshold of a host plant to not experience an economic loss during infestation when compared to a susceptible plant (Painter, 1951;

Panda and Khush, 1995; Koegan and Ortman, 1978). Research into sources of HPR in soybeans has primarily focused on the mechanisms of antibiosis and anti xenosis. Some of the biochemical and morphological factors affecting plant resistance are presence of; gossypol, phenolic compound, DIMBOA, oryzanone in plants (Glenn *et al.*, 1971), while temperature, light, relative humidity, soil fertility are known environmental factors that affect the ability of plants to resist pest attacks (Painter, 1951).

Host-plant resistance can be a valuable tool for the management of the soybean aphid. The mechanisms of resistance will allow growers to produce soybeans while using fewer chemical management strategies; this, in turn, will save on expenses as well as preserve communities of natural enemies. Owing to lack of information, the present study has been initiated not only to study an overall population situation of chewing and biting insect pests of soybean in Umudike but also to discover sources of host-plant resistance within the soybean germplasm.

2. Materials and Methods:

The experiment on the influence of genotype on the expression of host plant resistance in soybean was conducted in 2014 and 2015 planting seasons at the National Root Crops Research Institute (NRCRI), Umudike situated at Latitude 05⁰28' N, Longitude 06⁰52' E and Altitude 122m above sea level in 2015 cropping season. Umudike has a total rainfall of about 2000-2500mm per annum with annual average temperature of about 260C.

The predominant vegetative type is rain forest (NEST, 1991). However, the soil was classified as sandy loam ultisol. The soybean genotypes were obtained from National Cereals Research Institute, Badegi, Nigeria (Table 1). The seeds were planted at 2 seeds per hill with spacing of 75 × 5cm in a plot area of 2 × 1m. Which gave plant population density of 533,332 plants/ha. The experiments were laid out in a Randomized Complete Block Design with four replications. Weeding was done regularly and manually to reduce inter-species competition.

Table 1: Six genotypes of soybean evaluated

Genotypic code	Name of genotype
V1	TG x 923 – ZE
V2	TG x 579
V3	TG x 1014 – ZED
V4	TG x 1019 – ZED
V5	TG x 360 – OZD
V6	TG x 1448

Pest scouting frequency.

Aphis craccivora: This was observed weekly on 20 randomly selected soybean stands in the 2 middle rows of each plot. Each was counted and mean calculated. Four observations were made beginning from 2WAP between 8.00 a.m. and 10.00 a.m. A hand lens and diagnostic manual for the identification of insect pathogens published by Poinar and Thomas (1978) was used for confirmation of insect identity.

Table 2: Average Rainfall and Temperature pattern of the environment between May and August 2014 and 2015.

Month	Rainfall (cm)		Temperature (OC)	
	Amount	Days	Max	Min
May	246.8	15	32.6	23.4
June	371.1	21	29.8	23.5
July	131.9	19	27.3	24.4
August	363.7	23	27.3	23.2

Pod damage: Pod damage were determined in the field at maturity by visual rating on a scale of 1-9 (Jackai and Singh, 1988) from the 2 central rows of each plot. Holes and presence of frass on pods and sticking of pods were used as pod damage index.

2. Data Analyses:

The data for the two years were pooled as there were no significant differences between years. Agronomic and insect pests damage parameters collected were subjected to uni- and multi-variate analyses to select promising genotypes. The procedures used include; Pearson Correlation Coefficient used to estimate the relationships between the yield and yield related traits Ofori (1996), while Path analysis was used to Quantify the contribution of causal variables to a targeted effect variable directly and indirectly through other variables (Akinola, 2012).

A Rank Summation Index (RSI) method was introduced to rank the genotypes for their overall performance as proposed by Ngwuta (2007). To obtain the RSI, genotypes were first ranked for each parameter (that is; 1= best genotype and 6 = poorest genotype) and the parameter ranks summed to generate overall performance of each genotype. Data for insect observation yield and yield related components were subjected to analysis of variance (ANOVA) which was used to compare variables using GenStat (2012) and Statistical Package for Social Sciences (SPSS). Amos SPSS was used for path coefficient analysis while significant means were separated by Fisher's Least Significant Difference Test (LSD), at 5% level of significance.

3. Results and Discussion:

The highly significant differences in variety observed for grain yield and all the other traits is an indication that the studied population is genetically diverse for all the traits studied. This observation is consistent with the findings of Aduloju *et al.* (2009). From Table 3, TG X 1019 – ZED (V4) was observed to be the tallest genotypes (39.23cm), while TG X 1448 (V6) was the shortest (28.97cm) genotype.

This variation in heights could be attributed to genotypic differences among the genotypes. The number of leaf beetle and Aphid increased from 6 WAP to 9WAP and decreased at 12 WAP. The decrease in the population could probably be ascribed to weather factors which could have possibly hindered their migratory activity as rains were heavy and frequent at that period. The decreased number of leaf beetle and Aphid as indicated in this study agree with the findings of Degri and Hadi (2000) who reported from Bauchi, the absence of Aphid on field cowpea under heavy rain fed condition.

Perhaps, leaf beetle and Aphid would prefer a warm weather mixed with rains as encountered in the early cropping season in the area. The least number of; Leaf beetle, Soybean looper and Aphid per plant recorded on TG X 1014-ZED (V3) and TG X 1019 – ZED (V4) at different weeks under study showed that resistant genotypes harboured the least numbers. However, TG X 360 - OZD (V5) genotype exhibited moderate resistant, while TG X 923-ZE (V1), TG X 579 (V2) and TG X 1448 (V6) appeared as susceptible ones. These variations in genotypes susceptibility to infestation caused by these insect pests may be due to the presence of anti-xenosis (non-preference) and/or antibiosis phenomena, as described by Van Emdan (1987), who indicated that anti-xenotic plants can be avoided or less colonized by pests seeking food or oviposition site. However, he described Antibiosis as the position of some property by the plant, which directly or indirectly affects the performance of pests in term of survival, growth, development rate, fecundity, etc.

Onyishi *et al.* (2013) reported that genotypes, which recorded the least number of insect pests indicate that they possessed morphological and biochemical factors that made them less preferred by insect pests. The data of pod number per plant and pod length observed in Table 3, indicates that TG X 579 (V2) produced the highest number of pods per plant (30.20), followed by TG X 1448 (V6) (27.33) while TG X 360 - OZD (V5) produced the longest pod (11.30cm). This may be due to the genotypic variation among the soybean genotypes. The results corroborate the findings of Kelechukwu *et al.* (2007) who reported that the number of pods and pod length of cowpea is dependent on the type of variety as

certain varieties are genetically more in number and longer than others.

The lowest number of damage pod (3.13) recorded in TG X 1014-ZED (V3) may be as a result of their resistance and chemical constitution which made them be avoided by these insects. This view is in agreement with Zaren (1987) who believed that the variation in cultivar susceptibility to pest infestation may be due to antibiosis, morphological and physiological character of plant and the number of glands and hairs. Again, this supported Harriman *et al.* (2014) that maintained that reasonable silicate deposits in leaves of some crops make them unattractive to leaf feeding insect pests since it slows down the rate of digestion of pests. The variations observed among the genotype in seed number per pod and grain yield could be attributed to their genetic dissimilarity.

This implied that seed number per pod and grain yield were genetically controlled. However, earlier studies conducted by several researchers revealed varietal differences in the grain yield of soybean (Sanginga *et al.*, 2000; Nirmal *et al.*, 2001) and this accounted for the varietal variations in yield in this study. The reliability of a parameter to be selected for breeding programme among other factors is dependent on the magnitude of its coefficient of variations (CV). It shows the extent of variability in relation to the mean of the population. While a lower value of CV generally depicts low variability among the tested sample; a high proportion CV indicates high variation. The CV recorded in all the parameters studied was low.

3.1. Rank Summation Index

The identification of the best genotypes supports the usefulness of selection index, in this case, rank summation index (RSI) for selection purpose was used (Ngwuta *et al.*, 2007). To obtain the RSI, genotypes were first ranked for each parameter (that is 1 = best and 6 = poorest) and parameter ranks summed to generate overall performance of each genotype. Hence, the lower the RSI of any genotype, more desirable and the better is its agronomic performance. Therefore, the ranking of the 6 soybean genotypes (Table 5) for best performance using damage and yield attributes showed that genotype TG X 1448 (V6) had the best overall performance levels with a Rank Summation Index (RSI) value of 17. This was followed by TG X 1014-ZED (V3) that had the RSI value of 20.

3.2. Correlation:

Selection based on the detailed knowledge of magnitude and direction of association between yield and its attributes is very important in identifying the

key characters, which can be exploited for crop improvement through suitable breeding programme. Correlation between yield and yield components were computed for soybean genotypes (Table 6). Stronger and positive correlations were found between grain yield and pod number per plant ($r = 0.907^*$), seed number per plant ($r = 0.691^*$) and pod length ($r = 0.535$).

These results showed that any positive increase in such characters will suffice the boost in grain yield. These findings were in similar with the results of Burhan (2007). It indicates that grain yield can be increased whenever there is an increase in characters that showed positive and significant association with grain yield. Hence, these characters can be considered as criteria for selection for higher yield as these were mutually and directly associated with yield. On the other hand, negative and significant correlations were determined between grain yield and number of damage pod per plant ($r = -0.616^*$). These results were in unison with Kavita and Reddi (2001) and Reedy *et al.* (1997).

2.7. Path Coefficient Analysis

Grain yield, which is accepted as a major economic character in soybean and due to its complex nature depends on all other yield components. Change in anyone of the components could ultimately disturb the balance. In order to get a clear picture of the interrelationship between these traits, the direct and indirect effects of different characters were worked out using path coefficient analysis (figure 1.) in respect of the grain yield (Singh *et al.*, 2004).

The Path coefficient analysis based on grain yield as a dependent variable revealed that pod number per plant and pod length evolved the highest positive direct influence, 1.80 and 0.65 respectively. Conversely, seed number per plant and number of damage pod per plant had a negative and low direct effect (-0.14 and -0.33 respectively) on grain yield. Besides, most of these traits exhibited indirect influence on grain yield. Thus, these traits could be used more confidently as the selection criteria in the grain yield improvement of soybean. Similar results in support of our results were given by other researchers (Oktem, 2008; Burhan, 2007).

4. Conclusion

Rank summation index (RSI) results identified TG X 1448 (V6) with RSI value of 17 as the overall best performer in terms of resistance, yield and other yield related attributes. While TG X 1019 – ZED (V4) with RSI value of 25 is the least performed genotype. Using path coefficient analysis for selection criteria, pod number per plant and pod length could be used as a selection criterion due to its highly positive direct

effect on grain yield also indirect effects on all other characters.

Corresponding Author:

Chidi J. Harriman,
Department of Agronomy, Michael Okpara
University of Agriculture, Umudike, Abia State.
E-mail: harrimanchidi@gmail.com

References

- 1- Aduloju, M.O., Mahmood, J. and Abayomi Y.A. (2009). Evaluation of soybean [Glycine max (L) Merrill] genotypes for adaptability to a southern Guinea savanna environment with and without P fertilizer application in north central Nigeria. *African Journal of Agricultural Research* 4 (6): 556-563.
- 2- Akinola, N. A. (2012). Path Analysis Step by Step Using Excel. *Journal of Technical Science and Technologies*, 1(1):9-15: 2298-0032.
- 3- Anonymous. (2001). *Economic Survey*. 1st Edn. Government of Pakistan Finance Division Economic Advisor Wing, Islamabad, Pakistan, pp: 43-44.
- 4- ASA. (2012). *American Soybean Association Annual bulletin*: www.soygrowers.com
- 5- Burhan, A. (2007). Relationship among yield and some yield characters in soybean. *J. Biol. Sci.*, 7: 973 – 976.
- 6- Degri, M. M. and Hadi, H. M. (2000). Field evaluation and economies of some insecticides against the major insect pests of cowpea (*Vigna unguiculata* (WALP) in Bauchi, Nigeria. *ESN Occasional Publication* 32 (113- 118).
- 7- Dugje, I.Y., L.O. Omoigui, F. Ekeleme, R. Bandyopadhyay, P. Lava Kumar, and A.Y. Kamara. (2009). *Farmers' Guide to Soybean Production in Northern Nigeria*. International Institute of Tropical Agriculture, Ibadan, Nigeria. 21 pp.
- 8- F.A.O. (2005). *Statistics Agriculture Data* 2005.
- 9- Genstat. (2012). *Genstat for Windows, Discovery, 4th edition*. Lawes Agricultural Trust, Rothamsted Experimental Station, UK.
- 10- Ghosh, S. and Senapati, S.K. (2009). *Seasonal fluctuations in the population of Leucinodes orbonalis L.* Precision agriculture 10 (5): 443-449.
- 11- Giller, K.E. and Dashiell, K.E. (2007). *Glycine max (L.) Merrill*. In: van der Vossen HAM and Mkamilo GS (Eds.) Plant Resources of Tropical Africa 14. Vegetable Oils. PROTA Foundation, Wageningen. Netherlands/Backhuys Publishers, Leiden, Netherlands/CTA, Wageningen, Netherlands. pp 74 – 78.
- 12- Glenn, W.T., Getahm, A. and Cress D. C. (1971). *Resistance in Barley to the Greenbug, Schizaphisgraminum*. Toxicity of phenolic and flavonoid compounds and related substances. *Ann. ENT. Soc Amer.*, 64 (3), 718-722.
- 13- Harriman, J.C., Ngwuta, A.A., Onyishi, G. C. and Nze, E.O., Janeth, O. O. and Ndulue, N. K (2014): *Genotypic Performance of 15 Maize Cultivars for Stem Borer Resistance in Owerri West, South Eastern Nigeria*. International Journal of Advanced Research (2014), Vol.2, Issue 8, 800-815.
- 14- Jackai, L.E.N. and Singh, S.R. (1988) *Screening Techniques for Host Plant Resistance to Insect Pests of cowpea*. *Tropical Grain Legume Bulletin* 35: 2-18.
- 15- Kavita, S. and Reddi, S.R.N. (2001). *Correlation and path analysis of yield components in rice*. *The Andhra Agricultural Journal*, 48(3-4): 311-314.
- 16- Kelechukwu, N. E., Adewale, M. O. and Ezekial, A. A. (2007). *Aluminium, influence on performance of some cowpea (Vigna unguiculata) varieties on Nigeria Alfisol*. *World J. Agric. Sci.*, 3(4): 512-522.
- 17- Koegeen, M., and E. E. Ortman. (1978). *Antixenosis- a new term proposed to replace Painter's 'nonpreference' modality of resistance*. *Bull. Entomol. Soc. Am.* 24:175-176.
- 18- Naik, V., Babu, C., Rao, P., Arjuna, K.P.V. and Srinivasa, R.V. (2008). Seasonal incidence and management of *Leucinodes Orbonalis* Guenee on Brinjal. *Annals of plant Protection Sciences* .16 (2):85-91.
- 19- NEST. (1991). *Nigeria Environmental Study Action*. Nigeria Threatened Environment: A National Profile. Nigeria.
- 20- Ngwuta, A.A. (2007). Evaluation of thirteen cultivars of Bambara groundnut (*Vigna subterranean* L. Verdc.) in Umudike, rainforest agroecological area of Nigeria. *International Journal of Agriculture and Rural Development*. 9: 120-122.
- 21- Nirmal, D.E., R.A.J. Kumar and G. Kalloo, (2001). *Diet versatility in cowpea (Vigna unguiculata) genotypes*. *Indian J. Agric. Sci.*, 71: 598-601.
- 22- Ofori, I. (1996). *Correlation and path-coefficient analysis of components of seed yield in Bambara groundnut (Vigna subterranean)*. *Euphytica*, 91: 102-107.
- 23- Oktem, A. (2008). Determination of selection criteria for cowpea using path coefficient analyses. *Grain Research Communication* 36 (4): 561-570.

- 24- Onyishi, G.C., Harriman, J.C., Ngwuta, A.A., Okporie, E.O. and Chukwu, S.C. (2013): Efficacy of some cowpea genotypes against major insect pests in southeastern agro-ecology of Nigeria. *Middle-East Journal of Scientific Research* 15 (1):114-121.
- 25- Orawu, M., Adipala, E. and Warren H. (2001). Influence of cowpea/sorghum intercropping on occurrences of disease and insect pests in Eastern Uganda. In. *African Crop Science Conference Proceedings*, Vol. 5: 409–412.
- 26- Painter, R. H. (1951). Insect resistance in crop plants. *Soil Science*, 72(6), 481.
- 27- Painter, R.H. (1951). *Insect Resistant In Crop Plants*. MacMillan, New York. 520 pp.
- 28- Panda, N. and G. S. Khush. (1995). *Host plant resistance to insects*. Cab International, Wallingford.
- 29- Poinar, G.C. Jr. and Thomas, G.M. (1978). *Diagnostic Manual for Identification of Insect Pathogens*. Plenum Press, New York, pp: 232.
- 30- Ragsdale, D. W., McCornack, B. P., Venette, R. C., Potter, B. D., Macrae, I. V., Hodgson, E. W., O'Neal, M. E., Johnson, K. D., O'Neil, R. J., DiFonzo, C. D., Hunt, T. E., Glogoza, P. A. and M. E. Cullen. (2007). Economic Threshold for Soybean Aphid (Hemiptera: Aphididae). *J. Econ. Entomol.* 100 (4): 1258-1267.
- 31- Ragsdale, D. W., Voegtlin, D. J. and R. J. O'Neil. 2004. Soybean aphid biology in North America. *Ann. Entomol. Soc. Am.* 97:204-208.
- 32- Rahmam, S.M.M., Alam, M.Z. and Ali, M. (2006). Suppression of brinjal shoot and fruit borer by some IPM packages. *International Journal of Sustainable Agricultural Technology*, 2 (3): 21-26.
- 33- Raju, S. V. S., Bar, U. K., Shanker, U., & Kumar, S. (2007). Scenario of infestation and management of eggplant shoot and fruit borer, *L. orbonalis* Guen. India. *Resistant Pest Manage. Newslett*, 16(2), 14-16.
- 34- Reddy, J.N., De, R.N. and Suriya Rao, A.V. (1997). Correlation and path analysis in low land rice under intermediate (0 – 50cm) water depth. *Oryza*, 34 (3):187 – 190.
- 35- Sanginga, N., O. Lyasse and B.B. Singh, (2000). Phosphorus uses efficiency and nitrogen balance of cowpea breeding lines in a low P soil of the derived savanna zone in West Africa. *Plant Soil*, 220: 119-128.
- 36- Singh, V., Desphande, M.B., Choudri, S.V. and Nimbkar, N. (2004). Correlation and path coefficient analysis in safflower. *Newsletter*, 19:77-81.
- 37- Snelling, R. O. (1941). Resistance of plants to insect attack. *The Botanical Review*, 7(10), 543-586.
- 38- Tefera, H. (2011). *Breeding for Promiscuous Soybeans at IITA*. INTECH Open Access Publisher.
- 39- Van Emden, H. F. (1987). Cultural methods: the plant. *Integrated pest management*, 27-68.
- 40- Zaren, N. (1987). Evaluation of six cotton cultivars for their resistance to thrips and leafhoppers. *Iran Agricultural Research*, 4(2), 89-97.

Received January 22, 2016; revised January 26, 2016; accepted January 26, 2016; published online February 1, 2016.

Appendix

Table 3: Agronomic and damage traits variations of 6 soybean genotypes

GENOTYPE	PH (cm)	NL	D50%F	NLB/P AT;			NSL/P AT;			NA/P AT			NDL/P	PLD/P
				6WAP	9WAP	12WAP	6WAP	9WAP	12WAP	6WAP	9WAP	12WAP		
TG X 923-ZE (V1)	32.43	49.7	60.00	2.900	3.033	2.333	1.600	1.033	1.833	1.967	3.067	1.900	10.67	21.63
TG X 579 (V2)	31.03	33.7	57.67	2.567	2.633	1.867	1.400	0.767	1.633	1.133	1.833	0.800	7.90	23.80
TG X 1014-ZED (V3)	33.50	40.7	58.67	2.400	2.967	2.233	2.567	2.000	2.767	2.600	3.733	2.167	12.33	30.97
TG X 1019 - ZED (V4)	39.23	44.3	53.67	3.300	3.800	2.967	3.200	2.300	3.433	2.900	4.300	2.400	15.23	34.37
TG X 360 - OZD (V5)	32.43	42.7	54.67	2.800	2.933	2.500	2.033	1.833	2.400	2.533	3.267	2.000	11.67	27.30
TG X 1448 (V6)	28.97	39.7	57.00	2.600	3.133	2.100	1.733	1.400	2.000	1.567	2.067	1.367	9.70	24.50
MEAN	32.93	41.8	56.94	2.761	3.083	2.333	2.089	1.556	2.344	2.117	3.044	1.772	11.25	27.09
LSD _(0.05)	3.424	8.12	NS	NS	0.6517	0.6959	0.3782	0.2692	0.4131	0.3062	0.4844	0.3038	2.320	6.931
CV (%)	1.0	6.1	1.7	1.3	0.9	5.8	5.7	5.3	4.1	15.1	2.8	3.8	3.7	3.5

PH = Plant height (cm), NL = Number of leaves, D50%F = Days to 50% flowering, NLB/P = Number of leaf Beetle per plant, NSL/P = Number of soybean Looper per plant, NA/P = Number of Aphid per plant, NDL/P = Number of damaged leaf per plant, PLD/P = Percentage leaf damage per plant (%).

Table 4: Genotypic variation of 6 soybean cultivars on the number of pods per plant, pod length, number of damaged pod per plant, percentage damaged pod per plant, seed number per pod and grain yield.

GENOTYPE	POD NO. PER PLANT	POD LENGTH (CM)	NO. OF DAMAGED POD PER PLANT	PERCENTAGE DAMAGE POD PER PLANT (%)	SEED NUMBER PER POD	GRAIN YIELD (kg/ha)
TG X 923-ZE (V1)	25.00	10.53	5.67	22.77	3.833	2871.8
TG X 579 (V2)	30.20	7.80	6.97	23.07	4.767	3084.2
TG X 1014-ZED (V3)	23.00	9.37	3.13	13.67	3.000	2650.4
TG X 1019 - ZED (V4)	20.43	9.70	4.40	21.50	3.567	2135.5
TG X 360 - OZD (V5)	19.90	11.30	3.53	17.70	3.167	2498.4
TG X 1448 (V6)	27.33	8.67	4.67	17.10	4.100	2969.3
MEAN	24.31	9.56	4.73	19.30	3.739	2701.
LSD _(0.05)	1.583	1.441	1.154	5.182	0.5077	125.4
CV (%)	3.2	3.5	3.0	1.6	2.3	1.2

Table 5: Plant traits, their ranks and rank summation index (RSI) of 6 soybean genotypes

Genotype	NPPP	R ₁	PL	R ₂	NDPPP	R ₃	PDPPP	R ₄	NSPP	R ₅	GY	R ₆	RSI
TG X 1448 (V6)	27.33	2	8.67	5	4.67	4	17.10	2	4.10	2	2969.3	2	17
TG X 1014-ZED (V3)	23.00	4	9.37	4	3.13	1	13.67	1	3.00	6	2650.4	4	20
TG X 923-ZE (V1)	25.00	3	10.53	2	5.67	5	22.77	5	3.83	3	2871.8	3	21
TG X 579 (V2)	30.20	1	7.80	6	6.97	6	23.07	6	4.77	1	3084.2	1	21
TG X 360 - OZD (V5)	19.90	6	11.30	1	3.53	2	17.70	3	3.167	5	2498.4	5	22
TG X 1019 - ZED (V4)	20.43	5	9.70	3	4.40	3	21.50	4	3.57	4	2135.5	6	25

NPPP = Number of pod per plant, PL = Pod length (cm), NDPPP = Number of damaged pod per plant, Percentage damaged pod per plant, Number of seed per pod, GY = Grain yield (kg/ha), R₁-R₆ = Rank₁ to Rank₆, RSI = Rank summation index.

Table 6: *Pearson correlation matrix of some yield parameters of 6 soybean genotypes evaluated.*

	(1)PNPP	(2)SNPP	(3)PL	(4)NDPPP	(5)GY
1.Pod no. per plant	1				
2. Seed no. per plant	0.893*	1			
3. Pod length	-0.807	0.759	1		
4. no. of damage pod per plant	0.790	-0.934**	-0.562	1	
5. Grain yield per hectare	0.907*	0.691*	0.535	-0.616*	1

*. Correlation is significant at the 0.05 level (2-tailed).
 **. Correlation is significant at the 0.01 level (2-tailed).

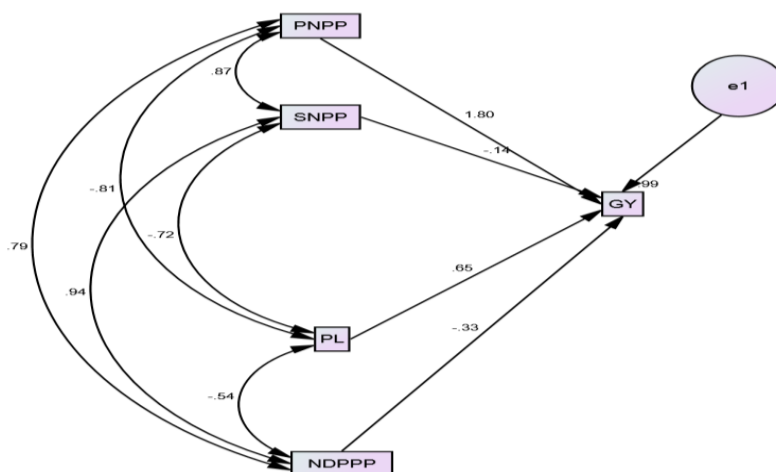


Figure 1. Path Diagram

NDPPP = Number of damaged pod per plant, PL = Pod length, PNPP = Pod number per plant, GY = Grain yield, SNPP = Seed number per plant.



Application of Thermal Imaging Sensor to Early Detect Powdery Mildew Disease in Wheat

Tarek Y. Bayoumi^{1*} • A. A. Abdullah²

¹Agronomy Department, Faculty of Agriculture, Suez Canal University, 41522 Ismailia, Egypt

²Botany Department, Faculty of Agriculture, Suez Canal University, 41522 Ismailia, Egypt

dr.tarekbayoumi@yahoo.com

Abstract: The potential of remote sensing as a tool to identify Powdery mildew disease in an early infection stage and to accurately quantify the severity of infection is crucial in plant disease assessment and management. Powdery mildew is one of the most harmful disease causing great losses in wheat yield. Remote sensing data were obtained in the thermal infrared spectral ranges. A greenhouse study was conducted to assess changes in leaf temperature of wheat plants during infection by powdery mildew to evaluate leaf reflectance measurements. Thermal images of plant disease under different environmental conditions in the field are a cutting-edge research. The variations in temperature between infected and healthy leaves of wheat and the variation between air and leaf-surface temperatures under greenhouse conditions were sensed for early detection of disease. Results revealed that infection with powdery mildew pathogen induced changes in leaf temperature from 0.37 °C (after one hour from the infection) to 0.78 °C at (21 days after infection with the pathogen) and metabolism, contributing to a distinct thermal signature characterizing the early and late phases of the infection. These changes in leaf temperature during Powdery mildew development resulted in a considerable heterogeneity in temperature distribution of infected leaves. The maximum temperature difference within a thermogram of wheat leaves allowed the discrimination between healthy and infected leaves before visible symptoms appeared.

To cite this article

[Bayoumi, T. Y. and Abdullah, A.A. (2016). Application of Thermal Imaging Sensor to Early Detect Powdery Mildew Disease in Wheat. *J. Middle East North Afr.sci*, 2(2), 56-63]. (p-ISSN 2412- 9763) - (e-ISSN 2412-8937). <http://www.jomenas.org>. 6

Keywords: Powdery mildew; Disease prediction; Infrared thermal imagery; Wheat; remote sensing; early detection.

1. Introduction

To implement timely control strategies through plant monitoring, an accurate quantification of disease and damage caused by biotic and abiotic stressors in plants is required. Currently, visual disease and damage quantification methods are the most common (Guan and Nutter, 2002; Steddom et al., 2004,) but these techniques are subject to bias and can be inaccurate (Richardson et al., 2001; Turner et al., 2004 and Bayoumi et al., 2014). Imprecise and inaccurate data may cause costly errors when management and policy decisions are based on biased damage evaluation. The future and the priorities of agriculture have been shifted from agricultural production towards environmental and ecological issues. The aim of modern agriculture is it not only to increase and optimize production but also to produce safe and healthy of high quality food. The over exploitation of resources in agriculture has led to environmental

degradation such as plant diseases. In this regard, powdery mildew infections on wheat represent an important, increasingly growing problem. Wheat (*Triticum aestivum* L.) is one of the important field crops grown in Egypt and across the world. 50 % of relative wheat yield losses may occur when mean temperature change is >2.3 °C, or when carbon dioxide concentration is <395 ppm (Wilcox and Makowski, 2014).

Spread and complexity of disease problems under climate change have led farmers to apply intensive chemical compounds, which result in increased the resistance of pests and pathogens (Coakley et al., 1999). Moreover, plant disease reduces global food production by at least 10% up to 30% (Christou and Twyman, 2004; Strange and Sco, 2005). Specifically, powdery mildews are obligate parasitic fungi which infect wide range of crops (about 700 species of powdery mildews existing

in about 7600 plant species) including cereals, cucurbits, fruit trees and ornamental crops (Bravo et al., 2004), thereby causing significant losses of crop yields when compared to other plant diseases.

Mild weather results in increased powdery mildew growth. Spores germinate at leaf temperatures between 6° to 33°C; the optimum temperature for growth is 25°C. At 21° to 30°C, rapid germination and mycelium growth takes place. During favorable temperature periods, the time between spore germination and production of spores by the new colony takes only 5 days. High temperatures that do not harm the plant can harm the fungus; spores and mildew colonies can be killed at extended durations of temperatures above 33°C. The fungus is destroyed completely when air temperatures rise above 35°C for 12 hours or more if colonies are directly exposed to UV light

Wheat is most susceptible to powdery mildew infection during different stages of development under warm, humid environmental conditions that favor growth of fungus. Application of fungicides is still essential for disease management (Samobor et al., 2005). It is, therefore, important to accurately monitor the occurrence and severity of the disease in order to time fungicide applications. In this context, quantitative information on powdery mildew infection on Wheat is necessary. The conventional method for disease severity assessment in the field mainly relies on direct observation (Nilsson, 1995). This method is repeated ten times on sowing and in addition, it may vary considerably among assessors. Until now, rapid and comprehensive powdery mildew detection methods are not available in practice.

As an alternative method, remote sensing can be used to non-destructively assess plant diseases rapidly over a large area without physical contact with sampling units. Detection of crop stress is an important application of remote sensing (Piarulli et al., 2012). Thermal remote sensing is the branch of remote sensing that deals with the acquisition, processing and interpretation of data acquired primarily in the thermal infrared (TIR) region of the electromagnetic spectrum (Prakash, 2000). Thermal remote sensing differs from optical remote sensing by measuring emitted radiations from the surface of the target object, whereas optical remote sensing measures reflected radiations of the target object under consideration (Sabins, 1996). Thermal properties of plant leaves are affected by a complex heterogeneous internal structure that contains a certain amount of water per unit area. For that reason, it is possible to have research on individual plant with thermal remote sensing because of the versatility, accuracy and high resolution of the infrared thermography (Hu et al., 2011). Nevertheless, accurate

thermal measurements depend on environmental conditions, which influence the thermal properties of the visualized crop. Therefore, calibration of images according to weather conditions is necessary for comparison between image data obtained during different measuring periods and growth seasons (Nilsson, 1995). Nevertheless, to our knowledge, not significant attention has been paid so far to the assessment of thermal imagery on Wheat disease. Thus, the main goal of this research is to evaluate the performance of thermal imagery to detect powdery mildew infection of Wheat. The specific objectives of this study were to: Assess the potential of thermal imagery to detect powdery mildew disease; evaluate the disease severity of wheat leaves infected by powdery mildew, and assess the impact of environmental conditions during measurement of wheat for the assessment and quantification of powdery mildew in the field.

2. Materials and Methods:

2.1. Artificial Infection of Wheat Plants in the Greenhouse.

To test the principal suitability of thermography for the recognition of plant infection, the responses of wheat plants (*Triticum aestivum*) to an infection by powdery mildew was analyzed in greenhouse experiments in 2012/2013 and 2013/2014, at Faculty of Agriculture Farm's of the Suez Canal University (SCU). A moderate susceptible wheat population to powdery mildew disease resulted from crossing between (Sids1 X Sakha 61) and was used in this study. This population was obtained from the Department of Agronomy, Suez Canal University from previous breeding program (Bayoumi et al., 2014).

The wheat plants were sown in 50 cm² diameter pots. Thirty pots were filled with soil that contains a mixture of clay: peat moss 1:1. All plants were watered and fertilized as required. Twenty days after sowing (plants had reached the second leaf stage, 15 to 20 cm height), fifteen pots were selected for inoculation and the remained pots were used as a control. Inoculation was done on the youngest fully expanded leaves of five plants per pot.

Leaves were gently rubbed with clean moistened finger to remove waxy layer from the surface of leaves. Fungal spores were collected from infected wheat leaves, which were shaken before inoculation to remove the old spores; after that spores were removed with a fine brush and directly applied on the leaf surface of target susceptible plant leaves with a paint brush and by dusting spores from infected leaves plant according to (Lebedeva and Peusha 2006; Kathrin et al., 2011). Figure 1 shows the typical symptoms of powdery mildew occurrence

on wheat field-grown on spikes, stem of plants, and leaves, compare to typical healthy plants and leaves.



Figure1. typical symptoms of powdery mildew occurrence on wheat field-grown on (A) spikes (B) stem of plants (C) leaves and (D) typical severe symptoms on plants and leaves.

2.2. Thermo-graphic Measurements, Data Acquisition, and Analysis

The physiological changes in wheat during development of powdery mildew in leaves temperature were determined using visible and thermal imaging techniques under greenhouse by using Fluke Thermal Imager Ti32 (Fluke Thermography, USA), temperature measurement range -20°C to $+600^{\circ}\text{C}$, with $\pm 2^{\circ}\text{C}$ or 2 % accuracy, infrared spectral band $7.5\ \mu\text{m}$ to $14\ \mu\text{m}$ (long wave), field of view $23^{\circ} \times 17^{\circ}$ and have infrared sensor size of 320×240 . Both transmission correction and emissivity were 85 % and 0.98, respectively. For more accuracy, the span of auto adjusted thermal image is manually set in order to detect maximum temperature of the entire display. Thermal images were taken between 12:00 AM to 3:00 PM. The temperature difference (TD) within healthy and infected leaves was studied by taking thermal and color reflectance images from control leaves and inoculated leaves and recording disease severity day by day after inoculation. Digital thermal image analyzed with the software package Smart View® version 3.5.31, which allowed for correction of object emissivity after images had been recorded. However, leaf emissivity was set to 0.98 according to (Lindenthal et al., 2005). The minimum differential between leaves in healthy plant and infected plant were determined using the following equation according to (Chiwaki et al., 2005).

Temperature Differential (T.D) = Temperature of leaves in infected plant – Temperature of leaves in healthy plant

2.3 Humidity, Air Temperatures and Leaf Area Determination

Total leaf areas of wheat and disease severity were estimated from captured images using Image J software (version 1.48s, USA). Disease severity was measured as relative between total leaf area and the infected leaf area as a percentage according to (Feng et al., 2011) and (Nunes -Maciel et al., 2013). Infrared thermal images of wheat plants were obtained from the period before the appearance of external symptoms until the disease conditions existed. Each thermal image was taken for two wheat plants healthy and infected in each frame of image. Immediately after inoculation, disease assessment inoculated plants were assessed daily for powdery mildew development and taken the image. At the first visible symptom, area measurements for disease rating used the Image J software (The lesion as well as the yellowish halo and the faded area surrounding the lesion were all included in the assessment of disease severity. Color pictures were taken with a digital camera (Canon A 2500) at the time of taken thermal image. Air temperature and Relative Humidity were recorded at image time. Humidity and air temperatures in the greenhouse were periodically measured using Humidity and Temperature Meter (Jenway, model 5075, serial No.: 43424, USA) in the same time of capturing thermal images of healthy and infected leaves.

After scanning, the leaves and shoots of the measured plants were harvested and the fresh weight was determined at once. The visible degree of infection was monitored according to the guidelines of (Chaerle et al., 2006) on a percentage scale. Plant samples were then dried at 60°C and total dry matter was determined.

3. Statistical Analysis:

All analyses were conducted using SPSS 11.0 (SPSS Inc., Chicago, IL). Data were analyzed by standard analysis of variance. When the F values were significant, mean comparisons were performed with the least significant difference value at significance level of $P= 0.05$. All experiments were conducted at least twice.

4. Results and Discussion:

4.1. Changes in Leaf Temperature

No visible signs of infection were recognized in inoculated leaves between the beginnings of the experiment and the first measurements. During the following 20 days, number of mildew hyphae and conidia increased on the leaves and led finally to the senescence of the plants. However, even when the leaves were populated with mildew colonies in the late stage of infection, green islands of apparently healthy leaf areas could be observed among the colonies. Table 1 shows changes in temperatures

(T.D) of normal and infected leaves after infection with *Blumeria graminis tritici* under greenhouse .The relationship between the severity of powdery mildew and temperature differential °C (T.D) within a whole leaves temperature of wheat plants were investigated at 14 periods of symptoms development to determine the changes in leaves temperature of wheat as a result infected with powdery mildew. After one hour from the inoculation, there was slightly decrease in temperature differential of the infected wheat leaves (TD= -0.02 °C) with no symptoms were shown. After that, the decreasing in TD of infected leaves increasing with increasing of disease severity and spreading of lesion leaves reached to the highest decreasing (TD= -0.64) at 6 day after inoculation(DAI), where the disease severity (DS=2.41%). Thereafter, there is a gradually retreating in decreasing of TD at eight DAI from TD= -0.62 and DS=2.46% to TD= -0.37 and DS=30.9% at 21 DAI.

Table 1: changes in temperatures (t.d) of normal and infected leaves after infection with *Blumeria graminis tritici* under greenhouse.

DAI	T.D °C	DS %	Air temperature °C	Relative humidity %
0.04	-0.02	0	25.90	82.00
0.08	-0.05	0	25.50	82.00
2	-0.32	0	28.50	82.00
3	-0.55	0	25.50	87.00
5	-0.63	01.03	27.90	85.00
6	-0.64	02.41	25.00	79.00
8	-0.62	02.46	21.00	80.70
9	-0.61	09.09	26.50	83.00
12	-0.45	15.48	23.90	80.60
13	-0.44	19.20	25.00	81.00
14	-0.45	25.20	24.60	80.60
17	-0.42	26.30	29.90	78.50
18	-0.40	26.80	30.88	81.00
21	-0.37	30.90	30.00	85.00

DAI = days after inoculation with pathogen, Ds% = disease severity of powdery mildew %, * 0.04 DAI = 1 hour after infection with pathogen, ** 0.08 DAI = 2 hours after the infection

4.2. Visual Diagnosis of Temperature Differentials on Infrared Thermal Images

The aforementioned disease symptoms were observed at 5 DAI after the infection (DAI), Figure 2 illustrate representative pseudo color thermal images in the thermal infrared region from a healthy and infected, respectively which explains the dynamics of leaf temperature of healthy and infected leaves which

inoculated with powdery mildew. The analysis of thermal images showed that powdery mildew of wheat development caused a decrease in leaf temperature of inoculated leaves at the point of effective infection and before the symptoms become visible. This might be due to dense of colonies and impact of the disease on the physiological processes in the infected leaves, such as the concentration of salicylic acid and Stomata lock-open, as well as the water potential. The results were agreement with (Stoll et al., 2008; Oerke and Steriner, 2010).

They were reported that dense colonies of powdery mildew, in contrast, were associated with a temperature only slightly lower 0.2 °C than healthy leaves. In later stages, powdery mildew tends to slightly increase leaves temperature because of reduced water potential of disease leaf area and spatial and temporal analysis of leaf temperature improved the differentiation between healthy and infected leaves. Prokopov et al., 2010 reported that powdery mildew infection caused decrease in salicylic acid content after 3 days, but on the 7thday of infection it increased significantly in wheat and powdery mildew attack disrupted stomatal behavior and impair stomatal opening, and hence leaf water conductance .The present results,however indicate that the effect of infection can be detected as early as three days after inoculation, as demonstrated by changes especially in leaf temperature and before symptoms become visible.

4.3. Leaves Temperature Distribution

Table 2 shows the leave temperature distribution according to leaves position. Inoculated plant after two days of inoculation (2 DAI) showed slightly decreasing in leaf temperature in lower and middle leaves which recorded in lower leaves (TD =-0.61) and middle(TD =-0.50), while TD increasing (TD= 0.15) on the upper leaf in infected plant. After 3 days of inoculated showed slightly decreased in TD on upper (TD=0.12), while middle and lower leaves still decreasing (TD=-0.86, and 0.91respectively). In all of previous days, no symptoms appearance in infected leaves plant. At 5day after inoculation, symptoms began to appearance on the lower leaves as small lesion, where TD of lower and middle leaves continued decreased (Δ TD=-0.99, and-0.98respectively).

Upper leaf is still decreasing (TD=0.11). The 6 and 8 days of inoculation were showed the maximum decreasing in lower leaves (Δ TD=-1.04, and -1.07respectively). Middle leaves show stability (Δ TD=-0.99) and upper leaves (TD=0.10, 0.11respectively). The 9 DAI showed increase on TD on lower leaves (-0.97), while stability TD in middle and upper leaves (TD=-0.98, 0.10respectively). The

12 DAI showed decrease on TD of upper and middle leaf temperature suddenly (TD = -0.32, -1.08 respectively), and increase TD on lower (TD=0.06). On the other hand, from 13 DAI to 21 DAI were showed continuation increasing but slightly on TD on lower leaves while a decreased in TD upper leaves and beginning increasing in bottom leaves.

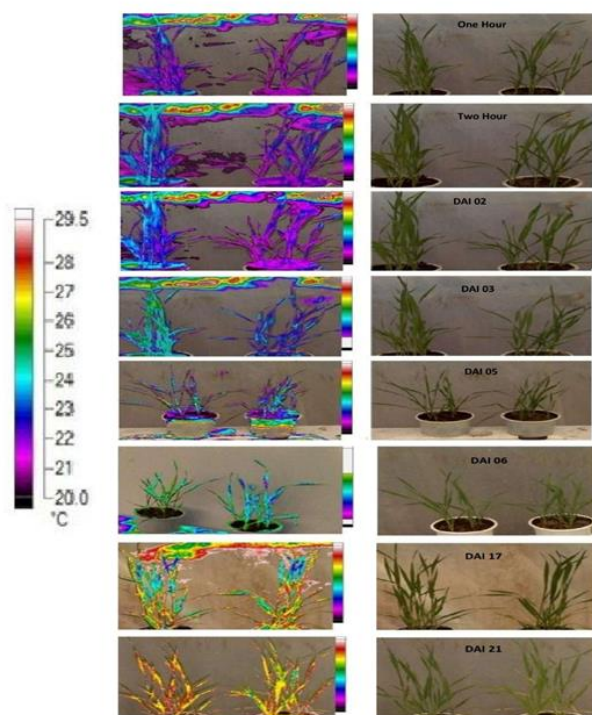


Figure 2. Dynamics of leaves temperature of healthy wheat leaves (right) and thermal images of leaves inoculated (left) with *Blumeria graminis tritici* after one hour to 21 days after inoculation

Table 2: Distribution of leaves temperature according to position of leaves plants.

DAI	Temperature differential (°C)			Mean TD plant °C
	T.D on upper leaves	T.D on Middle leaves	T.D on Lower leaves	
2	0.15	-0.50	-0.61	-0.32
3	0.12	-0.86	-0.91	-0.55
5	0.11	-0.98	-0.99	-0.62
6	0.10	-0.99	-1.04	-0.64
8	0.11	-0.99	-1.07	-0.65
9	0.10	-0.98	-0.97	-0.62
12	-0.32	-1.08	0.06	-0.45
13	-0.41	-1.00	0.09	-0.44
14	-0.50	-0.97	0.13	-0.45
17	-0.79	-0.72	0.26	-0.42
18	-0.90	-0.69	0.40	-0.40
21	-1.70	0.15	0.45	-0.37

4.3. Visualization of Leaves Temperature with Plant Position

Figure 3 shows the distribution of leaves temperature according to position on leaves plant using thermal image techniques. A decreasing in the leaves temperature of the lower and middle leaves compare to upper leaves in plant and before symptoms become visible. Thereafter at five DAI symptoms were appeared on the lower leaves first, coincided decrease in leaves temperature. Decreasing in leaves temperature coincided with the progression of the disease on the leaves of the plant with the occurrence of stability in leaves temperature of middle leaves this decreasing reach to a maximum at 8 DAI day where (TD = -1.07). Leaves temperature of lower leaves were increasing at 9 DAI (TD=-0.97) to reach its maximum increasing at 21 DAI where (TD =0.45) as a result of yellowing leaves and death tissue and destruction of the cells as a result of developing the disease. However, middle leaves were decreased in leaves temperature at 2DAI (TD=-0.5) and reach to a maximum decreasing at 12

DAI (TD = -1.08) coincided with a slightly decreased in the leaves temperature of upper leaves (TD=-0.32). The temperature of middle leaves increasing at 13 DAI (TD=-1) because of the beginning of the yellowing of leaves and death of some of the tissue. Develop of the disease reached to maximum increasing at 21 DAI (TD =0.15) as a result an increased rate of death and death tissue and destruction of the cells while continuing decreasing in the upper leaves temperature.

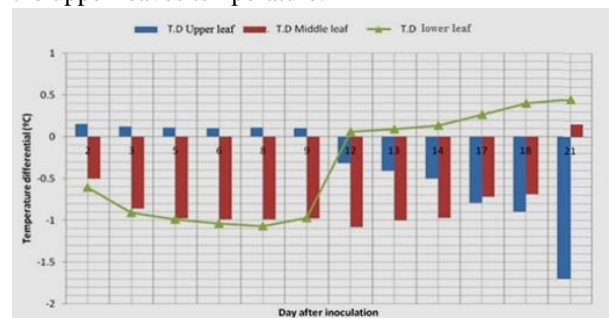


Figure 3. Distribution of leaves temperature according to position on leaves plant using thermal image techniques

5. Overall Discussion:

Crop protection decisions are currently determined at the greenhouse scale. As demonstrated by Secher (1997), disease control might be optimized if fungicides are applied on a site-specific scale, resulting in more sustainable agricultural cropping systems and reduced environmental impact. In order to apply fungicides on a site-specific scale, non-intrusive sensor technologies for disease

identification and tools to support fungicide spray decisions must be developed. Remote sensing and reflectance measurements have gone through rapid development over the past two decades and there is a trend towards the use of images in the application of stress identification for precision farming (Deguise and McNairn, 2000). The duration of the latency period is particularly important for powdery mildew, whose infection does not strictly depend on particular environmental conditions, like rainfall or the presence of free water on plant organs. Infection by this pathogen is virtually continuous and therefore, the epidemic progression mostly depends on the daily dose of inoculum able to infect the host, which in turn depends on how many infection cycles have been completed, leading to sporulating powdery mildew colonies (Xu, 1999). Based on our findings, how the powdery mildew of wheat develops on leaves and the possibility of being followed by using thermal imaging as a new technology to predict the powdery mildew disease at three days before symptoms become visible. Reliable differentiation between normal and infected leaves was observed after 1 hour from the infection due to the formation of fungal conidia under the epidermal layer. After hours from infection, the germ tube adsorbs water and solutes from the host cell wall to facilitate the infection process (Edwards, 2002). Powdery mildew consumes nutrients from the infected plant by its haustoria which grow inside epidermal cells (Bravo et al., 2004) and therefore within 2-4 days micro-colonies are visible on the leaf surface as gray fungal growths on the lower leaf (Figure 2 and Table 2). Powdery mildew infection causes changes in plant carbohydrate metabolism, as well as salicylic acid and oxylipins involved in inducing defense (Bockus et al., 2010). The reaction between pathogen and wheat leaves was observed after 7 days from the artificial infection of powdery mildew pathogen, leading to the appearance of fungal growth as a disease symptom on leaves.

The results were in agreement with those of (Awad et al., 2014 and Bayoumi et al., 2014). They were reported that thermal infrared has been proved by various researchers to be a useful tool for the pre-symptomatic effect of disease and pathogen on plant and allowed tracking of disease progression even at the early pre-symptomatic stage. Xin, et al., 2012 reported that during plant-pathogen infection, the physiological state of the infected tissue is altered, such as changes in photosynthesis, transpiration, stomata conductance, accumulation of salicylic acid and even cell death. This was related to leaf temperature. Ullah, (2013) was reported that foliar disease can directly be detected by using thermal images which were able to identify powdery mildew of barley and wheat and have the potential to identify

and quantify with high spatial resolution management zones in disease control and associated pathogens, as they are sensitive to physiological disorders associated with fungal attack as well as disease (Awad et al., 2014). In addition, leaf diseases often affect plant transpiration. A sequence of thermal modifications resulting from pathogen attack pre-symptomatic cooling followed by a temperature increase due to tissue desiccation described for sugar beet leaves infected with *Cercospora beticola* (Chaerle et al., 2006). A proven result, which can take a particular decision enables us to reduce the appearance of powdery mildew of wheat, spread early, and thereby reduce losses in crop of wheat.

6. Conclusion:

Thermal imaging has been growing fast and playing an important role in plant disease detection. In this study, a disease identification system was developed for wheat powdery mildew infections. To improve the system for identifying powdery mildew infections, thermal imagery was utilized, and results showed that the ability of this system was acceptable. In future research, it is desirable to develop an intelligent platform for real-time disease identification. This could be achieved by multi-sensing systems equipped with an artificial light source and a multi-sensor platform that moves in the crop fields and detects fungal diseases on plants' leaves. In order to increase the ability of real-time detection of a wide range of fungal diseases, our ongoing research is currently focused on developing an early warning system for disease detection.

7. Acknowledgments

This study was partially supported by the project entitled "Applying New Integrated Agronomic Techniques for Sustainable Agriculture in Marginal Soils of Sinai", as a basic and applied research grant from the Science and Technology Development Fund, Ministry of Scientific Research, Egypt.

Corresponding Author:

Tarek Y. Bayoumi,
Agronomy Department, Faculty of Agriculture, Suez Canal University, 41522 Ismailia, Egypt.
E-mail: dr.tarekbayoumi@yahoo.com

References

- 1- Awad, Y. M., Abdullah, A. A., Bayoumi, T. Y., Abd-Elsalam, K., & Hassanien, A. E. (2015). Early Detection of Powdery Mildew Disease in Wheat (*Triticum aestivum* L.) Using Thermal Imaging Technique. In *Intelligent Systems' 2014* (pp. 755-765). Springer International Publishing.

- 2- Bayoumi, T.Y, El-Hendawy, S., Yousef, M.S., Emam, M.A; S.A. Okasha (2014). Application of infrared thermal imagery for monitoring salt tolerant of wheat genotypes. *Journal of American Science* 2014; 10(12):227-234.
- 3- Bockus, W. W., Bowden, R. L., Hunger, R. M., Murray, T. D., & Smiley, R. W. (2010). *Compendium of wheat diseases and pests* (No. Ed. 3). American Phytopathological Society (APS Press).
- 4- Bravo, C., Moshou, D., Oberti, R., West, J., McCartney, A., Bodria, L., & Ramon, H. (2004). Foliar disease detection in the field using optical sensor fusion.
- 5- Bürling, K., Hunsche, M., & Noga, G. (2011). Use of blue-green and chlorophyll fluorescence measurements for differentiation between nitrogen deficiency and pathogen infection in winter wheat. *Journal of plant physiology*, 168(14), 1641-1648.
- 6- Chaerle, L., Leinonen, I., Jones, H. G., & Van Der Straeten, D. (2007). Monitoring and screening plant populations with combined thermal and chlorophyll fluorescence imaging. *Journal of Experimental Botany*, 58(4), 773-784.
- 7- Chiwaki, K., Nagamori, S., & Inoue, Y. (2005). Predicting bacterial wilt disease of tomato plants using remotely sensed thermal imagery. *Journal of Agricultural Meteorology (Japan)*.
- 8- Christou, P., & Twyman, R. M. (2004). The potential of genetically enhanced plants to address food insecurity. *Nutrition research reviews*, 17(01), 23-42.
- 9- Coakley, S.M., H. Scherm, and S. Chakraborty, Climate change and plant disease management. *Annual Review of Phytopathology*, 1999. 37(1): p. 399-426.
- 10- Deguise J.C., and H. McNairn: "Hyperspectral remote sensing for precision agriculture", in: Proceedings of Fifth International Conference on Precision Agriculture, Bloomington (USA), 2000, CD.
- 11- Edwards, H. H. (2002). Development of primary germ tubes by conidia of *Blumeria graminis* f. sp. *hordei* on leaf epidermal cells of *Hordeum vulgare*. *Canadian Journal of Botany*, 80(10), 1121-1125.
- 12- Feng, J., Wang, F., Hughes, G. R., Kaminskyj, S., & Wei, Y. (2011). An important role for secreted esterase in disease establishment of the wheat powdery mildew fungus *Blumeria graminis* f. sp. *tritici*. *Canadian journal of microbiology*, 57(3), 211-216.
- 13- Hu, Z., Du, W., & He, X. (2011, July). Application of infrared thermography technology for irrigation scheduling of winter wheat. In *Multimedia Technology (ICMT), 2011 International Conference on* (pp. 494-496). IEEE.
- 14- Lebedeva, T. V., & Peusha, H. O. (2006). Genetic control of the wheat *Triticum monococcum* L. resistance to powdery mildew. *Russian Journal of Genetics*, 42(1), 60-66.
- 15- Lindenthal, M., Steiner, U., Dehne, H. W., & Oerke, E. C. (2005). Effect of downy mildew development on transpiration of cucumber leaves visualized by digital infrared thermography. *Phytopathology*, 95(3), 233-240.
- 16- Nilsson, H. E. (1995). Remote sensing and image analysis in plant pathology. *Canadian Journal of Plant Pathology*, 17(2), 154-166.
- 17- Nunes Maciel, J. L., do Nascimento Junior, A., & Boaretto, C. (2013). Estimation of blast severity on rye and triticale spikes by digital image analysis. *International Journal of Agronomy*, 2013.
- 18- Oerke, E. C., & Steiner, U. (2010). Potential of digital thermography for disease control. In *Precision Crop Protection-the Challenge and Use of Heterogeneity* (pp. 167-182). Springer Netherlands.
- 19- Pál, M., et al., (2011). Changes in salicylic acid and polyamine contents following powdery mildew infection of near-isogenic Thatcher-based wheat lines carrying different Lr genes *Acta Biologica Szegediensis*, 55(1): 139-141.
- 20- Piarulli, L., Gadaleta, A., Mangini, G., Signorile, M. A., Pasquini, M., Blanco, A., & Simeone, R. (2012). Molecular identification of a new powdery mildew resistance gene on chromosome 2BS from *Triticum turgidum* ssp. *dicoccum*. *Plant science*, 196, 101-106.
- 21- Prakash, A. (2000). Thermal remote sensing: concepts, issues and applications. *International Archives of Photogrammetry and Remote Sensing*, 33(B1; PART 1), 239-243.
- 22- Prokopov, J., Mieslerov, B., Hlavčkov, V., Hlavinka, J., Lebeda, A., Nau, J. and Špundov, M. (2010). Changes in photosynthesis of *Lycopersicon* spp. plants induced by tomato powdery mildew infection in combination with heat shock pre-treatment. *Physiol Mol Plant Pathol*, 74:205-21.
- 23- Samobor, V., Vukobratović, M., and Jošt, M. (2005). Effect of powdery mildew (*Erysiphe graminis* D.C. f.sp. *tritici*) attack on yield and physical parameters of wheat (*Triticum aestivum* sp. *vulgare*) grain quality. *Agriculture*, 11(2):30-37.
- 24- Secher, B. J. M. (1997). Site specific control of diseases in winter wheat. Aspects of Applied Biology (United Kingdom).



- 25- Stoll, M., Schultz, H. R., & Berkelmann-Loehnertz, B. (2008). Exploring the sensitivity of thermal imaging for *Plasmopara viticola* pathogen detection in grapevines under different water status. *Functional Plant Biology*, 35(4), 281-288.
- 26- Strange, R. N., & Scott, P. R. (2005). Plant disease: a threat to global food security. *Phytopathology*, 43.
- 27-Ullah, S. (2013). *Thermal plants: characterizing vegetation parameters using mid to thermal infrared hyperspectral remote sensing* (Doctoral dissertation, Universiteit Twente).
- 28-Wilcox, J., & Makowski, D. (2014). A meta-analysis of the predicted effects of climate change on wheat yields using simulation studies. *Field Crops Research*, 156, 180-190.
- 29-Xin, M., Wang, X., Peng, H., Yao, Y., Xie, C., Han, Y., & Sun, Q. (2012). Transcriptome comparison of susceptible and resistant wheat in response to powdery mildew infection. *Genomics, proteomics & bioinformatics*, 10(2), 94-106.
- 30-Xu, X. M. (1999). Effects of temperature on the latent period of the rose powdery mildew pathogen, *Sphaerotheca pannosa*. *Plant pathology*, 48(5), 662-667.

Received January 26, 2016; revised January 27, 2016; accepted January 27, 2016; published online February 1, 2016.

The Journal of Middle East and North Africa Sciences

Monthly Journal Online

Publisher: JOMENAS Press

Address: Anwar St. PO Box 11415, Amman, Jordan.

Telephone: +962-6-5050852.

Emails: editorsmenaj@gmail.com / jmenas2015@gmail.com

Website: <http://www.jomenas.org>

